Master's thesis

NTNU
Norwegian University of Science and Technology
Faculty of Natural Sciences
Department of Physics

Tea Christiansen Rasmussen

The Dancing Variability of Central Stars of Planetary Nebulae

Uncovering Hidden Features Using Wavelet Analysis

Master's thesis in MSPHYS
Supervisor: Jon Andreas Støvneng
Co-supervisor: Jose Miguel González Pérez
May 2025

NTNU
Norwegian University of
Science and Technology

Tea Christiansen Rasmussen

The Dancing Variability of Central Stars of Planetary Nebulae

Uncovering Hidden Features Using Wavelet Analysis

Master's thesis in MSPHYS
Supervisor: Jon Andreas Støvneng
Co-supervisor: Jose Miguel González Pérez
May 2025

Norwegian University of Science and Technology
Faculty of Natural Sciences
Department of Physics

NTNU
Norwegian University of
Science and Technology

Abstract

Several central stars of planetary nebulae show complex light curves with rapid photometric variations. Jn1, NGC 246, NGC 6852, VV 47, and RX J2117 are all planetary nebula nuclei (PNN) characterized by hydrogen deficiency and bipolar shaped nebulae. These features may indicate a history of binary evolution. Previous observations of these objects suggest the possible presence of several low-amplitude, unstable modulation frequencies. As the photometric variation is of low amplitude and rapidly evolving in time, the main tool used in the analysis in this thesis is the wavelet transform. This is able to collect both time and frequency information from a non-stationary signal as opposed to the static Fourier transform. The motivation for this thesis is to look after interesting photometric features during short observing runs aimed at discovering new pulsators by using non-stationary analysis tools that may reveal signals hidden from conventional stationary methods. The presence of these transient modulation frequencies could encourage future research campaigns to follow these PNNs with longer observation runs so that the low-amplitude photometric variations can be studied properly. Another focus in this thesis is to look after features in the photometric variation, such as harmonic structures in the light curve, which can be related to interactions with a binary companion through an accretion disc. The analysis of all the 5 PNNs show several modulation signals where many of them have variations during the observation run. Jn 1, NGC 6852, VV 47 and RXJ 2117 also show modulation frequencies that could be harmonically related, indicating a possible interaction with a binary companion. The data and findings from this thesis are not conclusive, mainly because of the short observation runs and relatively low sample rate. They do however show promising features that hopefully gives rise to observation campaigns with longer runs of the 5 PNNs.

Sammendrag

Flere sentrale stjerner i planetariske tåker har komplekse lyskurver med hurtige fotometriske variasjoner. Jn 1, NGC 246, NGC 6852, VV 47 og RXJ 2117 er alle planetariske tåkekjerner (PNN) preget av hydrogenmangel og bipolarformede tåker. Disse trekkene kan indikere en historie med binær evolusjon. Tidligere observasjoner av disse objektene antyder mulig tilstedeværelse av flere ustabile modulasjonsfrekvenser med lav amplitude. Siden den fotometriske variasjonen har lav amplitude og utvikler seg raskt over tid, er hovedverktøyet som brukes i analysen i denne avhandlingen wavelet-transformasjonen. Den er i stand til å samle inn både tids- og frekvensinformasjon fra et ikke-stasjonært signal i motsetning til den statiske Fourier-transformasjonen. Motivasjonen for denne avhandlingen er å se etter interessante fotometriske trekk med kort observasjonstid med sikte på å oppdage nye pulsatorer ved å bruke ikke-stasjonære analyseverktøy som kan avsløre signaler skjult fra konvensjonelle stasjonære metoder. Tilstedeværelsen av disse forbigående modulasjonsfrekvensene kan oppmuntre fremtidige forskningskampanjer til å observere disse PNN-ene med lenger observasjonstid, slik at de fotometriske variasjonene med lav amplitude kan studeres på en grundig måte. Et annet fokus i denne avhandlingen er å se etter trekk i den fotometriske variasjonen, for eksempel harmoniske strukturer i lyskurven, som kan relateres til vekselvirkninger med en binær følgesvenn gjennom en akkresjonsskive. Analysen av alle de 5 PNN-ene viser flere modulasjonssignaler der mange av dem varierer i lysstyrke under observasjonene. Jn 1, NGC 6852, VV 47 og RXJ 2117 viser også modulasjonsfrekvenser som kan være harmonisk relatert, noe som indikerer en mulig interaksjon med en binær følgesvenn. Man kan ikke konkludere at PNN-ene er variable basert på dataen og funnene fra denne avhandlingen, hovedsakelig på grunn av de korte observasjonstidene og relativt lav samplingfrekvens. De viser imidlertid lovende trekk som forhåpentligvis gir opphav til observasjonskampanjer med lenger observasjonstid av de 5 PNN-ene.

Preface

This thesis was written during the school year 2024/2025 in collaboration with Andøya Space Education. It is written as a part of the Master of Science in Physics (MSPHYS) study programme at the Department of Physics at the Faculty of Natural Sciences. My supervisor at NTNU was Jon Andreas Støvneng, and my supervisor at Andøya Space Education was Jose Miguel González Pérez.

I would like to thank Jon Andreas Støvneng for the support and for being the interface to NTNU. I would like to thank Jose Miguel González Pérez for the supervision and guidance, as well as general support throughout the whole year.

The first section in this thesis presents the motivation for the thesis and why it is of interest. In the second section, relevant theory on star evolution both for the single and binary star system will be introduced, as well as some general theory on photometric variations and how they might look in solar-like stars, planetary nebula and white dwarfs, and in AM CVn type of objects. The choice of method and analysis tool will be covered in section three, while the observations and results will be presented in section four. The results and findings will be discussed in section five, and finally, the conclusion will be presented in section six.

Contents

List of Figures

List of Tables

Abbreviations

AGB Asymptotic Giant Branch

AM CV AM Canum Venaticorum

CE Common Envelope

FAP False Alarm Probability

FT Fourier Transform

HR-diagram Hertzsprung-Russell diagram

MS Main Sequence

PNN Planetary Nebula Nuclei

RGB Red Giant Branch

WD White Dwarf

WET Whole Earth Telescope

WFT Windowed Fourier Transform

WT Wavelet Transform

Chapter 1

Introduction

1.1 Motivation for thesis

For the past few decades, the study of pulsating stars has been crucial for understanding the interior structure of stars and also for testing stellar evolution theory. In order for a star to be categorized as a pulsating star, the observations must show signs of pulsations with amplitudes above a certain detection limit (1). Keeping this in mind, one can imagine a scenario where there is a pulsating or variable star, but with low amplitudes. Depending on how the observations and data processing is performed, the low-amplitude modulation frequencies might be drowned by noise or not visible due to the choice of method for data processing. The authors Hermes et al. states after performing a search for photometric variability in the white dwarf PG 0112+104 that: "The relatively low-amplitude pulsations observed in PG 0112+104 demonstrate that many white dwarfs that have been observed not to pulsate, mostly from the ground, may indeed vary but at amplitudes below historical detection limits." (2) In these cases, where the photometric variations have such low amplitudes, those variations might be more evident during certain time intervals in the observation run. If this is the case, it would be beneficial to use an analysis method that can work with a non-stationary signal instead of a method that assumes a stationary signal. In the latter method, one will effectively take the average of the whole run and consequently the low-amplitude photometric variations may be hidden in the noise (3).

By using such a method that takes into account non-stationary signals, one might be able to detect photometric variations that would have been ignored otherwise. This is one of the key points in the motivation for this thesis. The findings from this thesis are not meant to conclude that a possible variable star is in fact a variable star, but hopefully the findings can encourage future observation projects to invest in retrieving high quality data on the objects of interest in order to properly examine the possible low-amplitude modulation frequencies. This thesis will focus on short observation runs, which are typical of campaigns searching for new variable stars exhibiting low-amplitude photometric variability. Such scenarios are well-suited for the application of non-stationary methods, as they may uncover subtle photometric features that remain hidden when using stationary analysis techniques (1).

In particular, this thesis focuses on the photometric analysis of various objects that may be linked to the formation of peculiar white dwarfs. This alternative evolutionary pathway is motivated by the so-called "DB-problem". In spectroscopy one can characterize the chemistry of the outer layers of a star. The very hot pre-white dwarf can be classified as a DO that show strong ionized helium lines and have temperatures of the order of 100 000 K. As the DO cools down, hydrogen lines will appear in the spectrum of the white dwarf. Such white dwarfs showing hydrogen lines can be denoted as DA's, while a white dwarf showing helium lines is called a DB. What gives rise to the "DB-problem" is the fact that DB white dwarfs are rarely found in the temperature range of approximately 30 000 K to 45 000 K. This is unexpected because stellar evolution models suggest that white dwarfs should cool continuously through this range, and DBs should be present throughout (1).

For several decades, this "DB-problem" have puzzled white dwarf scientists. There are several theories on why we see this "DB-gap" between 30 000 K and 45 000 K, one of which is a binary system evolution where two stars are gravitationally bound to each other and orbit around their common centre of mass. Objects that are believed to be related to the "DB-gap" following the binary system evolution theory, are bipolar shaped PNNs (planetary nebula nuclei) presenting deficiency in hydrogen. Some of these objects show a quite complex and variable low-amplitude temporal spectrum(1). This makes it rather challenging to understand the nature of the photometric variations and interpret the evolutionary channels leading up to DB white dwarfs. Here an analysis that is able to work with non-stationary signals might be helpful. One of the goals of this master thesis is to find suitable candidates for further research in the attempt to explain the "DB-problem" as a result of binary system evolution. In addition to what is already mentioned above, such suitable candidates might show evidence of an accretion disc(1).

Chapter 2

Theory

One of the main object types of interest in this thesis are the central stars of planetary nebula presenting a bipolar shaped nebula and a lack of hydrogen in the spectra, since this group may be related to the DB-gap problem(1). In the next two following subchapters, there will be a brief introduction of the evolutionary channels that can create these PNNs: the single star evolution and the binary system evolution.

2.1 Single star evolution

A useful tool to show the evolution of a single star is the Hertzsprung-Russell diagram (HR-diagram). A HR-diagram shows the relation between the surface temperature of a star (on the x-axis) and its luminosity (on the y-axis) (4). Figure 2.1.1 shows an example of a simplified HR-diagram marked with different phases that are essential for the evolution of a low-to-intermediate-mass star (around 0.5–8 solar masses) (5). 90 percent of all the stars in the universe are in a phase called the main sequence (6).

In order for a star to be on the main sequence, there has to be hydrogen fusing into helium in the core of the star (4). From fig. 2.1.1, we can see that the main sequence stretches diagonally across the HR-diagram from the top left corner to the bottom right corner. This is a stable phase where the star will spend most of its lifetime (4).

When all of the hydrogen in the core has fused into helium there is no longer a force counteracting the gravity force which will make the core contract. As the core contracts, the temperature inside will increase and ignite a hydrogen burning shell outside of the inert helium core as shown in fig. 2.1.2 (1, 4). Inside this shell, hydrogen will fuse into helium which creates a pressure that causes the outer layers of the star to expand. This gives a red giant star (RGB phase) (1, 4).

The core continues to contract until the temperature reaches a high enough temperature to ignite helium fusion in the core of the star. When this temperature is reached, helium will start to fuse into oxygen and carbon. Now the star has entered the horizontal branch (1, 4).

When all of the helium in the core has fused into carbon and oxygen we get a similar situation as for the RGB phase where the core contracts, the temperature in the core increases which ignites a shell of burning helium outside of the core. So now there is a core of carbon and oxygen with a burning helium shell on the

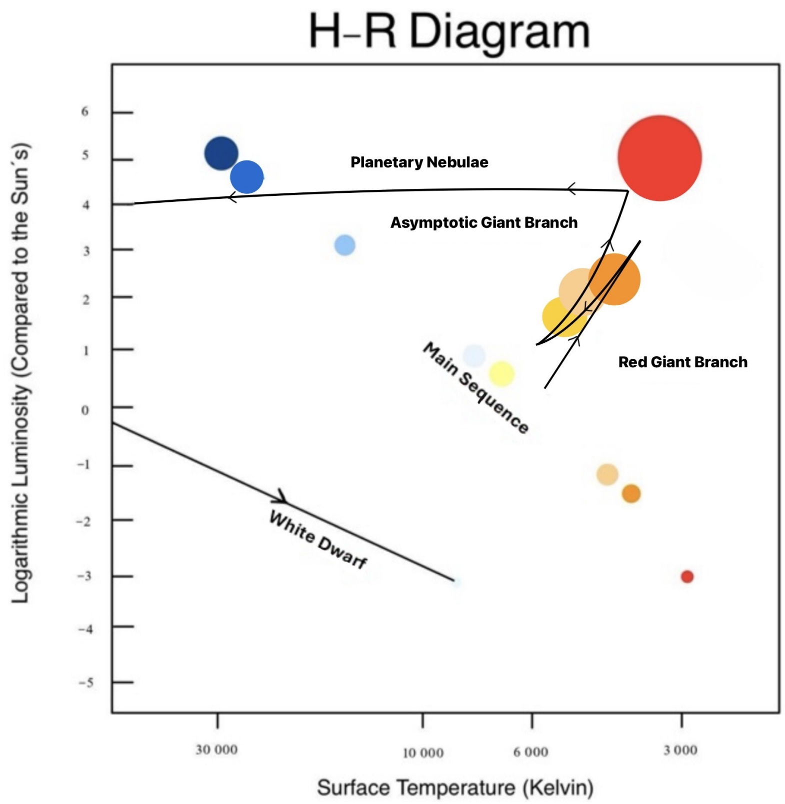

Figure 2.1.1: A simplified representation of HR-diagram marked with some of the most essential phases for low-to-intermediate-mass stars. Figure is inspired by (7).

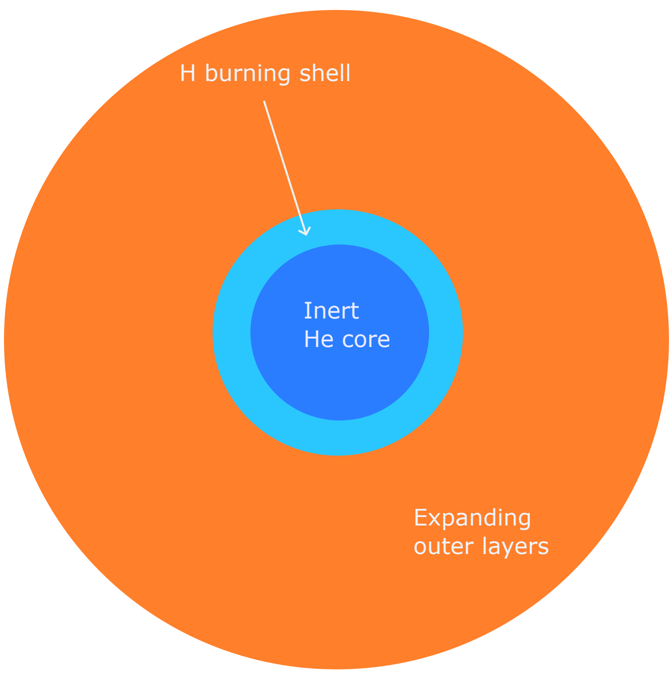

Figure 2.1.2: RGB composition. Figure inspired by (8) as cited by (9).

outside of the core and then a burning hydrogen shell outside of the helium shell again, as shown in fig. 2.1.3. This stage is called the asymptotic giant branch (AGB) (1).

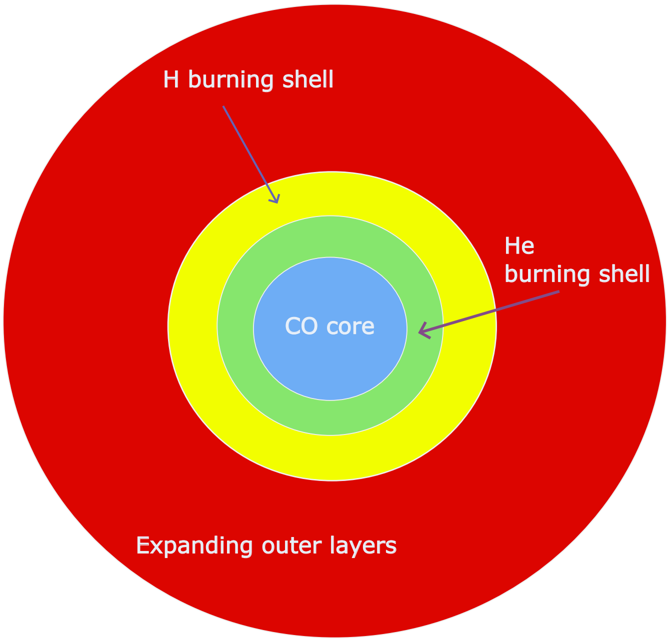

Figure 2.1.3: AGB composition. Figure inspired by (8) as cited by (9).

2.1.1 Planetary nebula and white dwarf

The core will continue to contract, but because the star in question is a low-to-intermediate-mass star, the temperature will not become high enough to ignite carbon fusion (1, 4). This means there is no energy in the core from the fusion process that counteract the gravity force. Instead, because of the high contraction of the core, there is now an electron degeneracy pressure that is counteracting the gravity force (1, 4). Helium flashes will eject the outer layers of the star and create a planetary nebula (1, 4).

As time goes by, the helium flashes will eject the outer layers of the star, and eventually the planetary nebula will vanish from the central star (the remnant of the star). Now the remnant star will cool off as a white dwarf which is quite hot, but because of its small size, also quite dim (low luminosity) (1, 4). Considering single evolutionary scenarios, most white dwarfs are predicted to be born as DA types, with a thin hydrogen layer on top of a helium envelope (1).

2.2 Binary system evolution

As mentioned in section 1.1, the "DB-problem" causes a puzzle when it comes to the evolution of white dwarfs. There are theories that suggests a single star evolution with convective properties that can explain the observations(1). In this thesis however, we will look into the possibility that a binary system evolution can be the explanation of the "DB-problem".

The authors Postnov and Yungelson have investigated several channels for the formation of low-mass compact binaries with white dwarf components (10). For our case, the evolutionary channel that results in a degenerate white dwarf (WD) and a semidegenerate main sequence (MS) star is of interest. Both Jones (11) and Pérez (1) gives a thorough description of this evolutionary channel. It starts with a main sequence binary where the most massive star evolves into the giant phase (RGB or AGB), while the other is still at the main sequence. This situation is illustrated in fig. 2.2.1a where the giant star is at the left while the MS star is at the right while the dashed line marks the Roche lobe of the system. This means that everything inside the dashed line on the left side is gravitationally bound to the giant star, while everything inside the dashed line on the right side is gravitationally bound to the MS star. Material that is outside of the dashed line is either gravitationally bound to the system as a whole or not gravitationally bound at all. The giant star will start to expand as it is in its giant phase and fill its roche lobe as shown in fig. 2.2.1b. As it continues to expand it will start to transfer mass to its companion. Now there are two alternatives; the giant star shrink back as it loses mass to its companion or the mass transfer can become dynamically unstable and transfer mass faster and faster. If the latter alternative is the case, the Roche lobe of the companion star will also be filled as seen in fig. 2.2.1c. Now the mass has no other place to go but outside of the Roche lobe as shown in fig. 2.2.1d. The material outside of the Roche lobe is gravitationally bound to the system as a whole, not to a single star, and is called a common envelope (CE). Same as the binary system, the CE rotates, but it is not corotating with the binary system which in turn creates frictional forces between the binary system and the CE. These frictional forces decreases the orbit of the binary system and hence releasing gravitational energy that will be absorbed by the CE. When the released gravitational energy exceeds the binding energy of the envelope, the CE will be ejected and form a planetary nebula.

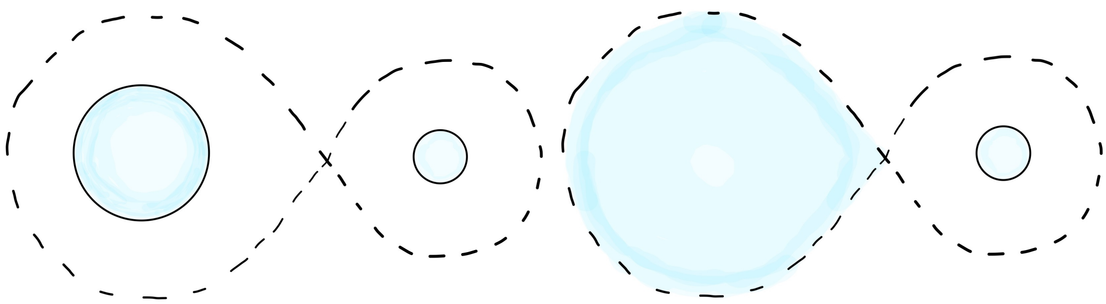

(a) Phase 1 **(b)** Phase 2

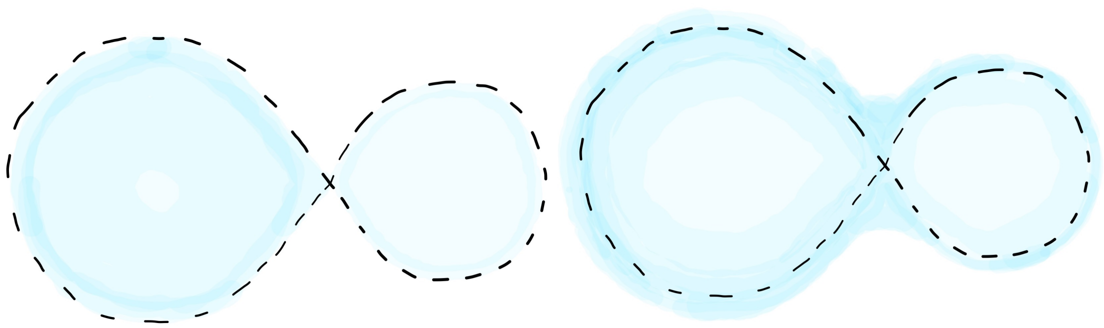

(c) Phase 3 **(d)** Phase 4

Figure 2.2.1: Common envelope evolution. Figure is inspired by (11).

These four phases that are illustrated in fig. 2.2.1 illustrates the common envelope evolution, but this is only the first common envelope stage. After the first

CE stage the previously giant star becomes a white dwarf while the companion or donor star that was previously a MS star now evolves into the giant branch and becomes a giant star. The second common envelope stage happen when the companion star overfills its Roche lobe and we get a similar situation as shown in fig. 2.2.1 but now with the roles of the companions reversed. The companion or helium star is initially non-degenerate, but becomes semi-degenerate as the mass loss stops the helium fusion in the core of the companion (10). The result will be a close binary system in which a significant fraction of hydrogen has been effectively removed, and where mass transfer is expected to be dominated by helium.

2.3 Photometric variations

This thesis focuses on photometric variability, which may combine intrinsic stellar pulsations with signatures of interaction with a close companion. Therefore, the nature of these potential sources of variability is introduced. Some stars exhibit regular variations in their brightness due to intrinsic properties, these are known as pulsating stars. The study of the stellar structure due to the star's intrinsic oscillations is called asteroseismology. One can extract quite some information about the interior of a star by studying its oscillations as for example its interior composition stratification. In addition, the features of the photometric variations might also show signs of interaction with a close companion in a binary system (1, 12).

2.3.1 Solar-like oscillations

There are many different kinds of pulsations modes in stars. The Sun for example, have two non-radial modes known as p-modes (p from pressure) and g-modes (g from gravity). The p-modes or pressure waves are trapped inside the star where they bounce between the surface and the deeper layers due to refraction. Here the pressure gradient within the star causes the sound of speed to change with the depth which in turn causes the refraction. For g-modes on the other hand, the restoring force is buoyancy which is caused by gravity, hence the name (4).

There are stars ranging from low-mass ($M \lesssim 2M_{\odot}$) main-sequence stars to evolved red giants that excite stochastically driven oscillations. Stochastic oscillations happen when the energy from the turbulent convection of the star transfers into energy of global oscillations. The driving mechanism behind the oscillations in the Sun is stochastic, which is why these types of oscillation are often referred to as solar-like oscillations (12).

The solar-like oscillations have a finite mode lifetime and varies from a few minutes to about hundred days. A typical Fourier spectrum for such solar-like oscillations will have peaks corresponding to all the different oscillation modes, but with different amplitudes. This can be helpful in identifying the oscillation modes (12).

2.3.2 Photometric variation in PNNs and white dwarfs

The pulsations seen in PNNs and white dwarfs are generally speaking non-radial g-modes (1). According to the Starrfield et al. (13, 14) the non-radial g-modes are triggered by the κ and γ mechanisms which comes from a cyclical ionization and recombination process of carbon and oxygen. This mechanism happens in the outer layers of hot, hydrogen-deficient white dwarfs, but is also valid for the pulsations in the PNNs. If one considers a scenario where the PNN have episodes with enhanced mass loss that is time dependent, it is plausible that this could explain an irregular change in amplitude of the photometric variation on a time scale of weeks, but not days however (1).

Another possible driving mechanism proposed by Kawaler et al.(15) is the ϵ mechanism where in this case the g-modes are triggered due to a remnant He-burning shell. Here the typical periods of the g-modes are between 70–200 s.

Such rapid changes observed in photometric studies of pulsating PNNs, can be due to intrinsic variations within the star, beating between modes that are close to each other in frequency, but can also be a result of binary system evolution or even a combination of all the above (1).

2.3.3 AM CVn

Another type of object that can be of interest in this thesis is the AM CVn type of stars. AM CVn stars are a type of cataclysmic variables that is believed to be a part of a close binary system with a low-mass semi-degenerate white dwarf that transfers mass to a normal-mass white dwarf via an accretion disc. They have orbital periods in the 5–65 min range (16). Even though the PNNs are not the same as AM CVns, it can be useful to look into the photometric features related to AM CVns as they are thought to be part of a binary system as well with no signs of hydrogen in its disc spectrum (17). Hence there might be similarities between the light curves of AM CVns and of the PNNs that can help in the interpretation of the analysis.

There are mainly three different phases for the AM CVn stars depending on how far it has evolved in time. The phase with the lowest orbital periods (usually less than 20 minutes) is called the high-state phase. In the light curve of such high-state AM CVn stars, one can see low-amplitude photometric variations with various periods. Among these periods you have the orbital period as well as the so-called superhump period. The latter is due to the precessing eccentric accretion disc (18). According to Solheim and Provencal (17) there are several AM CVn stars that show harmonic structures in the Fourier transform of their light curves. The same authors believes there is a relation between the observed harmonic structures and the physical structures in the disc. This can be helpful when analyzing the light curves of the PNNs, as harmonic structures might be an indicator of an accretion disc and hence probably a binary system. At the webpage of "Center for Backyard Astrophysics" (19), one can see the average light curves of AM CV and HP Lib, among others. The pulse shape present evidence of the presence of harmonics.

Also, another interesting observation was made by Solheim et al. (20) as a part of the Whole Earth Telescope (WET) project when doing an extensive photometry series on the AM CVn where they found 5 harmonically related frequencies, but did not detect the fundamental frequency. A possible explanation for this can be that the AM CVn is in a high state phase which means there is a high rate of mass transfer between the binaries that makes the disc strong in brightness. Because of this, the structure of the disc might be dominating.

Chapter 3

Method

3.1 Wavelet transform

Fourier analysis, or Fourier transform (FT), is a very common and useful process when one wants to find the sinusoidal components of a signal. In the case of a light curve from a variable star, the Fourier transform can help to find modulation frequencies and their corresponding power. There are however some limitations to the Fourier analysis, one of which is the assumption that the signal is stationary over time (its properties does not change significantly over time). For the purpose of this master thesis, this limitation is disadvantageous as it is expected that the modulation frequencies to be analyzed do change over time (3).

Wavelet transform (WT) on the other hand is capable to analyze non-stationary signals and to detect changes that occur during a time interval. When using WT on a signal, one obtains information on both time and frequency. For visualizing wavelet coefficients, a scalogram is often used (see fig. 4.2.6). In a scalogram the x-axis is time and the y-axis is frequency/period, while the power is represented by a color scale(3).

The windowed Fourier transform (WFT) is also an option as an analysis tool when looking at non-stationary signals. Here the Fourier transform is performed on a sliding segment of the signal where the segments can be windowed by an arbitrary function ((21) as cited in (22)). Kaiser and Torrence & Compo states that the WFT can be an inefficient tool when having several dominant frequencies present in a signal as the scaling in the WFT is predetermined. The wavelet transform on the other hand is scale independent and hence a better choice of analysis tool.

3.1.1 Morlet Wavelet

There are different types of wavelets; Morlet, Morse and Haar wavelet just to mention a few of them. One of the most common is the Morlet wavelet that represents a sinusoidal function modulated by a Gaussian function and which has equal variance in time and frequency (23). In a comparative analysis of wavelet transforms for time-frequency analysis performed by Silik et al.(23), the authors claims that the real Morlet wavelet provides the maximum information. Such a property is convenient for the purpose of this thesis where one key point is to extract as much information from the wavelet transform (scalogram) as possible.

3.2 Software

The program used to perform the Fourier- and wavelet transform was made in Jupyter notebook in Python code language. The starting point is the differential photometry data from short observing runs dedicated to detecting potential variability in planetary nebula nuclei. The original light curves were reduced by Pérez in his dissertation, using the multi-windowed methodology developed by Østensen (1). In the processing of the original data before applying the FT and WT, the clear outliers were removed and also filtered with a Butterworth high pass filter using the scipy.signal library (see SciPy documentation (24) for more details) with the cutoff frequency set to three times the lowest frequency in the signal. Then, for each data point, the mean value is subtracted so that the resulting light curve oscillates around 0. For the Fourier transform, the fft.rfft function from the numpy library that computes the discrete Fourier transform using the Fast Fourier Transform algorithm was used, as well as the fft.rfftfreq function that returns the discrete Fourier transform sample frequencies (see Numpy documentation (25) for more details). In order to retrieve the proper physical power, the output of the FT must be normalized. For all the PNNs except NGC 246 and RXJ 2117, the normalization argument was set to "ortho" which means that the transform is scaled by $\frac{1}{\sqrt{N}}$ where N is the number of samples. As NGC 246 and RXJ 2117 have considerable higher sample rate compared to the the three other PNNs, the normalization argument was set to "forward" which means that the transform is scaled by $\frac{1}{N}$. With this choice of normalization scaling, the light curve and FT plot shown in this thesis have the same order of magnitude as those presented in Pérez's dissertation. As the fft.rfft function might give a complex output, the absolute value of the output is calculated and used in the frequency spectrum.

For the wavelet transform, the cwt-function from the PyWavelets library was used with logarithmic scales, as suggested by Torrence and Compo (22), and with 1.5 as center frequency and 1.0 as bandwidth frequency (see PyWavelets documentation (26) for more details). Both the scales, center- and bandwidth frequency was chosen based on literature (22, 26) and trial & error method. Here it is assumed that the output from the wavelet transform is normalized with the scale factor of $\frac{1}{\sqrt{N}}$. In the same way as with the FT, the normalization of NGC 246 and RXJ 2117 uses a scale factor of $\frac{1}{N}$. See appendix A.1 for the Python script.

3.3 Synthetic light curves

One way to gain a good comprehension of how the wavelet transform behaves and how it responds to different kinds of signals is to make synthetic light curves where the parameters of the signal are under control, and then perform wavelet transform on it. With this method it is also possible to make synthetic light curves that resembles the type of signal that we expect, for example an AM CVn type of signal. This can help with identifying what kind of properties the signal and thus also the PNN-object itself may have. As mentioned in section 2.3.3, the AM CVn objects might show harmonic structures in the frequency spectrum because of the accretion disc. Therefore it might be useful to have a synthetic light curve with harmonics to see how the resulting scalogram will look like. The light curves of the AM CVn objects AM CV and HP Lib (19) have also been used for inspiration in the construction of the synthetic light curves.

The first scenario for the synthetic light curves is a signal made up of one fundamental frequency and its first and second harmonic, with frequencies set to 1000, 2000 and 3000 µHz, respectively, and intensity to 10, 3 and 2, respectively. The second scenario is similar to the one just mentioned but now with the third and fourth harmonic included as well with frequencies set to 4000 and 5000 µHz, respectively, and intensity set to 1 for both harmonics. By having different intensities one can see how the color in the scalogram changes with the intensity of the modulation signals. See appendix A.2 for the Python script. The third scenario takes inspiration from the AM CV and HP Lib light curves in terms of their pulse shape. See appendix A.3 for the Python script.

The settings used for the FT and the WT for the actual PNNs, as described in section 3.2, are the same ones used here. The Butterworth high pass filter was not applied to the synthetic light curves for scenario 1 and 2 that is shown in section 4.2, but it was applied before doing the FT. The cutoff frequency for the Butterworth high pass filter was set to two times the lowest frequency in the signal. In order for the synthetic light curves to be similar with the actual data from the PNNs, the sample rate for Jn 1 at 0.018 was used with the normalization scaling factor set to $\frac{1}{\sqrt{N}}$.

Chapter 4

Results

4.1 Observations

The observations used in this thesis are taken from the Nordic Optical Telescope with the Andalucia Faint Object Spectrograph and Camera in June 2000 and January 2001. The observers for this campaign were Robert Kamben and Jose M. González Pérez. For more details on the observations and reduction see the dissertation of Pérez (1).

Out of the 11 PNNs that were observed, 4 showed signs of pulsations. These 4 possible pulsators are Jn 1, NGC246, NGC6852 and VV 47. These are the ones that will be analyzed in this thesis in addition to RXJ 2117, which was also part of the campaign, but whose light curve and frequency spectrum was not included in the dissertation. The observed objects are all PNNs that are believed to be part of binary system evolution due to their lack of hydrogen and the bipolar shape of their nebula. This may indicate that the PNN have a close companion and previous interaction between the two (1).

The upcoming subchapters will show the light curve, the frequency spectrum (Fourier transform) and the scalogram (wavelet transform using the Morlet wavelet) of the 5 PNNs. The dashed red line in the frequency spectrum (as seen in the lower panel of fig. 4.2.4) marks the limit corresponding to the false alarm probability (FAP) set to 1/12 (for further explanation about FAP, see (1)). This means that if a peak in the frequency spectrum is above this limit of confidence, it has less than 1/12 percent chance to be due to noise. This is a rather relaxed criterium, but for the purpose of this thesis, which is not to conclude whether the PNNs are variable stars or not, but to look after features in the scalograms that might be hidden in the Fourier transform, this criterium is considered adequate by this author. Also, for the PNNs it is expected to see low-amplitude pulsations thus it is beneficial to have a more relaxed criterium so the low-amplitude peaks are not cut out because of a too high limit of confidence.

The y-axis in the light curve (as seen in the upper panel of fig. 4.2.4) shows the modulation intensity in mmi (milli modulation intensity), while the y-axis in the frequency spectrum as well as the colorbar of the scalogram shows modulation power in μmp (micro modulation power). The light curve and the frequency spectrum are shown separately, while the scalogram is shown together with the frequency spectrum (as seen in fig. 4.2.6a) with shared y-axis to make it easier to compare those two. The unit for the x-axis of the separate frequency spectrum is frequency, while the unit of the shared axis between the scalogram and the frequency spectrum is converted to periods. As the Nyquist frequency is the highest frequency that can be represented from a sampled signal without aliasing (27), the frequencies in the FT are shown up to the Nyquist frequency. The same max value goes for the corresponding periods shown in the combined scalogram and FT figure.

There is also a table for each PNN that shows both the dominating modulation periods from the scalogram (relative to all the modulation signals shown in the scalogram) and where in time during the observation run they present relevant power. The former indicates the areas of periods where power exists during the observation run. Due to the short runs, relatively low sample rate and the choice of wavelet, it is not possible to say what the exact modulation period is. That is why the third column from the left in the table shows an interval of periods and not an exact number. Both values, shown in the third and fourth column of the table, are read directly from the scalogram based on the color and the values are therefore approximate.

Before looking at the PNNs, the results of the synthetic light curves with corresponding scalogram and frequency spectrum will be presented. All of these plots have the same units as mentioned above and the frequencies in the FT are only shown up until the Nyquist frequency here as well.

4.2 Synthetic light curves

The synthetic light curve from the first scenario mentioned in section 3.3 is shown in the middle panel of fig. 4.2.1. The lower panel in fig. 4.2.1 shows the corresponding scalogram and frequency spectrum while the upper panel shows the three individual harmonics in different colors.

The wavelet transform clearly detects the amplitude differences between the harmonics as can be seen from the scalogram with the clear yellow/green color for the fundamental frequency and the more diffuse blue/green color for the first and second harmonic. One can also see from the scalogram that the period intervals are quite broad. This is most likely due to the limitations of the Morlet wavelet in terms of resolution in combination with the fact that the run is rather short with relatively low sample rate.

In the middle of the run, around 1000 s, corresponding to one cycle for the fundamental frequency signal, weak blue/green colors appear in between the period intervals from the harmonics. The same feature appears at the beginning and at the end of the run, but mainly between the first and second harmonic modulation periods. As the synthetic signal was made with only three harmonics, these weak blue/green period interval in between the harmonics cannot be real, but might be an effect of the beating between the real modes or an artifact of the wavelet analysis because the end of the light curve do not go towards zero.

The amplitudes seems to be decreasing towards the far left and right side of the scalogram. The actual harmonic signals have the same amplitudes for the whole run, so this observation is not a result of a physical change in the amplitudes during the run. Due to the fact that it is a start and end to the observation run and hence also the signal, the wavelet transform probably interprets this as a decrease in power.

The second scenario synthetic light curve is shown in the middle panel of fig. 4.2.2, and the lower panel shows the corresponding scalogram and frequency spectrum. The upper panel shows the five individual harmonic signals in different colors.

The scalogram for the second scenario shows many of the same features as discussed for the first scenario. One can also see that the third and fourth harmonic, which have the lowest amplitudes, are difficult to detect in the scalogram.

The synthetic light curve with the pulse shape from the third scenario can be seen in the upper panel of fig. 4.2.3, and the scalogram and frequency spectrum are shown in the lower panel. The scalogram for the third scenario also have some of the same features as seen from both the first and second scenario, which makes sense as the 10 and 20 s period are harmonically related. In addition one can see in the scalogram a trail of power with periods from 200 s and up to 10 at the middle of the run. This is probably due to the negative peak that appear about 24 s after the run has started.

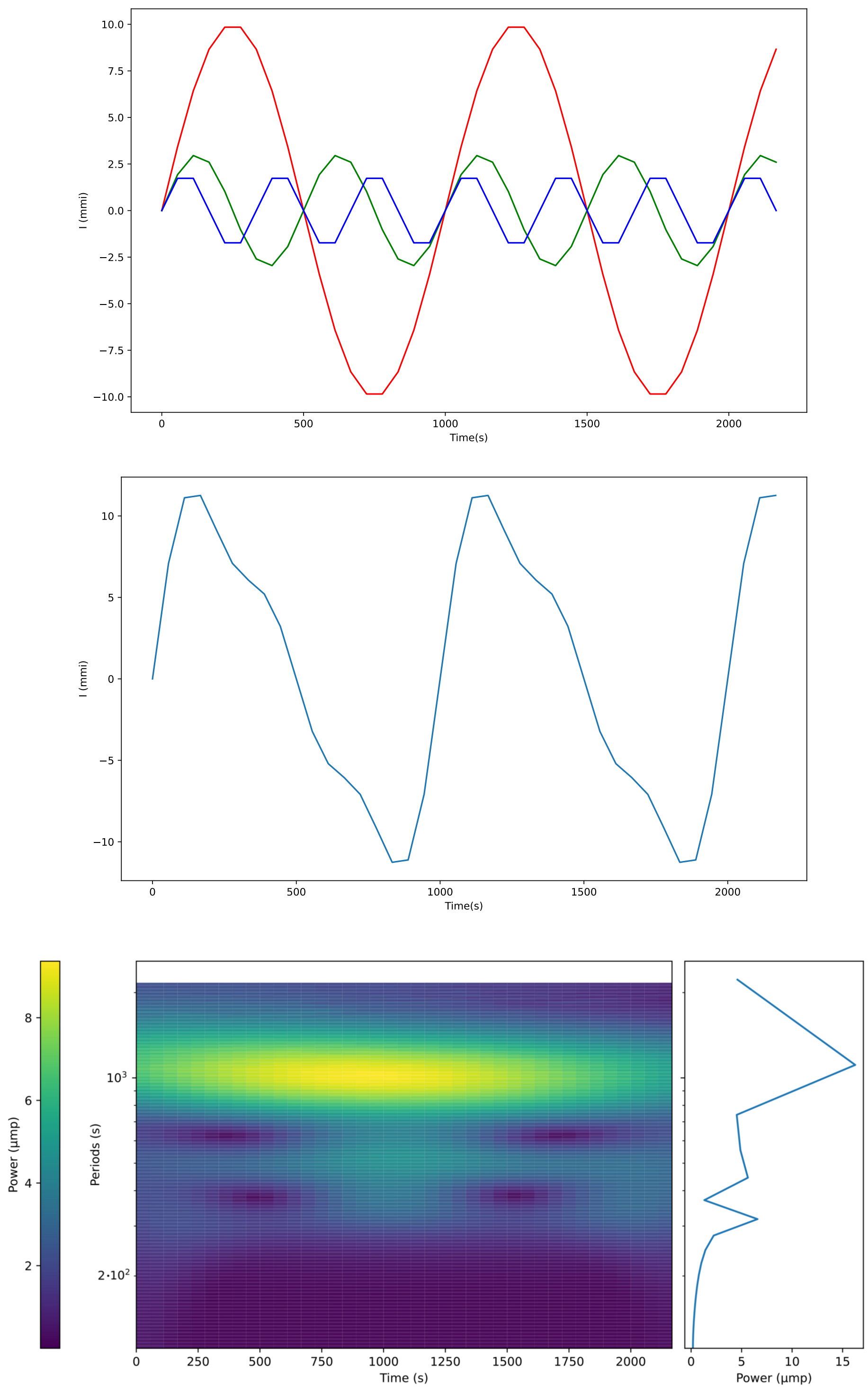

Figure 4.2.1: First scenario: the upper panel shows the three separate harmonics (the red, green and blue are the fundamental frequency, the first and second harmonic, respectively), while the panel in the middle shows the synthetic light curve. The lower panel shows the scalogram and frequency spectrum.

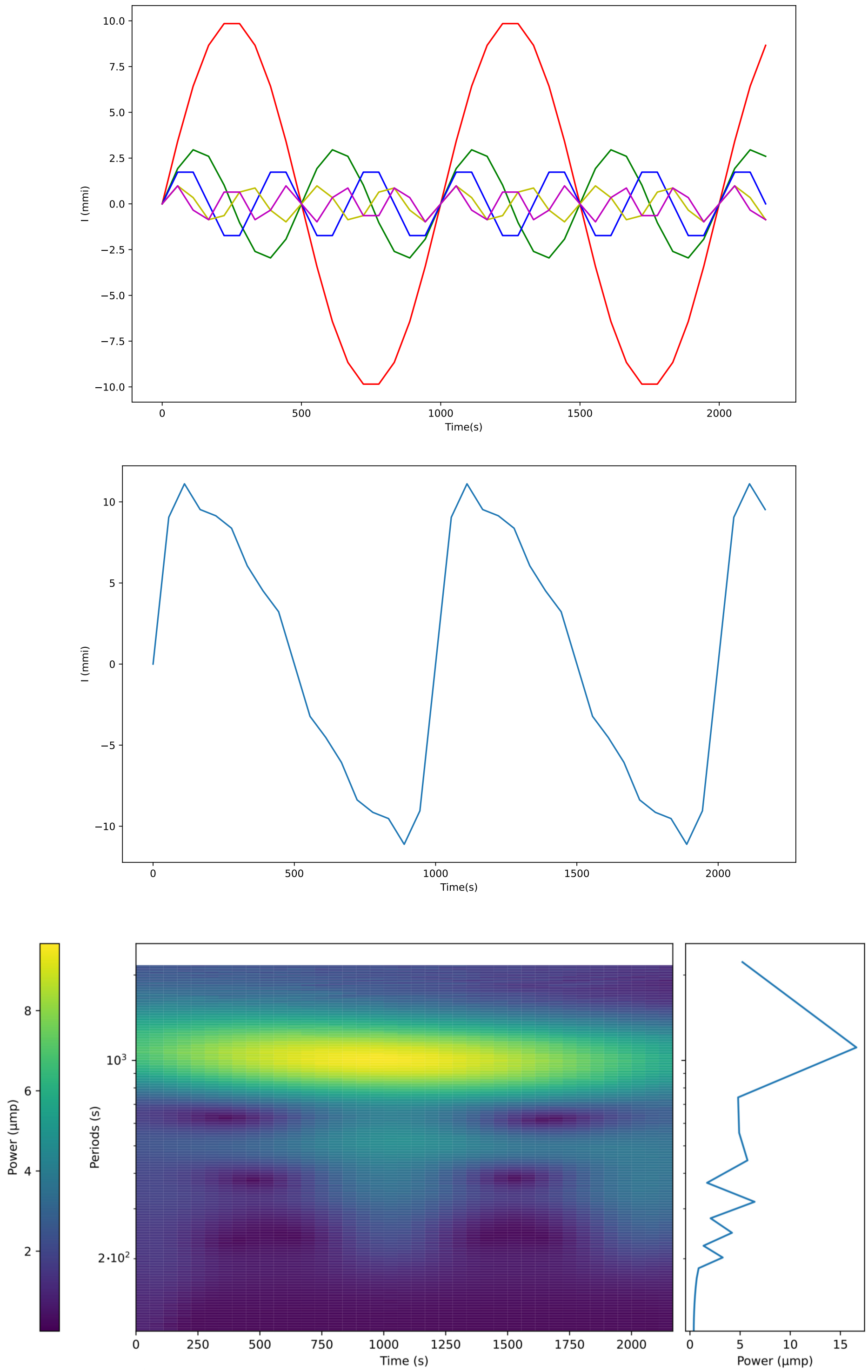

Figure 4.2.2: Second scenario: the upper panel shows the five separate harmonics (the red, green, blue, yellow and magenta are the fundamental frequency and first to fourth harmonic, respectively), while the panel in the middle shows the synthetic light curve. The lower panel shows the scalogram and frequency spectrum.

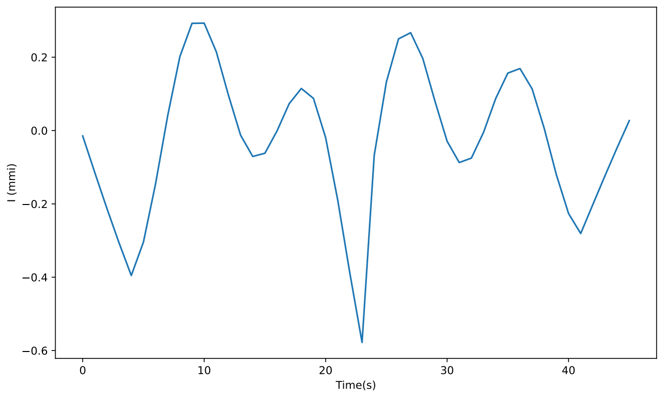

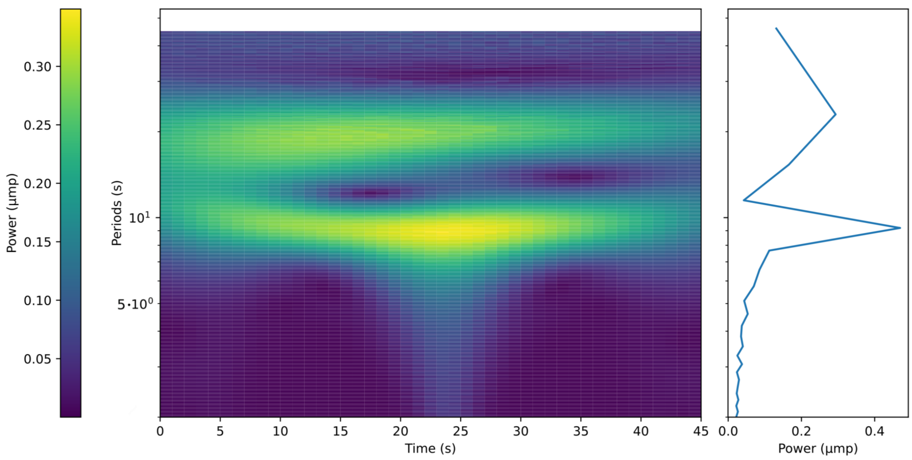

Figure 4.2.3: Third scenario: the upper panels shows the synthetic light curve and the lower panel the scalogram and frequency spectrum.

4.2.1 Jn 1

Figure 4.2.4 and fig. 4.2.5 show the light curve and the corresponding FT plot for the first and second run respectively of the PNN Jn 1. The first run was taken at July 19, 2000, while the second run was taken four days later, on July 23. Figure 4.2.6a and fig. 4.2.6b shows the scalogram together with the frequency spectrum for the first and second run, respectively, of Jn 1. Table 4.2.1 shows the overview of the dominant modulation periods from the wavelet analysis and where in time they appear during the observation run.

Table 4.2.1: Overview of the detected frequencies for Jn 1. The third column from the right shows period intervals from the scalogram represented with a **P**, while the fourth column shows where in time the corresponding modulation signal have relative high power represented with a **T**. The number in brackets in the second column is the length of the run.

Object	**Observation run**	**P**	**T**
JN1	First run	150–300 s	0–500, 2250–2750 s
	[3416 s]	700–1000 s	0–2000 s
	Second run	300–400 s	2000–2500, 3000–3500 s
	[4165 s]	400–500 s	2000–2500, 3400–4000 s
		500–600 s	500–1500 s

During the first run there are two dominant signals, one ranging in between 150–300 s and the other between 700–1000 s. The former seems to be recurring during this short run (approximately 1 hour), albeit with less power in the beginning of the run, while the latter signal only appear at the beginning of the run. In the second run there are three dominant signals with periods ranging in between 300–400 s, 400–500 s and 500–600 s. The two former signals seems to be recurring, but in the scalogram it looks like they are blending into each other. This might be due to beating between the present frequencies. Also, another interesting observation is the weak signal with the period interval between 900–1500 s which might be the same signal as the one in the first run, but now with less power. This signal looks quite narrow and weak in the beginning of the second run and then evolves to a stronger signal with a wider period interval. The 150–300 s signal from the first run might also be present in the second run, but with less power here as well. The dominant periods (or frequencies) might be harmonically related as seen from the values in the table 4.2.1. However, since these are broad period intervals, this relationship is not conclusive.

4.2.2 NGC 246

Figure 4.2.7 and fig. 4.2.8 shows the light curve and the corresponding FT plot for the first and second run respectively of NGC 246. The first run was taken on July 21, 2000, while the second run was taken three days later, on July 24. Figure 4.2.9a

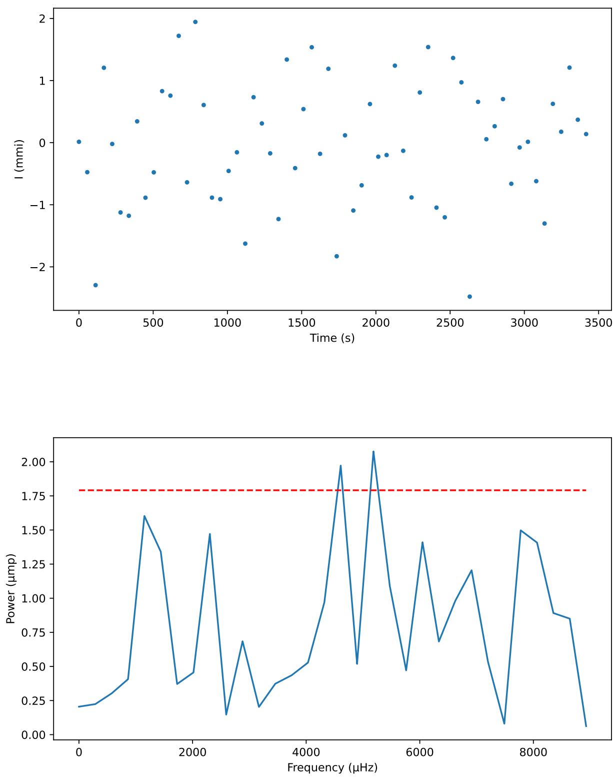

Figure 4.2.4: Jn 1: the upper plot shows the light curve, while the lower one shows the corresponding FT plot for the first run of Jn 1.

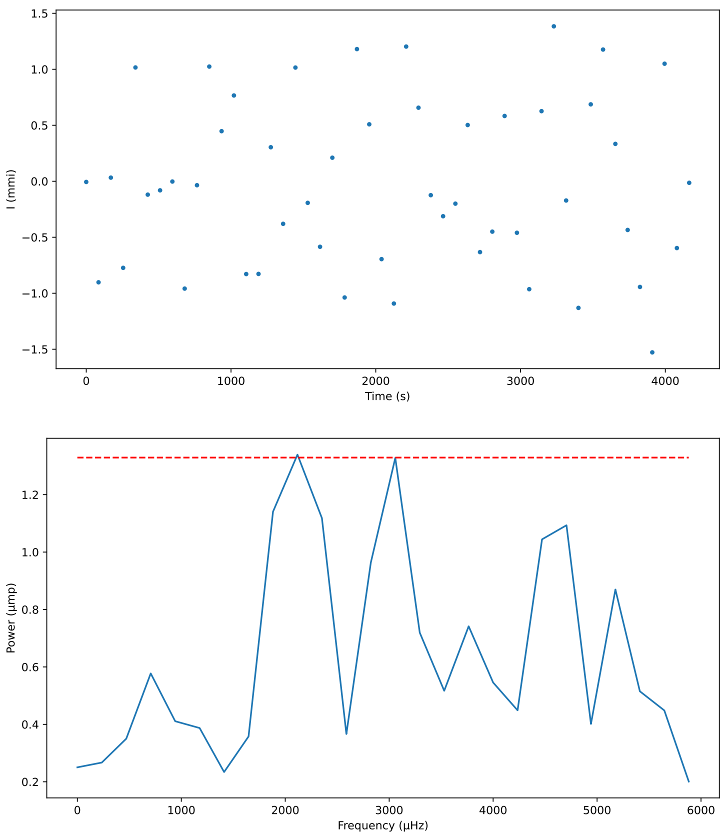

Figure 4.2.5: Jn 1: the upper plot shows the light curve, while the lower one shows the corresponding FT plot for the second run of Jn 1.

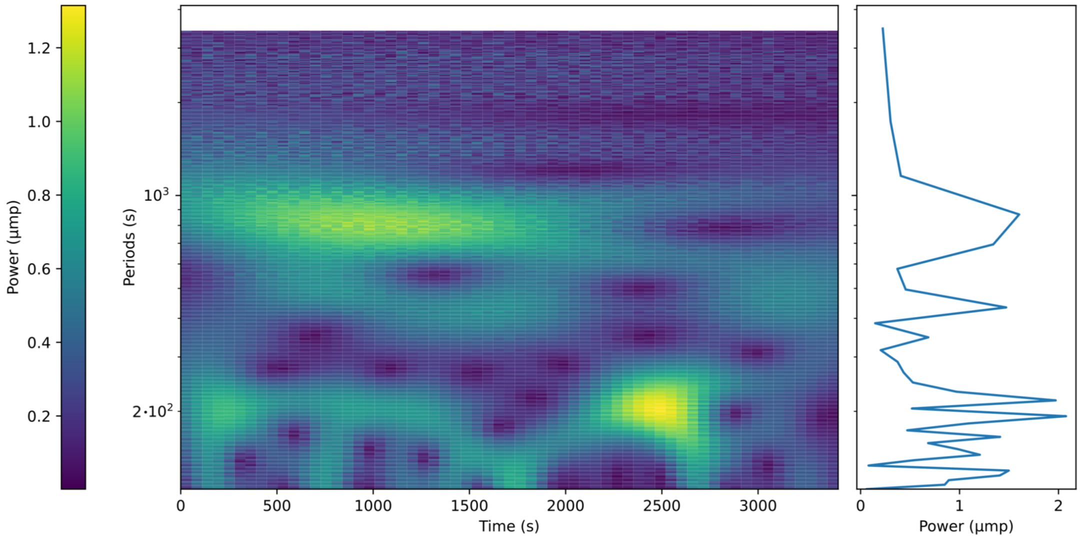

(a) Jn 1: scalogram and FT plot combined from first run

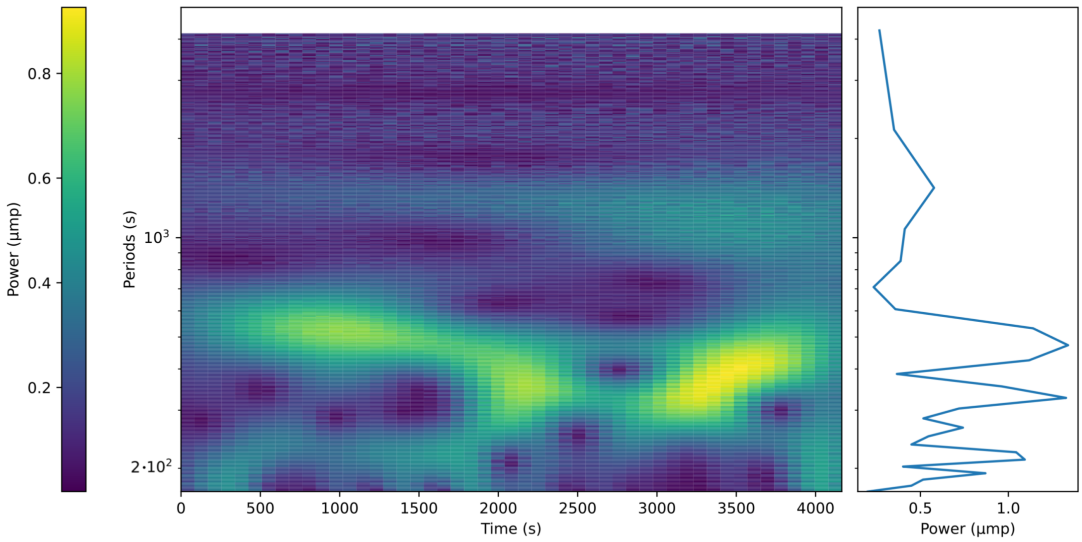

(b) Jn 1: scalogram and FT plot combined from second run

Figure 4.2.6: Jn 1: Scalogram combined with FT plot for first and second observation run.

and fig. 4.2.9b shows the scalogram together with the frequency spectrum for the first and second run, respectively. Table 4.2.2 shows the overview of the dominant modulation periods from the wavelet analysis and where in time they appear during the observation run.

For the first run of NGC 246 it seems to be a rather continuous signal with a period interval ranging between 1500–2500 s, although it looks like that the power of the signal in the middle and towards the end of the run is higher than in the beginning of the run. The second run shows some of the same features with a dominant signal with a period interval ranging in between 1500–2000 s, but here the signal is almost vanished in the beginning of the run.

Table 4.2.2: Overview of the detected frequencies for NGC 246. The third column from the right shows period intervals from the scalogram represented with a **P**, while the fourth column shows where in time the corresponding modulation signal have relative high power represented with a **T**. The number in brackets in the second column is the length of the run.

Object	**Observation run**	**P**	**T**
NGC246	First run [7359 s]	1500–2500 s	2500–6500 s
	Second run [11664 s]	1500–2000 s	6000–10500 s

4.2.3 NGC 6852

Figure 4.2.10 and fig. 4.2.11 show the light curve and the corresponding FT plot for the first and second run respectively of NGC 6852. The first run was taken on July 22, 2000, while the second run was taken the day after on July 23. Figure 4.2.12a and fig. 4.2.12b show the scalogram together with the frequency spectrum for the first and second run, respectively, of NGC 6852. Table 4.2.3 shows the overview of the dominant modulation periods from the wavelet analysis and when in time they appear during the observation run.

In the first run of NGC 6852 there are several dominant signals with period intervals ranging in between 2000–3000 s, 3000–5000 s and 5000–8000 s. The latter appears to be continuous with a rather stable power during the whole run. The second one is starting to increase in power at the middle of the run and blends with the former signal both in the beginning and at the end of the run. The 2000–3000 s signal is strongest at the beginning and at the end of the run, while almost negligible in the middle section of the run. Same as with Jn 1, the dominant periods (or frequencies) might be harmonically related as seen from the values in the table 4.2.3. In the second run there are also several significant signals. One of the signals is recurring with a period interval ranging in between 365–500 s that repeats two times during the run. There is another signal with only a slightly higher period interval, 500–600 s, that only appears toward the end of the run. The signal with the period interval 1000–2500 s appears around 3000s after the

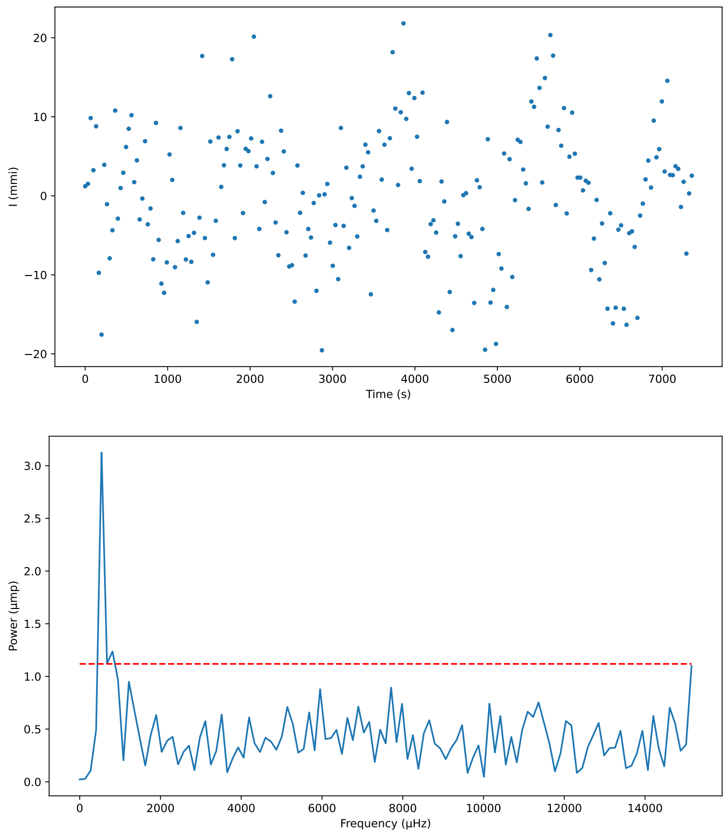

Figure 4.2.7: NGC 246: the upper plot shows the light curve, while the lower one shows the corresponding FT plot for the first run of NGC 246.

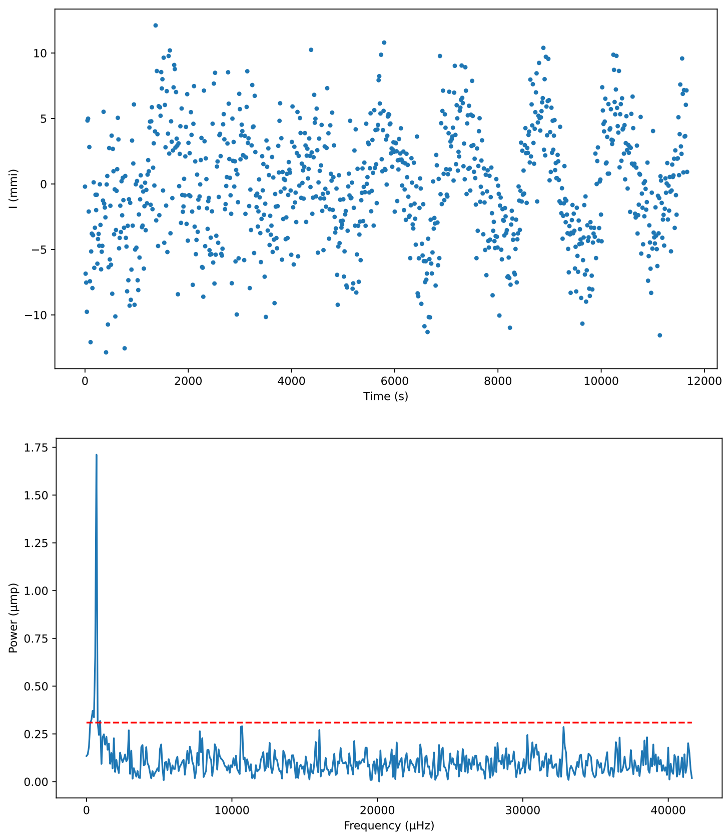

Figure 4.2.8: NGC 246: the upper plot shows the light curve, while the lower one shows the corresponding FT plot for the second run of NGC 246.

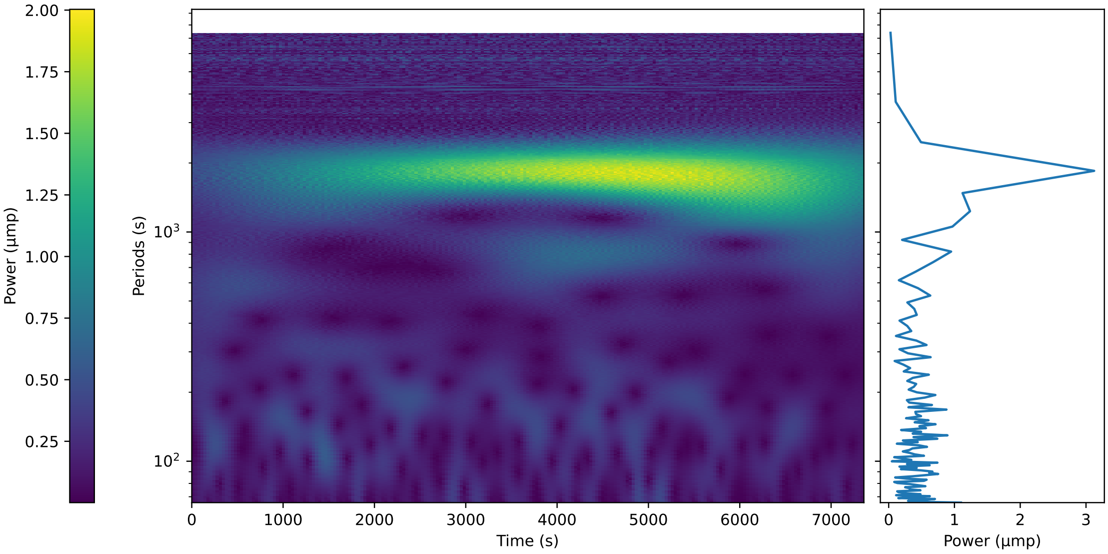

(a) NGC 246: scalogram and FT plot combined from first run

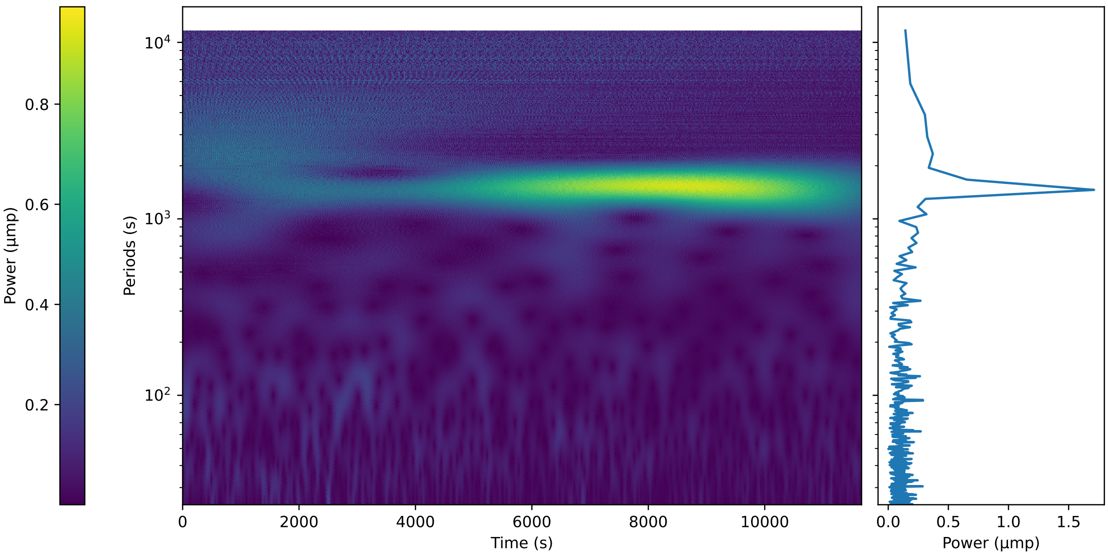

(b) NGC 246: scalogram and FT plot combined from second run

Figure 4.2.9: NGC 246: Scalogram combined with FT plot for first and second observation run.

run has started. This signal might actually be divided into three different signals as they seem to separate from each other in the beginning of the run until 3000 s into the run, then blend together until about 6000 s after the run started and then separate from each other again. Finally there is a signal with the period interval 3000–4000 s that seems to be rather continuous during the whole run except maybe at the very end of the run, and it increases in power towards the middle of the run about 6000 s after the run started. Overall there are many weak signals scattered all over the scalogram of the second run.

Table 4.2.3: Overview of the detected frequencies for NGC 6852. The third column from the right shows period intervals from the scalogram represented with a **P**, while the fourth column shows where in time the corresponding modulation signal have relative high power represented with a **T**. The number in brackets in the second column is the length of the run.

Object	**Observation run**	**P**	**T**
NGC 6852	First run	2000–3000 s	2000–4000 s
	[18000 s]	3000–5000s s	8000–14000 s
		5000–8000 s	0–18000 s
	Second run	365–500 s	3000–3500 s, 6500–7000 s
	[11700 s]	1000–2500 s	3000–6000 s
		3000–4000 s	0–9000 s

4.2.4 VV 47

Figure 4.2.13, fig. 4.2.14, fig. 4.2.15 and fig. 4.2.16 show the light curve and the corresponding FT plot for the first, second, third and fourth run respectively of VV 47. The first and second run are both taken at Jan 16, 2001. The first run was observed in the morning and the second run in the evening. The third and fourth run were taken the day after, on Jan 17, with the third run in the morning and the fourth run in the evening. Figure 4.2.17a, fig. 4.2.17b, fig. 4.2.17c and fig. 4.2.17d show the scalogram together with the frequency spectrum for the first, second, third and fourth run, respectively. Table 4.2.4 shows the overview of the dominant modulation periods from the wavelet analysis and where in time they appear during the observation run.

The first and fourth run of VV 47 do not show any significant dominant signals. The second and third run however, seems to have several dominant signals. For both of the last mentioned runs, it is quite hard to distinguish between the different individual signals as they appear to blend into each other during the run and then separate. Even so, for the second run one might distinguish the signals into two dominant signals with period intervals ranging in between 2000–3500 s and 4000–6000 s. Both signals seems to be recurring, or at least they have varying power during the run so they appear to be recurring, and they might also be harmonically related. During the third run one might distinguish the dominant signals into

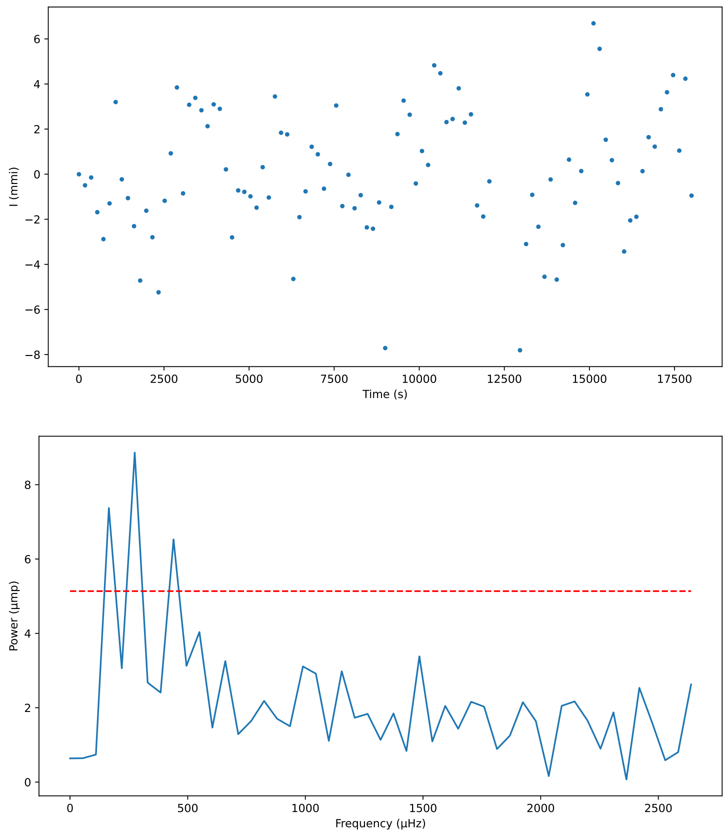

Figure 4.2.10: NGC 6852: the upper plot shows the light curve, while the lower one shows the corresponding FT plot for the first run of NGC 6852.

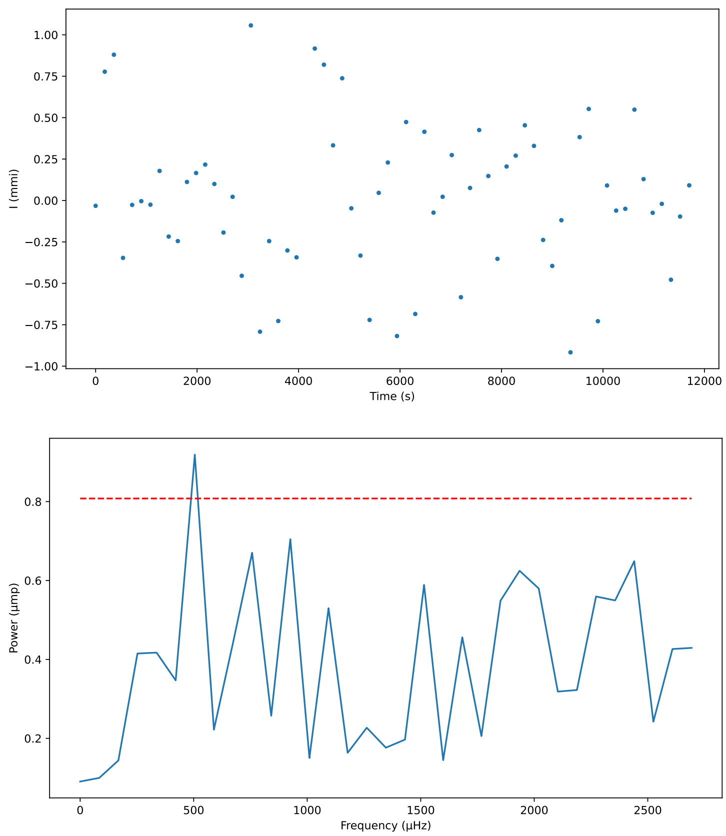

Figure 4.2.11: NGC 6852: the upper plot shows the light curve, while the lower one shows the corresponding FT plot for the second run of NGC 6852.

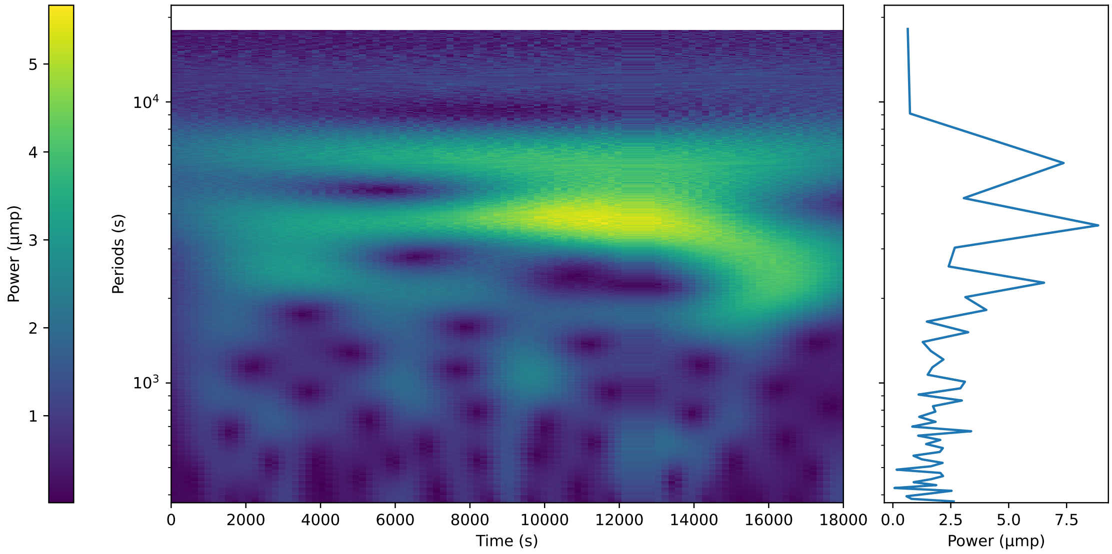

(a) NGC 6852: scalogram and FT plot combined from first run

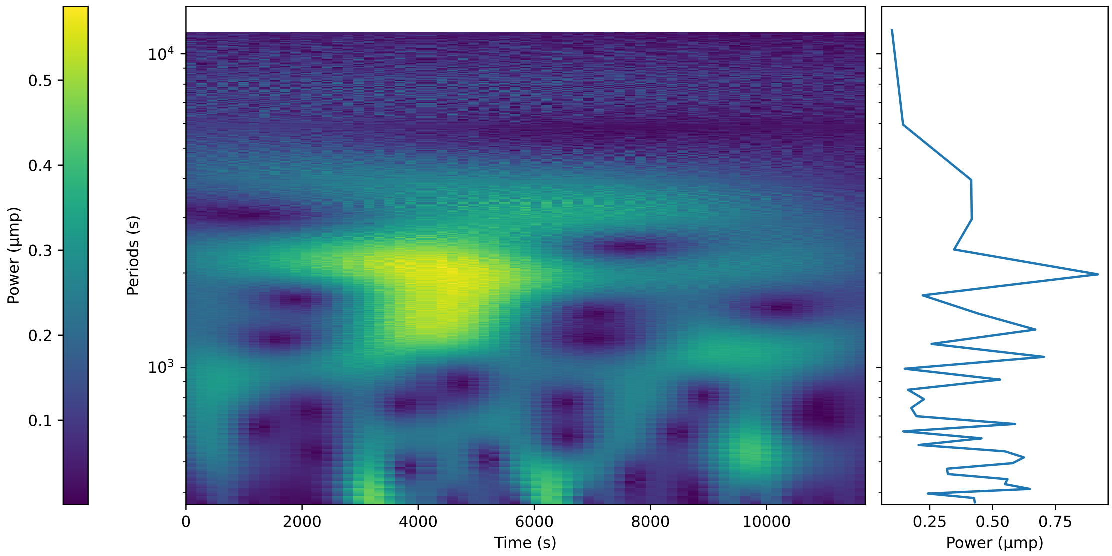

(b) NGC 6852: scalogram and FT plot combined from second run

Figure 4.2.12: NGC 6852: Scalogram combined with FT plot for first and second observation run.

4 different ones with period intervals ranging in between 200–300 s, 400–600 s, 600–900 s and 1500–2000 s. These signals have in general lower period (higher frequency) intervals than the ones shown in the second run. The modulation signal with lowest period interval (200–300 s) seems to be recurring and have a clear stronger power in the beginning of the run. The 400–600 s signal might be repeating twice during the run with less power the first time than the second time. However, it is hard to conclude as it is blended with the 600–900 s in the beginning of the run. The last dominant signal (1500–2000 s) seems to be continuous during the whole run, but is increasing in power towards the end of the run.

Table 4.2.4: Overview of the detected frequencies for VV 47. The third column from the right shows period intervals from the scalogram represented with a **P**, while the fourth column shows where in time the corresponding modulation signal have relative high power represented with a **T**. The number in brackets in the second column is the length of the run.

Object	**Observation run**	**P**	**T**
VV 47	First run	None	
	[20820 s]		
	Second run	2000–3500 s	8000–17000 s, 19000–22560 s
	[22560 s]	4000–6000 s	0–6000 s, 18000–22560 s
	Third run	200–300 s	500–1000 s, 2400–2600 s,
			3100–3600 s, 4500–5300 s
	[6300 s]	400–600 s	500–1400 s, 3600–4500 s
		600–900 s	300–1500
		1500–2000 s	0–6300 s
	Fourth run	None	
	[30240 s]		

4.2.5 RXJ 2117

Figure 4.2.18 shows the light curve and the corresponding FT plot for RXJ 2117. The observation run was taken at Jul 21, 2000. Figure 4.2.19 shows the scalogram together with the frequency spectrum for RXJ 2117. Table 4.2.5 shows the overview of the dominant modulation periods from the wavelet analysis and where in time they appear during the observation run.

The observation run of RXJ 2117 presents three dominant signals with period intervals ranging in between 700–1000 s, 1000–1500 s and 1500–2000 s. In a similar way as some of the other PNNs, the three signals appears to blending into each other during the run. The strongest signal is the one with lowest period interval

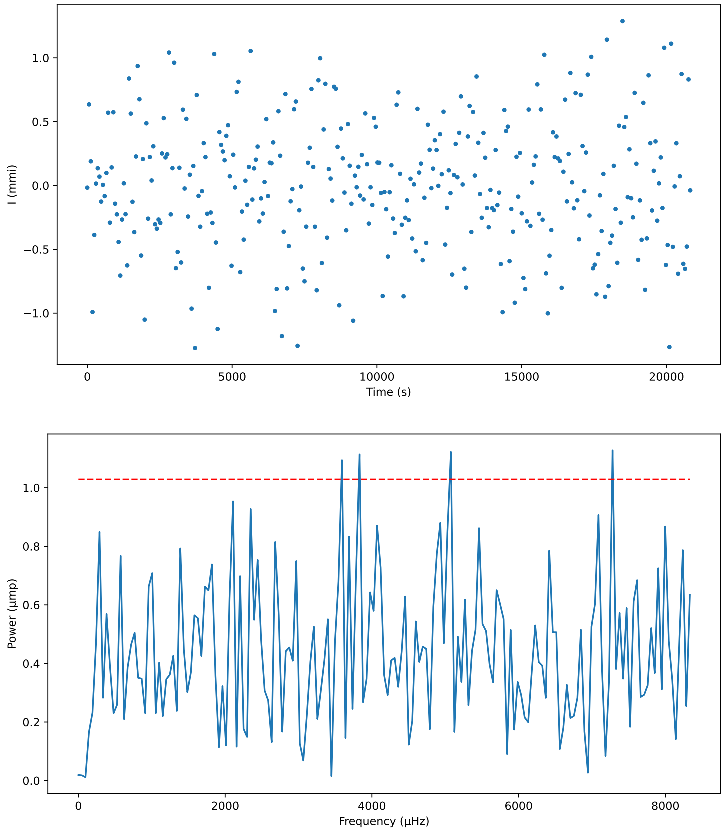

Figure 4.2.13: VV 47: the upper plot shows the light curve, while the lower one shows the corresponding FT plot for the first run of VV 47.

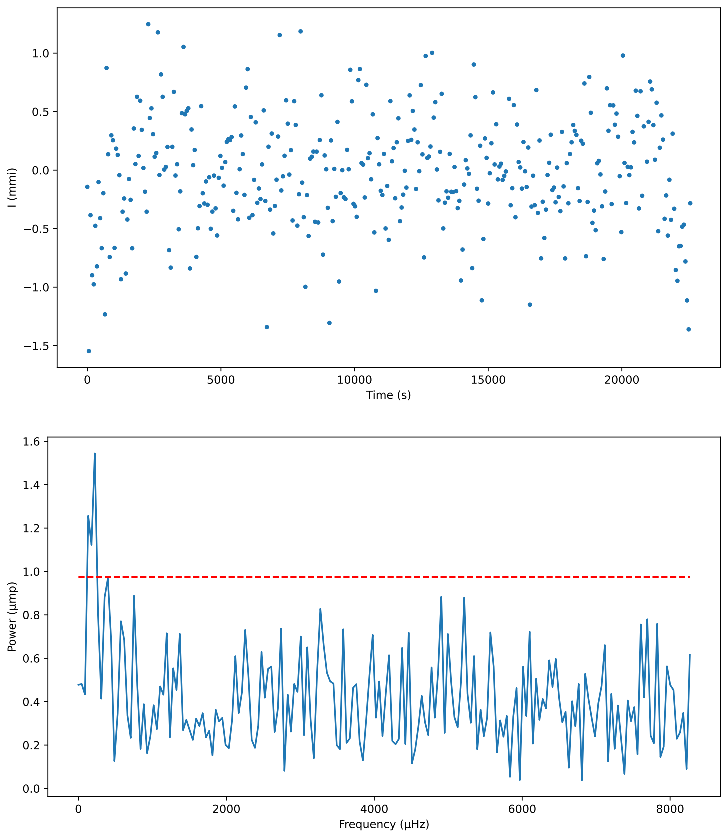

Figure 4.2.14: VV 47: the upper plot shows the light curve, while the lower one shows the corresponding FT plot for the second run of VV 47.

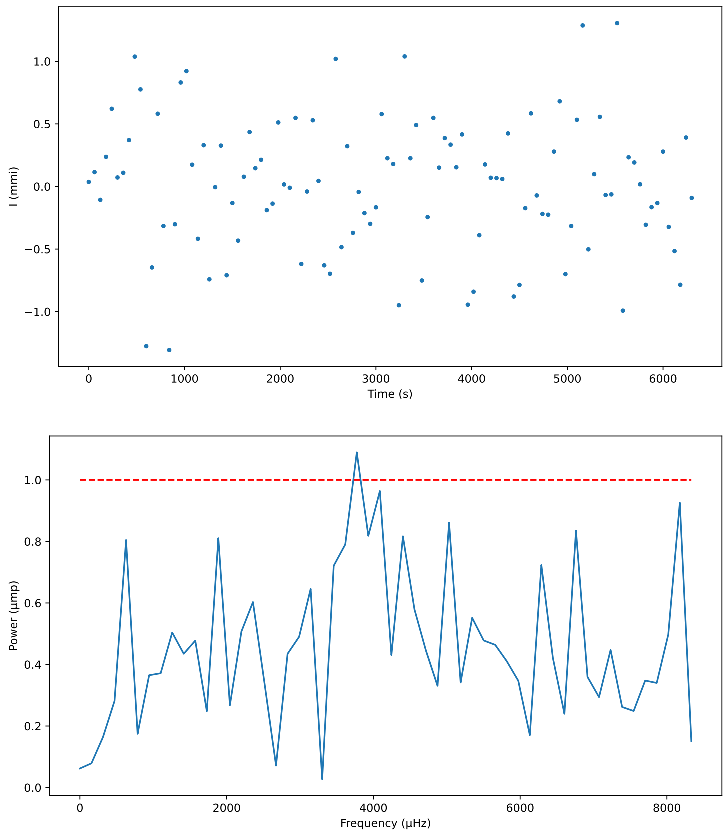

Figure 4.2.15: VV 47: the upper plot shows the light curve, while the lower one shows the corresponding FT plot for the third run of VV 47.

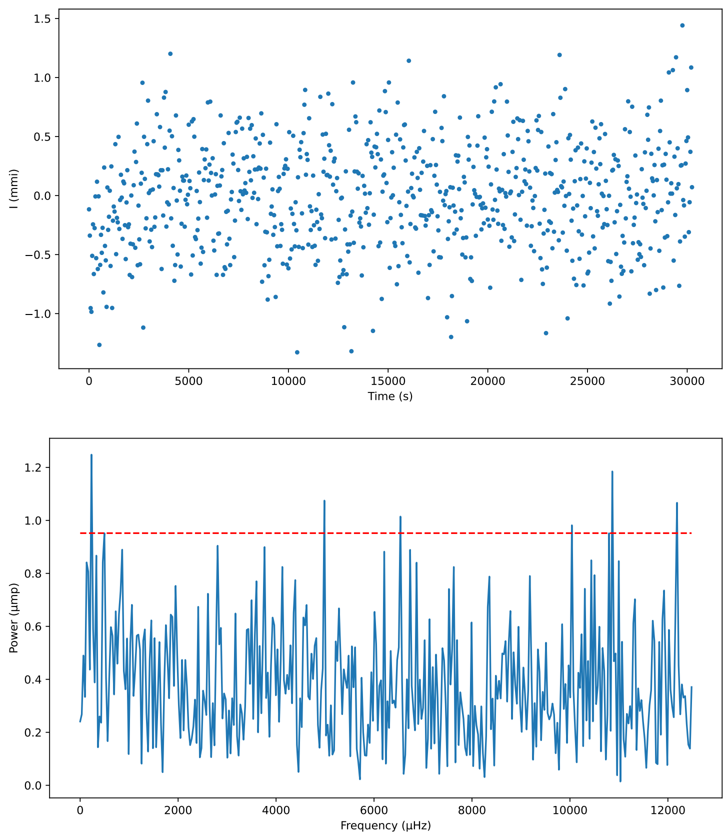

Figure 4.2.16: VV 47: the upper plot shows the light curve, while the lower one shows the corresponding FT plot for the fourth run of VV 47.

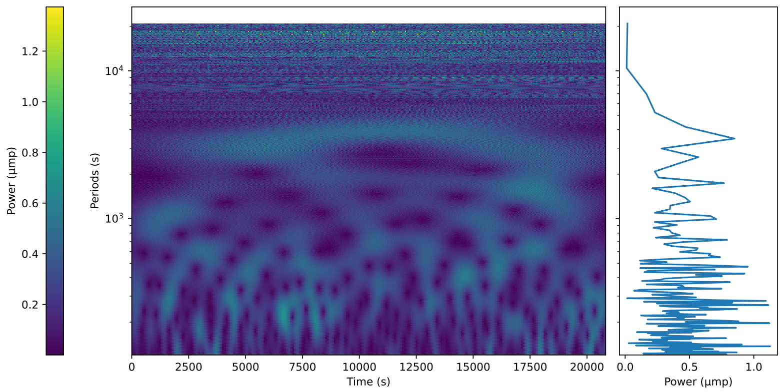

(a) VV 47: scalogram and FT plot combined from first run

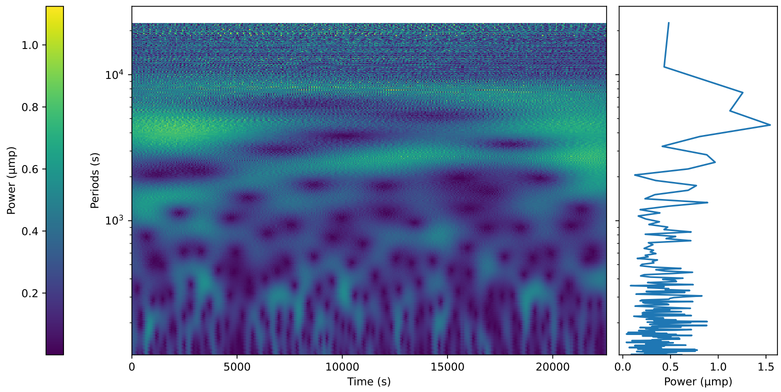

(b) VV 47: scalogram and FT plot combined from second run

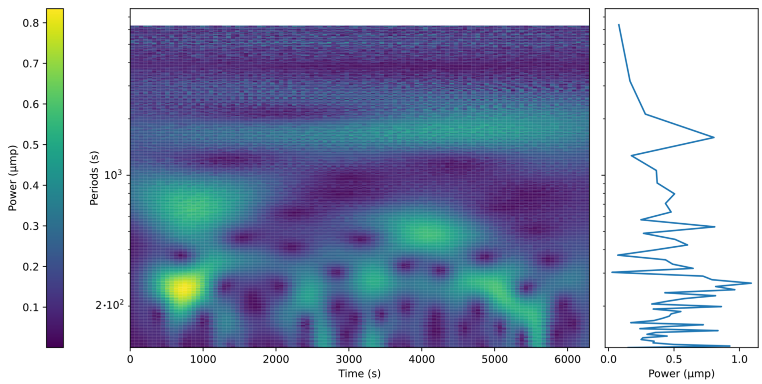

(c) VV 47: scalogram and FT plot combined from third run

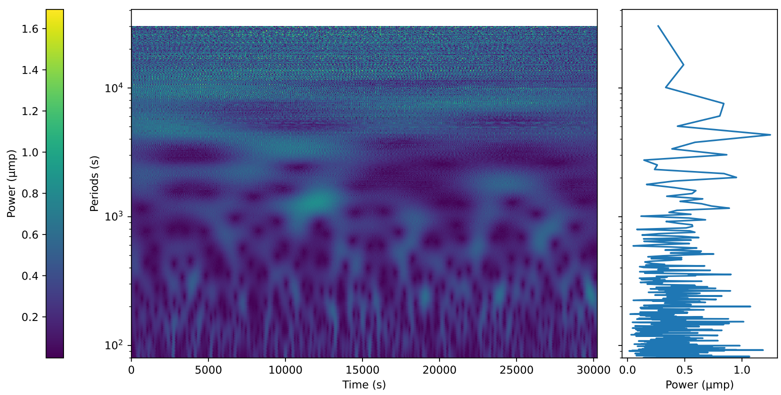

(d) VV 47: scalogram and FT plot combined from fourth run

Figure 4.2.17: VV 47: Scalogram combined with FT plot for first, second, third and fourth observation run.

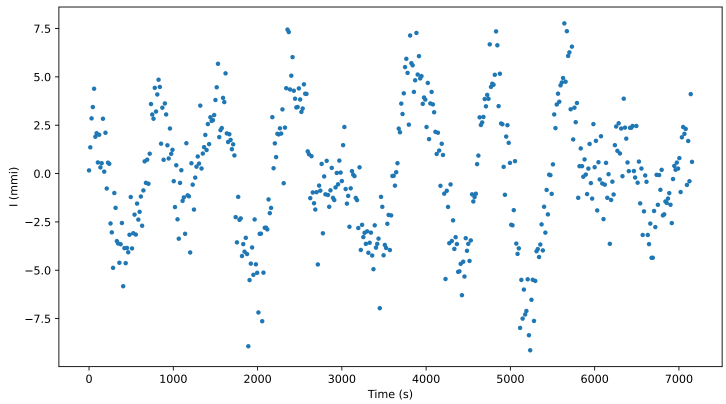

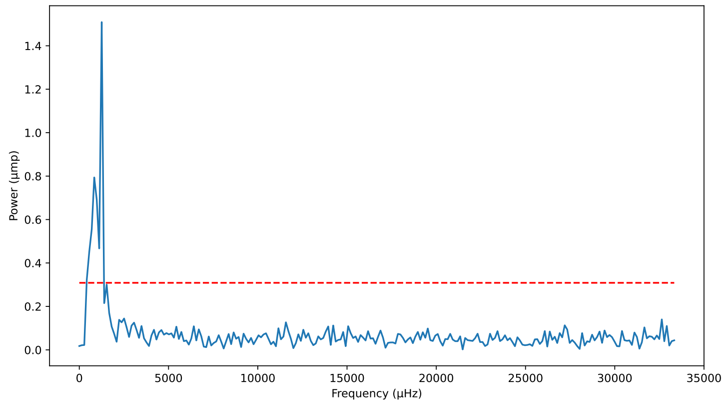

Figure 4.2.18: RXJ 2117: the upper plot shows the light curve, while the lower one shows the corresponding FT plot of RXJ 2117.

(700–1000 s) that repeats two times. The second occurrence shows a strong yellow color (high power of the signal).

Table 4.2.5: Overview of the detected frequencies for RXJ 2117. The third column from the right shows period intervals from the scalogram represented with a **P**, while the fourth column shows where in time the corresponding modulation signal have relative high power represented with a **T**. The number in brackets in the second column is the length of the run.

Object	**Observation run**	**P**	**T**
RXJ 2117	Only run	700–1000 s	500–2500 s, 4000–6000 s
	[7155 s]	1000–1500 s	1000–3500 s
		1500–2000 s	4000–6000 s

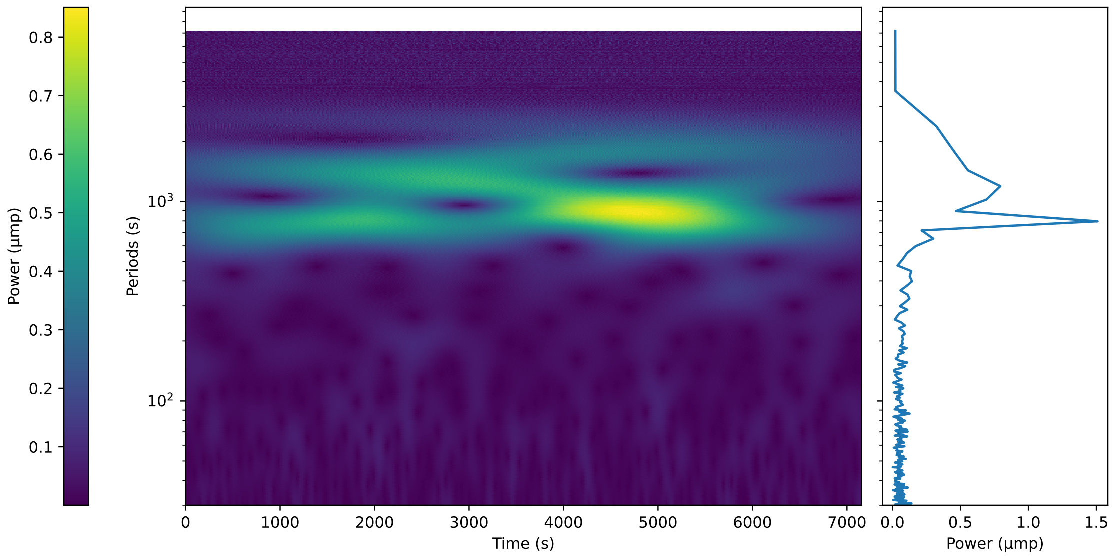

Figure 4.2.19: RXJ 2117: scalogram and FT plot combined

Chapter 5

Discussion

5.1 Jn 1

As seen in section 4.2.1 there are some modulation signals of interest shown in the scalogram of Jn 1. There seems to be rapid photometric variations for Jn 1 with modulation signals coming and going during both runs. As mentioned in section 2.3.2, this can be due to intrinsic pulsations of the star, beating between modes that are closely spaced in frequency, binary system interaction or a combination between these.

It is hard to say what the exact scenario for Jn 1 is with the scalograms available as they show complex photometric variations. However, the properties of the modulation signals observed in the scalograms can give some indication of what is going on. First of all, as mentioned in section 4.2.1, in the second run there are modulation signals that might be harmonically related, which can be an indicator of a binary system. As the modulation periods cannot be decided exactly with such short observation runs and relatively low sample rate, one cannot claim that this harmonic relation is a fact, but it is however a possibility.

Solheim et al. made an overview of the detected peaks in their frequency spectrum when observing AM CVn in a WET run during March/April 1990 (20, p. 946). The peaks with periods equal to 525.618, 350.407, 262.799 s, 210.244 s and 175.200 s was believed to be the first, second, third, fourth and fifth harmonic respectively. The period related to the fundamental frequency was 1028.48 s, but this was not detected in their frequency spectrum. If comparing the peaks detected by Solheim et al. with our dominating modulation signals, one can see that the first and second harmonic from the WET run are within the period intervals for the dominating modulation signals in the second run. The third, fourth and fifth harmonic from the WET run have periods lower than 300 s which is not the case for the dominating modulation signals from the second run. However, there are some weak modulation signals occurring at the bottom of the scalogram with periods less than 300 s that is comparable to the periods of the third, fourth and fifth harmonic from the WET run. Furthermore, in the first run, the modulation signal with the period interval of 150–300 s overlaps with the the third, fourth and fifth harmonic from the WET run. The period related to the fundamental frequency at 1028.48 s from the WET run is rather close to the 700–1000 s modulation signal from the first run, and in the second run there is a weak modulation signal that appears towards the end of the run that also looks like it may overlap with the

1028.48 s period. In other words, the dominating modulation signals or peaks in the scalogram of Jn 1 are comparable to the peaks from the AM CVn observation campaign. This might indicate that the Jn 1 is in fact a part of a binary system with an accretion disc which is the case of the AM CVn.

The fact that the modulation signals are coming and going during each individual run, and also that the overall modulation signals from the first run are somewhat different from the second run, may indicate highly dynamic processes. A possible scenario here could be that the first run shows modulation signals related to the intrinsic variations of the PNN while the second run shows modulation signals that relates to the interaction with the binary companion through the disc. Solheim et al. suggest that the peak they detected at 988.8 µHz with the corresponding period of 1011 second could be a g-mode pulsation. This period of 1011 second is comparable to the 700–1000 s modulation period interval found in the first run.

Considering the fact that the detected modulation frequencies has such low amplitude and power, it is a possibility that several modulation signals discussed above are not real. This argument goes for all the PNNs in this thesis as they show low amplitude variations. But as mentioned previously, the motivation for this thesis is not to conclude that the PNN is in fact variable, but to see if there are features in the scalograms in particular that should be investigated further with longer observation runs. Some of these key features may be hidden in the static FT. In this regard, Jn 1 is definitely of interest as there are several modulation frequencies in the scalogram that changes rapidly during the observation runs.

5.2 NGC 246

The scalograms of NGC 246 show mainly two modulation signals of interest as seen in section 4.2.2. The two period ranges have an overlap between 1500–2000 s and can therefore be the same signal appearing in the two different runs. However, the signal from the first run also have a period interval between 2000–2500 s, which is different from the modulation signal in the second run. In addition, the modulation signal from the first run is in general stronger in power when the period is close to 2000 s, while the second run modulation signal is stronger in power when the period is close to 1500 s. This might indicate that the two modulation signals are two different signals.

Both of the modulation signals also seems to be varying in power during the runs with color intensity increasing towards the middle of the runs and decreasing again when reaching the end of the runs. This behaviour might indicate there are intrinsic pulsations that varies rapidly. However, that seems unlikely as the scalogram shows changes in power that happens within hours, even minutes, which intrinsic pulsations (g-modes) related to the κ and γ mechanisms cannot account for, even when considering enhanced mass loss from the PNN (1).

The same feature with decreasing power towards the far left and right side of the scalogram was observed in the synthetic light curves in section 4.2 and suggested to be due to the wavelet transform's inability to deal properly with the start and the end of the observation run. This might indicate that the mentioned feature is not a result of real physical properties related to NGC 246, and that the modulation signal might in fact be continuous for the whole run. Another possible explanation for this varying power can be beating between modes with close frequencies. It could also be a result of interactions with a binary companion, but as there are no clear signs of harmonics, this seems unlikely.

Even though the data is not conclusive and NGC 246 do not show as many possible modulation signals as Jn1 for example, it is still an interesting object to continue observing. With longer observation runs one might be able to find further details about the modulation frequencies that appear in the scalogram.

5.3 NGC 6852

NGC 6852 has scalograms rich in modulation signals. An interesting observation is that there are several modulation signals that appear in one run but are absent in the other. Furthermore, the power of the modulation signals varies during the observation runs. As with Jn 1, NGC 6852 presents features indicating highly dynamic processes. A possible explanation for this behaviour can be interactions with a binary companion as there are several of the modulation signals that can be harmonically related to each other. This applies both when looking at the modulation signals in each separate run or if considering the modulation signals from both runs together.

The scalogram at the end of the second run shows power at periods of 500–600 s, which could be harmonically related to the power found at periods of 365–500 s and 1000–2500 s. This may indicate a similar scenario as discussed for Jn 1 in section 5.1, where the first run might show modulation signals related to the intrinsic variations of the PNN while the second run shows modulation signals related to the interaction with the binary companion. Modulation periods observed in the first run could indicate the presence of intrinsic pulsations as they are in a higher period range than those observed in the second run. The modulation periods from the first run might also be related to interactions with a close companion, considering that the AM CVn family has orbital periods of up to around 65 minutes. The exception might be the 5000–8000 s period that corresponds to 83–133 minutes. The second run shows power that may again be related to this interaction, and a possible harmonic structure, which strengthens the idea of an accretion disk being present.

One of the features seen in the harmonic synthetic light curves in section 4.2 was power located sporadically in between the harmonic period intervals. This same feature can be seen in the scalograms of the NGC 6852 which might indicate that these weaker modulation signals seen in between the dominating modulation signals are a consequence of beating between modes. On the other hand, this feature could also be due to an artifact of the wavelet analysis.

Again, the data is not conclusive, but do show intriguing features from these short runs that are difficult to see in the static frequency spectrum. Because of these transient features, NGC 6852 may be an interesting object to observe with longer observation runs.

5.4 VV 47

VV 47 shows interesting modulation signals mainly in the second and third run as seen in section 4.2.4. The scalograms of the first and fourth run do not show sections of modulation signals with high power but scattered, rather weak signals all over the scalograms. The second and third run present stronger indications of modulation signals. Even though the modulation frequencies of the first and fourth run add up to peaks that are above the false alarm probability in the frequency spectrums, the modulation signals in the scalogram do not tell us much because of the scattering and the relative low power. Therefore the focus will be on the second and third observation run of VV 47.

Before looking closer at the modulation signals from the two runs just mentioned, there is another point to be made. In all the observation runs, but especially in the longest runs (first, second and fourth run), there are similar patterns in the low period (high frequency) and high period (low frequency) range. In the lower period range the modulation signals are elongated in the vertical direction, while in the high period range the modulation signals become more elongated in the horizontal direction and pixelated. These features are probably due to the fact that for the Morlet wavelet the frequency resolution will decrease at higher frequencies and increase at lower frequencies and, as a result of the uncertainty principle, the time resolution will increase at higher frequencies and decrease at lower frequencies (28).

The scalograms for the second and third run for VV 47 have similarities with the two runs from NGC 6852 with one run showing more continuous higher period modulation signals, while the other shows more sporadic modulation signals in the lower period range. The modulations signals in the third run of VV 47 could be harmonically related as was the case for NGC 6852. Modulation periods observed in the second run might be related to intrinsic pulsations as they are at a higher period range compared to the third run. However, most of the modulations periods from the second run are below 65 minutes and therefore can indicate the presence of an interacting binary companion.

In his dissertation, Pérez considers that the peak he found in the third run of VV 47 at 3826 µHz might be a good candidate for a low-k order g-mode driven by the ϵ mechanism, among other things because of its short period (high frequency). The scalogram of the third run shows a modulation signal with a period ranging between 200–300 s that overlaps with the 3826 µHz (300 s in period) peak found by Pérez. As mentioned in section 4.2.4 the 200–300 s period signal seems to be recurring and varying in power during the run, which agrees with the prediction that the g-modes driven by the ϵ mechanism are unstable (1, p.58).

VV 47, with its wide range of periods, is certainly an object worth taking a closer look at, hopefully with longer observation runs. One cannot conclude that VV 47 is variable with these short runs, but with the features that the scalograms are showing, not to mention that one of the possible modulation signals could be connected to the ϵ mechanism, it might be a good investment to investigate the possible modulation signals further.

5.5 RXJ 2117

The PNN RXJ 2117 is one of the few PNNs that has been observed in long campaigns with excellent resolved frequency spectrum and that shows amplitude variations (29, 30). The scalogram of RXJ 2117 is quite clean without much noise and displays some clear modulation signals.

Again, the modulation signals seems to be varying in power during the run, and might be harmonically related to each other. The feature that was seen in the scalograms of the harmonic synthetic light curves and NGC 6852, with power located in between the dominating modulation signals, seems to be present in the scalogram of RXJ 2117 as well. This might indicate that beating between modes occur.

Vauclair et al. reported that for RXJ 2117 most of the peaks with significant power are found in the range 650–1600 µHz (30) which corresponds to 625–1539 s in period. The modulation periods found in this thesis from the scalogram is ranging between 700–2000 s which is not that different from the range of significant peaks reported by Vauclair et al. This might indicate that the modulations periods found for RXJ 2117 in this thesis are real modulation periods.

Chapter 6

Conclusion

The wavelet transform of the 5 PNNs show some promising and interesting features. The scalograms show several modulation periods, with many of them presenting significant variation in power during the observation runs. Jn 1, NGC 6852, VV 47 and RXJ 2117 also have modulation frequencies that could be harmonically related, sharing photometric features similar to those observed in hydrogen-deficient close binary systems, such as members of the AM CVn family. This may indicate the presence of an accretion disc and hence a binary companion. It could provide additional evidence linking these types of objects and support the idea that features such as bipolar nebulae and hydrogen deficiency are possible outcomes of close binary evolution channels. Some of the runs show evidence of interesting intrinsic pulsations that vary rapidly over time, such as the mode observed for VV 47, possibly triggered by the ϵ mechanism. Due to the short observations and relatively short sample rate, the data and findings from this paper are not conclusive, but nevertheless they do encourage having future observation campaigns on these 5 PNNs with longer runs.

The observation campaign the data of this thesis is gathered from can be thought of as a pre-selection of objects that might be interesting to study further. The thesis has focused mainly on short observation runs, usually aimed at discovering new pulsators that are expected to have short periods. For such short runs, the static FT might not be the best choice as unstable low-amplitude modulations might be hidden in the noise. The wavelet transform on the other hand is able to detect time-dependent modulation signals and can show its development during the observation runs. In other words, when having such "pre-selection" observation campaign, it might be a good solution to use the wavelet transform when analyzing the light curves. Compared to static approaches like Fourier Transform, wavelet analysis can be more efficient in detecting modulation frequencies in short observing runs, and a unique tool for discovering those that are highly dynamic, thus enabling the extraction of more detailed information about the underlying processes.

References

(1) J. M. González Pérez. “From Close Binary White Dwarfs to White Dwarfs”. Tromsø: University of Tromsø, 2004.

(2) J. J. Hermes et al. A Deep Test of Radial Differential Rotation in a Helium-Atmosphere White Dwarf: I. Discovery of Pulsations in PG 0112+104. The Astrophysical Journal 835.2 (Feb. 1, 2017), p. 277. ISSN: 0004-637X, 1538-4357. arXiv: `1612.07807 [astro-ph]`.

(3) P. Sleziak, K. Hlavčová, and J. Szolgay. Advantages Of A Time Series Analysis Using Wavelet Transform As Compared With A Fourier Analysis. Slovak Journal of Civil Engineering 23.2 (June 1, 2015), pp. 30–36. ISSN: 1338-3973, 1210-3896.

(4) F. LeBlanc. An Introduction to Stellar Astrophysics. Hoboken, N.J.: Wiley, 2010. ISBN: 1-119-96497-0.

(5) A. I. Karakas. “Low- and Intermediate-Mass Stars”. Handbook of Supernovae. Cham: Springer International Publishing, 2017, pp. 461–481. ISBN: 3-319-21845-X.

(6) Types - NASA Science. Sept. 22, 2020. URL: `https://science.nasa.gov/universe/stars/types/` (visited on 05/13/2025).

(7) Chandra :: Educational Materials :: The Hertzsprung-Russell Diagram. URL: `https://chandra.harvard.edu/edu/formal/variable_stars/bg_info.html` (visited on 05/12/2025).

(8) B. Carroll and D. Ostlie. An Introduction to Modern Astrophysics. 2nd edition. Pearson, 2006.

(9) K. Oman. Red Giant Branch and Asymptotic Giant Branch. Physics Stack Exchange. eprint: `https://physics.stackexchange.com/q/74691`.

(10) K. A. Postnov and L. R. Yungelson. The Evolution of Compact Binary Star Systems. Living reviews in relativity 17.1 (2014), pp. 3–3. ISSN: 2367-3613.

(11) Centro de Astrobiologia (CAB), director. Common Envelope Evolution: From Binary Star Chrysalis to Cosmic Butterfly. Jan. 25, 2021.

(12) S. Hekker. CoRoT and Kepler Results: Solar-like Oscillators. Advances in Space Research 52.9 (2013), pp. 1581–1592. ISSN: 0273-1177.

(13) S. Starrfield et al. Nonradial Instability Strips Based on Carbon and Oxygen Partial Ionization in Hot, Evolved Stars. The Astrophysical Journal 281 (June 1984), p. 800. ISSN: 0004-637X, 1538-4357.

(14) S. Starrfield, A. N. Cox, and R. B. Kidman. AN ANALYSIS OF NONRADIAL PULSATIONS OF THE CENTRAL STAR OF THE PLANETARY NEBULA Kl-161'2. ApJ. . . (June 1985).

(15) S. D. Kawaler et al. The Helium Shell Game - Nonradial g-Mode Instabilities in Hydrogen-Deficient Planetary Nebula Nuclei. The Astrophysical Journal 306 (July 1986), p. L41. ISSN: 0004-637X, 1538-4357.

(16) G. Ramsay et al. Physical Properties of AM CVn Stars: New Insights from *Gaia* DR2. Astronomy & Astrophysics 620 (Dec. 2018), A141. ISSN: 0004-6361, 1432-0746.

(17) J. E. Solheim and J. L. Provencal. First Attempt on Discoseismology of Am CVN Stars - What Can the Harmonic Structure of the Observed Amplitude Spectra Tell Us? Open Astronomy 7 (1998), pp. 277–286.

(18) G. Nelemans. AM Cvn Stars. 2005.

(19) An Atlas of Orbital Light Curves of Cataclysmic Variables – CBA. URL: `https://cbastro.org/cataclysmic-variables/an-atlas-of-orbital-light-curves-of-cataclysmic-variables/` (visited on 04/29/2025).

(20) J.-E. Solheim et al. Whole Earth Telescope Observations of AM Canum Venaticorum - Discoseismology at Last. Astronomy and Astrophysics 332 (Mar. 1998), pp. 939–957.

(21) G. Kaiser. A Friendly Guide to Wavelets. Boston: Birkhäuser Boston, 2011. ISBN: 978-0-8176-8110-4 978-0-8176-8111-1.

(22) C. Torrence and G. P. Compo. A Practical Guide to Wavelet Analysis. Bulletin of the American Meteorological Society 79.1 (Jan. 1998), pp. 61–78. ISSN: 0003-0007, 1520-0477.

(23) A. Silik et al. Comparative Analysis of Wavelet Transform for Time-Frequency Analysis and Transient Localization in Structural Health Monitoring. Structural durability & health monitoring 15.1 (2021), pp. 1–22. ISSN: 1930-2991.

(24) Butter — SciPy v1.15.2 Manual. URL: `https://docs.scipy.org/doc/scipy/reference/generated/scipy.signal.butter.html` (visited on 04/29/2025).

(25) Discrete Fourier Transform (Numpy.Fft) — NumPy v2.2 Manual. URL: `https://numpy.org/doc/2.2/reference/routines.fft.html` (visited on 04/29/2025).

(26) Continuous Wavelet Transform (CWT) — PyWavelets Documentation. URL: `https://pywavelets.readthedocs.io/en/latest/ref/cwt.html` (visited on 11/05/2024).

(27) E. Onajite. Seismic Data Analysis Techniques in Hydrocarbon Exploration. Waltham, MA: Elsevier, 2014.

(28) P. A. Abhang, B. W. Gawali, and S. C. Mehrotra. Introduction to EEG- and Speech-Based Emotion Recognition. 1st ed. Chantilly: Elsevier Science & Technology, 2016. ISBN: 0-12-804490-X.

(29) R. E. Nather et al. The Whole Earth Telescope - A New Astronomical Instrument. The Astrophysical Journal 361 (Sept. 1990), p. 309. ISSN: 0004-637X, 1538-4357.

(30) G. Vauclair et al. Asteroseismology of RXJ 2117+3412, the Hottest Pulsating PG 1159 Star. Astronomy & Astrophysics 381.1 (Jan. 2002), pp. 122–150. ISSN: 0004-6361, 1432-0746.

(31) Dsp_notebooks/Notebooks/Baseband_modulation/02_pulse_shaping.Ipynb at Main · Strath-Sdr/Dsp_notebooks. GitHub. URL: `https://github.com/strath-sdr/dsp_notebooks/blob/main/notebooks/baseband_modulation/02_pulse_shaping.ipynb` (visited on 05/14/2025).

Appendices

Appendix A

Python code

A.1 Photometry analysis

Photometry analysis with WT and FT

In [3]:

```
# Libraries
import tkinter as tk # GUI
import tkinter.filedialog as fd # file dialogs
import tkinter.messagebox as mb # message boxes

import matplotlib
import matplotlib.ticker as ticker

import matplotlib.pyplot as plt
import numpy as np
import math
from scipy import signal

import pywt

from pylab import*
```

In [4]:

```
# -*- coding: utf-8 -*-
"""
A simple script for loading csv files as structured numpy arrays. Uses tkinter
to simplify the process of getting file paths, and prints the available column
names in the csv file to the terminal. Terminal messages can be disabled.

Note: The messages make some assumptions on variable names.

Andøya Space Education

Created on Thu Oct 3 2024 at 15:10:42
Last modified [dd.mm.yyyy]: 21.10.2024
@author: bjarne.ådnanes.bergtun
"""

# ================================ Functions ================================ #


def get_file_path(file_path, print_to_terminal = True):
    if file_path == '':
        # First a root window is created and put on top of all other windows.
        root = tk.Tk()
        root.withdraw()
        root.wm_attributes('-topmost', 1)

        # On top of the root window, a filedialog is opened to get the CSV file
        # from the file explorer.
        file_path = fd.askopenfilename(
            title = 'Select rocket data to import',
            filetypes = (('CSV files','.csv'),('All files','.*')),
            parent = root,
            )

        if print_to_terminal:
            # Alert the user of ways of speeding up the process
            print('\nFile path:\n' + file_path)
    return file_path


def load_data(file_path, print_to_terminal = True):
```

```
    # Get file path, if not already given
    file_path = get_file_path(file_path, print_to_terminal)

    six_cols_list = ['C:/Users/teach/OneDrive/Heldagsprøve/NTNU/Master/Observation d
                     'C:/Users/teach/OneDrive/Heldagsprøve/NTNU/Master/Observation d
                     'C:/Users/teach/OneDrive/Heldagsprøve/NTNU/Master/Observation d

    if file_path in six_cols_list:

        # Load data
        data = np.genfromtxt(
        file_path,
        usecols = (0,6),
        encoding = 'windows-1252', # 'utf-8',
        )
    else:
        data = np.genfromtxt(
        file_path,
        usecols = (0,4),
        encoding = 'windows-1252', # 'utf-8',
        )

    return data
```

In [5]:

```
# Generating data

# The file path can be written in here.
file_path_array = ['C:/Users/teach/OneDrive/Heldagsprøve/NTNU/Master/Observation dat
                   'C:/Users/teach/OneDrive/Heldagsprøve/NTNU/Master/Observation dat
                   'C:/Users/teach/OneDrive/Heldagsprøve/NTNU/Master/Observation dat
                   'C:/Users/teach/OneDrive/Heldagsprøve/NTNU/Master/Observation dat
                   'C:/Users/teach/OneDrive/Heldagsprøve/NTNU/Master/Observation dat
                   'C:/Users/teach/OneDrive/Heldagsprøve/NTNU/Master/Observation dat
                   'C:/Users/teach/OneDrive/Heldagsprøve/NTNU/Master/Observation dat
                   'C:/Users/teach/OneDrive/Heldagsprøve/NTNU/Master/Observation dat
                   'C:/Users/teach/OneDrive/Heldagsprøve/NTNU/Master/Observation dat
                   'C:/Users/teach/OneDrive/Heldagsprøve/NTNU/Master/Observation dat
                   'C:/Users/teach/OneDrive/Heldagsprøve/NTNU/Master/Observation dat

july_19th_2000 = ['C:/Users/teach/OneDrive/Heldagsprøve/NTNU/Master/Observation data

july_20th_2000 = ['C:/Users/teach/OneDrive/Heldagsprøve/NTNU/Master/Observation data

july_21st_2000 = ['C:/Users/teach/OneDrive/Heldagsprøve/NTNU/Master/Observation data

july_22nd_2000 = ['C:/Users/teach/OneDrive/Heldagsprøve/NTNU/Master/Observation data
                  'C:/Users/teach/OneDrive/Heldagsprøve/NTNU/Master/Observation data

july_23rd_2000 = ['C:/Users/teach/OneDrive/Heldagsprøve/NTNU/Master/Observation data
                  'C:/Users/teach/OneDrive/Heldagsprøve/NTNU/Master/Observation data

january_16_2001 = ['C:/Users/teach/OneDrive/Heldagsprøve/NTNU/Master/Observation dat

january_16_17_2001 = ['C:/Users/teach/OneDrive/Heldagsprøve/NTNU/Master/Observation
                      'C:/Users/teach/OneDrive/Heldagsprøve/NTNU/Master/Observation

january_17_18_2001 = ['C:/Users/teach/OneDrive/Heldagsprøve/NTNU/Master/Observation


# Normalization list for forward" normalization"

ortho_norm_array = ['C:/Users/teach/OneDrive/Heldagsprøve/NTNU/Master/Observation da
```

```
                'C:/Users/teach/OneDrive/Heldagsprøve/NTNU/Master/Observation dat
                'C:/Users/teach/OneDrive/Heldagsprøve/NTNU/Master/Observation dat
```

In [6]:

```
def filter_high_val(ave_diff_phot,lim_val):
    for i in range(len(ave_diff_phot)):
        if ave_diff_phot[i] > lim_val:
            print(i)

def filter_low_val(ave_diff_phot,lim_val):
    for i in range(len(ave_diff_phot)):
        if ave_diff_phot[i] < lim_val:
            print(i)

def butter_highpass(cutoff, f_nyquist, order=6):
    normal_cutoff = cutoff/f_nyquist
    b, a = signal.butter(order, normal_cutoff, btype='high')
    return b, a

def butter_highpass_filter(data, cutoff, f_nyquist, order=6):
    b, a = butter_highpass(cutoff, f_nyquist, order=order)
    y = signal.filtfilt(b, a, data)
    return y

# making Lego function for scaleogram
def lego_func(cwtmatr,power_perc):
    mid_val = np.average(cwtmatr)
    dimensions = cwtmatr.shape
    rows, columns = dimensions
    power_perc_str = str(power_perc)
    print("Detected frequency from WT with power percentage equal to " +
          power_perc_str + ": ")
    for i in range(rows):
        for j in range(columns):
            if cwtmatr[i][j] < power_perc * mid_val:
                cwtmatr[i][j] = 0
#             else:
#                 cwtmatr_str = str(cwtmatr[i][j])
#                 print(cwtmatr_str + "\n")


# FALSE alarm probability function
def FAP(time,yf,FALSE_val):
    N = len(time)
    P_ave = 0
    for i in range(len(yf)):
        P_ave += (np.abs(yf[i]))**2
    P_ave = P_ave/N
    P_obs = math.log(N*(1/FALSE_val))*P_ave
    return P_obs


# printing the most dominant frequencies from FT-plot
def dom_freqs(xf, yf, P_obs_amp):
    index = np.where(yf == max(yf))[0]
    xf_max_str = str(xf[index])
    if max(yf) > P_obs_amp:
        print("This is the most dominant frequency: " + xf_max_str)

    yf_new = np.delete(yf,index)
    xf_new = np.delete(xf,index)

    index_2 = np.where(yf_new == max(yf_new))[0]
    xf_new_max_str = str(xf_new[index_2])
```

```
    if max(yf_new) > P_obs_amp:
        print("This is the second most dominant frequency: " + xf_new_max_str)

    yf_new_2 = np.delete(yf_new,index_2)
    xf_new_2 = np.delete(xf_new,index_2)

    index_3 = np.where(yf_new_2 == max(yf_new_2))[0]
    xf_new_2_max_str = str(xf_new_2[index_3])
    if max(yf_new_2) > P_obs_amp:
        print("This is the third most dominant frequency: " + xf_new_2_max_str)

    yf_new_3 = np.delete(yf_new_2,index_3)
    xf_new_3 = np.delete(xf_new_2,index_3)

    index_4 = np.where(yf_new_3 == max(yf_new_3))[0]
    xf_new_3_max_str = str(xf_new_3[index_4])
    if max(yf_new_3) > P_obs_amp:
        print("This is the fourth most dominant frequency: " + xf_new_3_max_str)

    yf_new_4 = np.delete(yf_new_3,index_4)
    xf_new_4 = np.delete(xf_new_3,index_4)

    index_5 = np.where(yf_new_4 == max(yf_new_4))[0]
    xf_new_4_max_str = str(xf_new_4[index_5])
    if max(yf_new_4) > P_obs_amp:
        print("This is the fifth most dominant frequency: " + xf_new_4_max_str)

    yf_new_5 = np.delete(yf_new_4,index_5)
    xf_new_5 = np.delete(xf_new_4,index_5)

    index_6 = np.where(yf_new_5 == max(yf_new_5))[0]
    xf_new_5_max_str = str(xf_new_5[index_6])
    if max(yf_new_5) > P_obs_amp:
        print("This is the sixth most dominant frequency: " + xf_new_5_max_str)

    yf_new_6 = np.delete(yf_new_5,index_6)
    xf_new_6 = np.delete(xf_new_5,index_6)

    index_7 = np.where(yf_new_6 == max(yf_new_6))[0]
    xf_new_6_max_str = str(xf_new_6[index_7])
    if max(yf_new_6) > P_obs_amp:
        print("This is the seventh most dominant frequency: " + xf_new_6_max_str)

    yf_new_7 = np.delete(yf_new_6,index_7)
    xf_new_7 = np.delete(xf_new_6,index_7)

    index_8 = np.where(yf_new_7 == max(yf_new_7))[0]
    xf_new_7_max_str = str(xf_new_7[index_8])
    if max(yf_new_7) > P_obs_amp:
        print("This is the eight most dominant frequency: " + xf_new_7_max_str)
```

In [7]:

```
def get_plot(file_path_array):

    time = load_data(file_path_array)[:, 0]
    diff_phot = load_data(file_path_array)[:, 1]

    ave_diff_phot = diff_phot - np.mean(diff_phot)

    if file_path_array == 'C:/Users/teach/OneDrive/Heldagsprøve/NTNU/Master/Observat
        time = time[:-17]
        diff_phot = diff_phot[:-17]
```

```
        ave_diff_phot = diff_phot - np.mean(diff_phot)

    elif file_path_array == 'C:/Users/teach/OneDrive/Heldagsprøve/NTNU/Master/Observ
        time = time[:-17]
        diff_phot = diff_phot[:-17]

        ave_diff_phot = diff_phot - np.mean(diff_phot)

    elif file_path_array == 'C:/Users/teach/OneDrive/Heldagsprøve/NTNU/Master/Observ
        time = time[:-90]
        diff_phot = diff_phot[:-90]

        ave_diff_phot = diff_phot - np.mean(diff_phot)

    elif file_path_array == 'C:/Users/teach/OneDrive/Heldagsprøve/NTNU/Master/Observ
        time = np.delete(time,262)
        time = np.delete(time,347)
        ave_diff_phot = np.delete(ave_diff_phot,262)
        ave_diff_phot = np.delete(ave_diff_phot,347)

    elif file_path_array == 'C:/Users/teach/OneDrive/Heldagsprøve/NTNU/Master/Observ
        time = np.delete(time,71)
        time = np.delete(time,70)
        time = np.delete(time,69)
        time = np.delete(time,68)
        ave_diff_phot = np.delete(ave_diff_phot,71)
        ave_diff_phot = np.delete(ave_diff_phot,70)
        ave_diff_phot = np.delete(ave_diff_phot,69)
        ave_diff_phot = np.delete(ave_diff_phot,68)

    elif file_path_array == 'C:/Users/teach/OneDrive/Heldagsprøve/NTNU/Master/Observ
        time = np.delete(time,23)
        ave_diff_phot = np.delete(ave_diff_phot,23)

    # Butterworth highpass filter
    sampling_period = np.diff(time).mean()
    sample_length = time[-1]
    f_min = 1/sample_length
    f_nyquist = (1/sampling_period)*(1/2)
    cutoff = 3*f_min
    ave_diff_phot = butter_highpass_filter(ave_diff_phot, cutoff, f_nyquist)

    ave_diff_phot = ave_diff_phot/1000

    # plot signal
    # making title for plot
    name = file_path_array[81:]
    title = name[:-4]

    fig_LC = plt.figure(figsize=(9,5))
    plt.plot(time,ave_diff_phot,'.')
    plt.xlabel('Time (s)')
    plt.ylabel('I (mmi)')

    file_name_lightcurve = title + '_lightcurve.' + 'pdf'
    plt.savefig('C:/Users/teach/OneDrive/Heldagsprøve/NTNU/Master LaTex/Pictures and
                + file_name_lightcurve, format = 'pdf', dpi = 300)


    # plot fourier transform for comparison
    from numpy.fft import rfft, rfftfreq

    yf = rfft(ave_diff_phot,norm="ortho")
    if file_path_array in ortho_norm_array:
```

```
    yf = rfft(ave_diff_phot,norm="forward")
xf = rfftfreq(len(ave_diff_phot), sampling_period)

yf = np.abs(yf)

# set scale for the x-axis in the FT_plot
scale_x = 1e-6
xf_scaled = (1/scale_x)*xf

# FALSE alarm probability
FALSE_val = 1/12
P_obs = FAP(time,yf,FALSE_val)
P_obs_amp = math.sqrt(P_obs)
P_obs_array = np.full_like(xf,P_obs_amp)

fig_FT = plt.figure(figsize=(9,5))
plt.plot(xf_scaled, yf)
plt.plot(xf_scaled, P_obs_array, color='red', linestyle='dashed')
plt.xlabel("Frequency (μHz)")
plt.ylabel("Power (μmp)")
plt.yscale("linear")

file_name_FT = title + '_FT.' + 'pdf'
plt.savefig('C:/Users/teach/OneDrive/Heldagsprøve/NTNU/Master LaTex/Pictures and
            + file_name_FT, format = 'pdf', dpi = 300)

plt.show()


# perform CWT
wavelet = "cmor1.5-1.0"

# Calculating scales
scale_min = 2
scale_max = 2 * f_nyquist/f_min

# logarithmic scale for scales, as suggested by Torrence & Compo:
widths_1 = np.geomspace(scale_min, scale_max, num=500)
cwtmatr, freqs = pywt.cwt(ave_diff_phot, widths_1, wavelet,
                          sampling_period=sampling_period)
# absolute take absolute value of complex result
cwtmatr = np.abs(cwtmatr[:-1, :-1])
if file_path_array in ortho_norm_array:
    cwtmatr = cwtmatr/(np.sqrt(len(ave_diff_phot)))

# converting frequency to period
periods = 1/freqs

# plot result using matplotlib's pcolormesh (image with annoted axes)
plt.rcParams['figure.constrained_layout.use'] = True

fig, axs = plt.subplots(1, 2, figsize=(10,5), sharey=True,
                        gridspec_kw={'width_ratios': [3 ,1]})
pcm = axs[0].pcolormesh(time, periods, cwtmatr)
axs[0].set_yscale("log")
axs[0].set_xlabel("Time (s)")
axs[0].set_ylabel("Periods (s)")
fig.colorbar(pcm, ax=axs[0], location='left',label="Power (μmp)")


# plot fourier transform with scaleogram
# converting frequency to period for FT
periods_FT = 1/xf
```

```
    plt.plot(yf, periods_FT)
    axs[1].set_xlabel("Power (µmp)")
    axs[1].set_yscale("log")

    file_name_scaleogram_and_FT = title + '_scaleogram_and_FT.' + 'pdf'
    plt.savefig('C:/Users/teach/OneDrive/Heldagsprøve/NTNU/Master LaTex/Pictures and
                + file_name_scaleogram_and_FT, format = 'pdf', dpi = 300)
```

In [8]:
```
#Plot all signals with corresponding wavelet and fourier transform plots

for i in range(len(file_path_array)):
    get_plot(file_path_array[i])
```

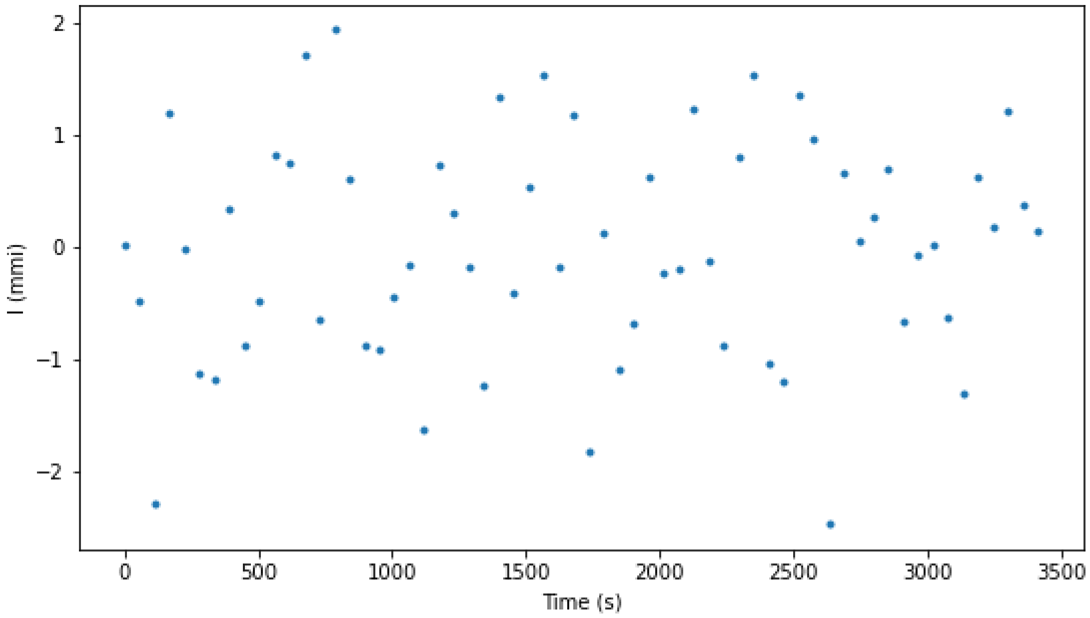

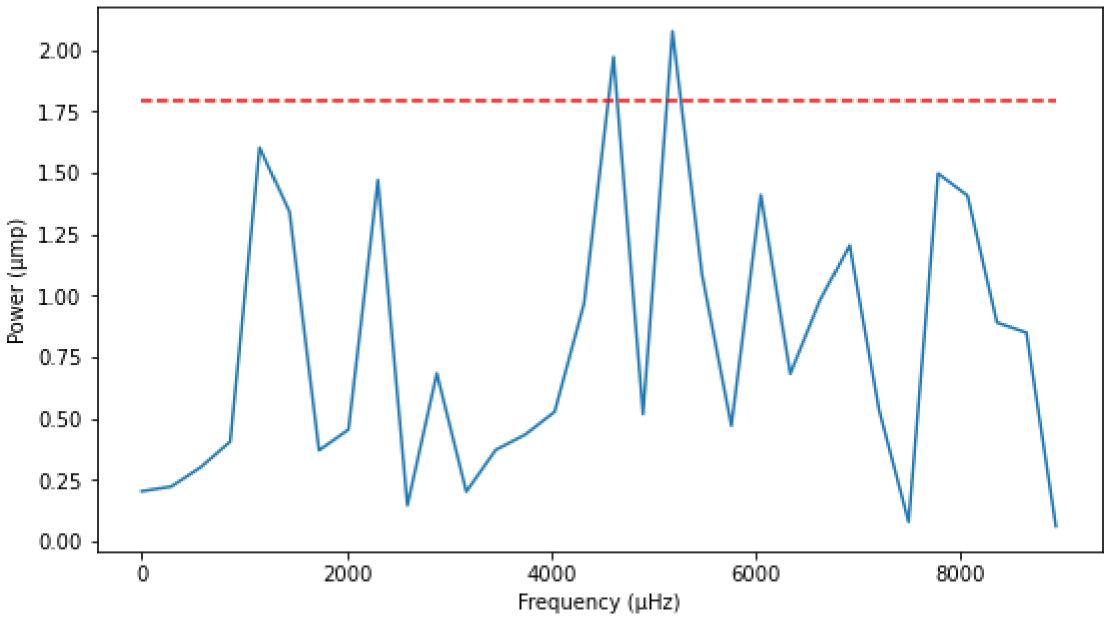


```
C:\Users\teach\AppData\Local\Temp/ipykernel_13912/2588248293.py:135: RuntimeWarning:
divide by zero encountered in true_divide
  periods_FT = 1/xf
```

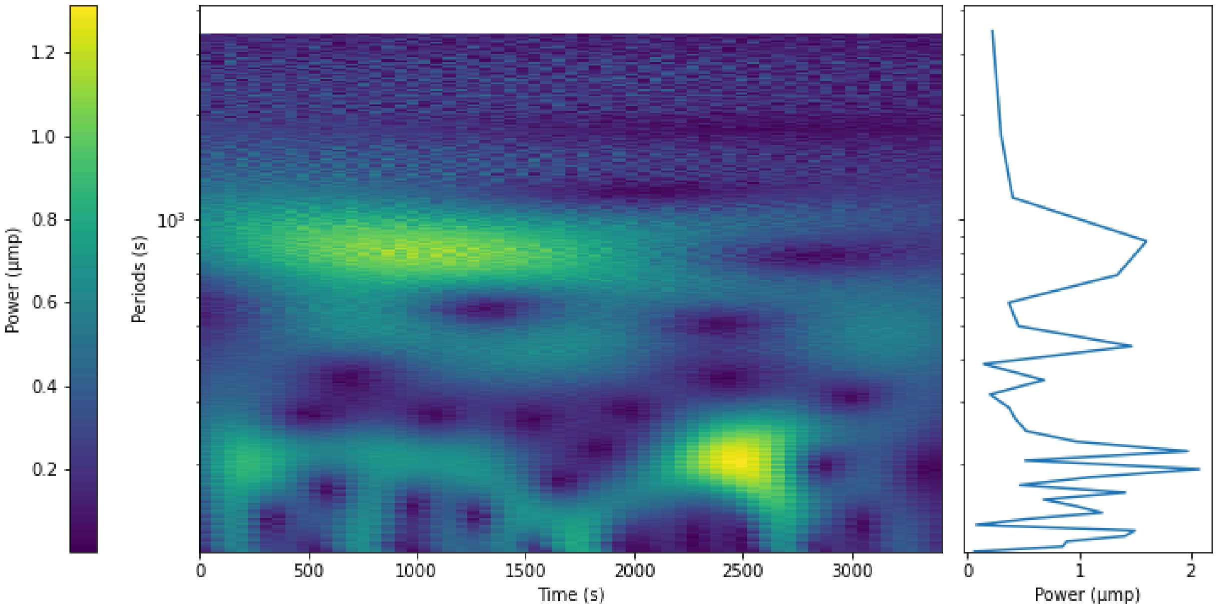
Power (μmp)
Periods (s)
Time (s)
Power (μmp)

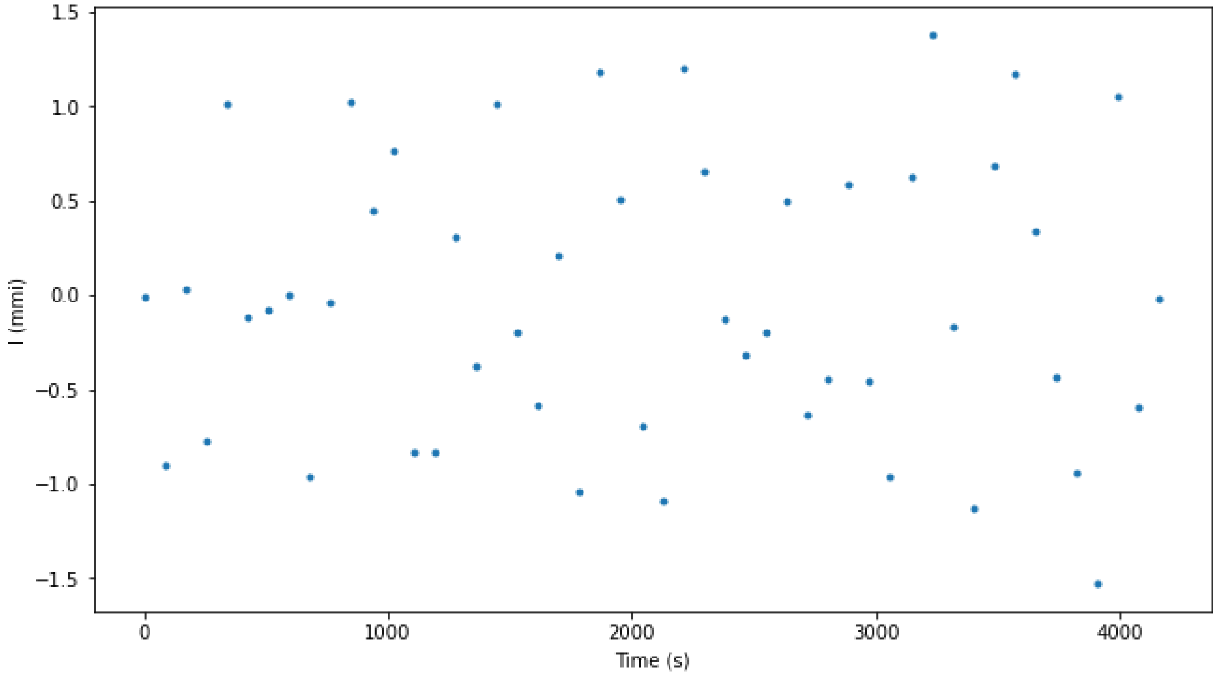
I (mmi)
Time (s)

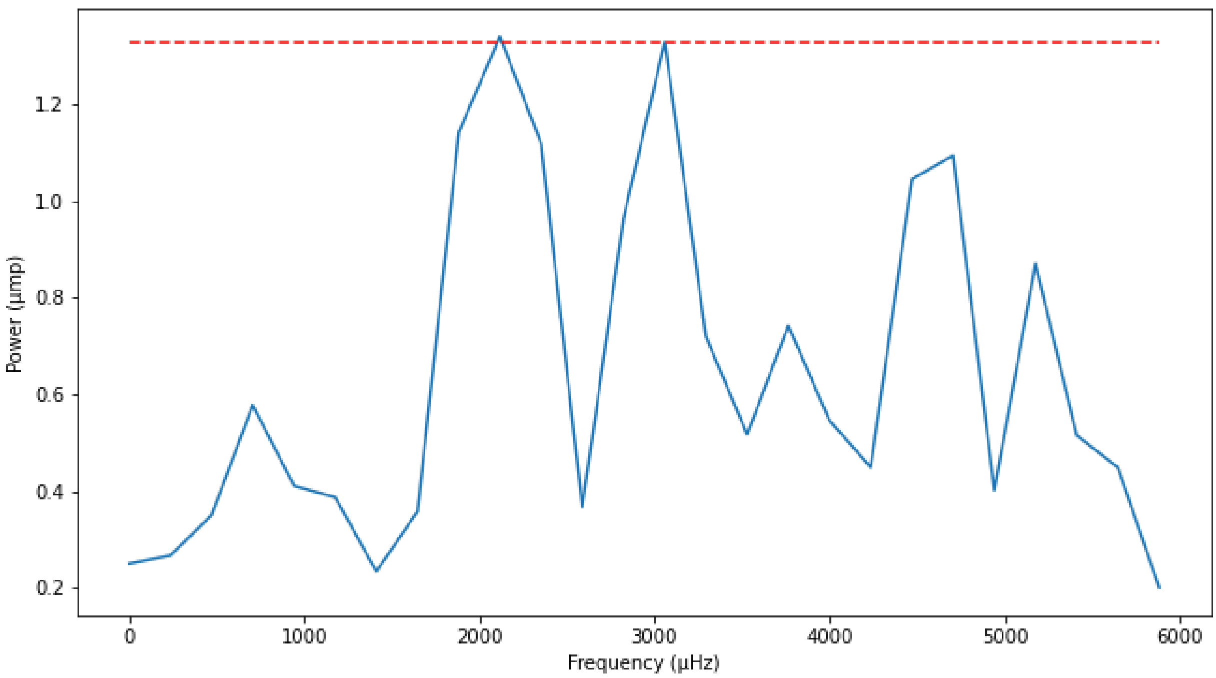
Power (μmp)
Frequency (μHz)

```
C:\Users\teach\AppData\Local\Temp/ipykernel_13912/2588248293.py:135: RuntimeWarning:
divide by zero encountered in true_divide
  periods_FT = 1/xf
```

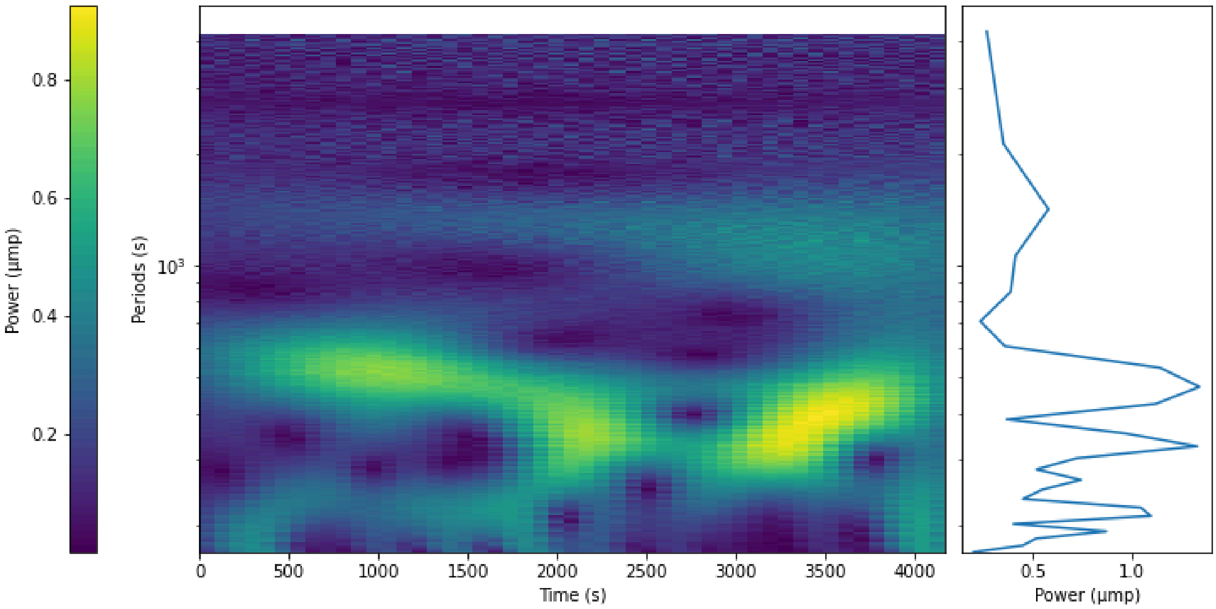

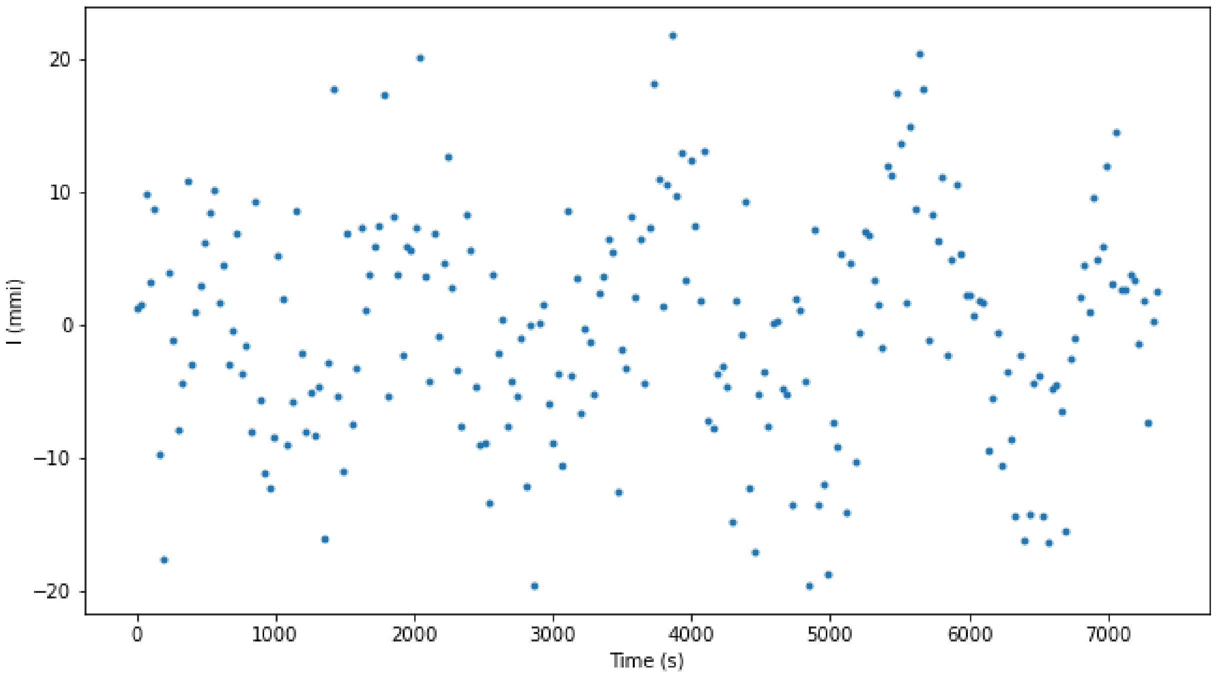

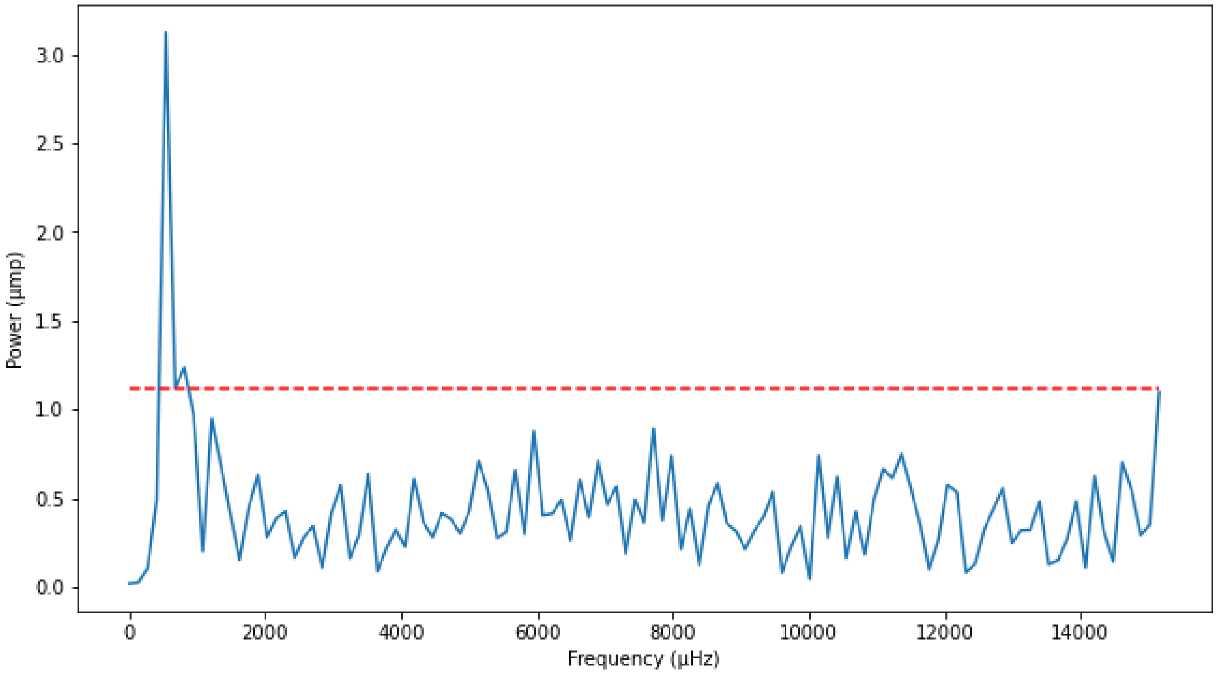


```
C:\Users\teach\AppData\Local\Temp/ipykernel_13912/2588248293.py:135: RuntimeWarning: divide by zero encountered in true_divide
  periods_FT = 1/xf
```

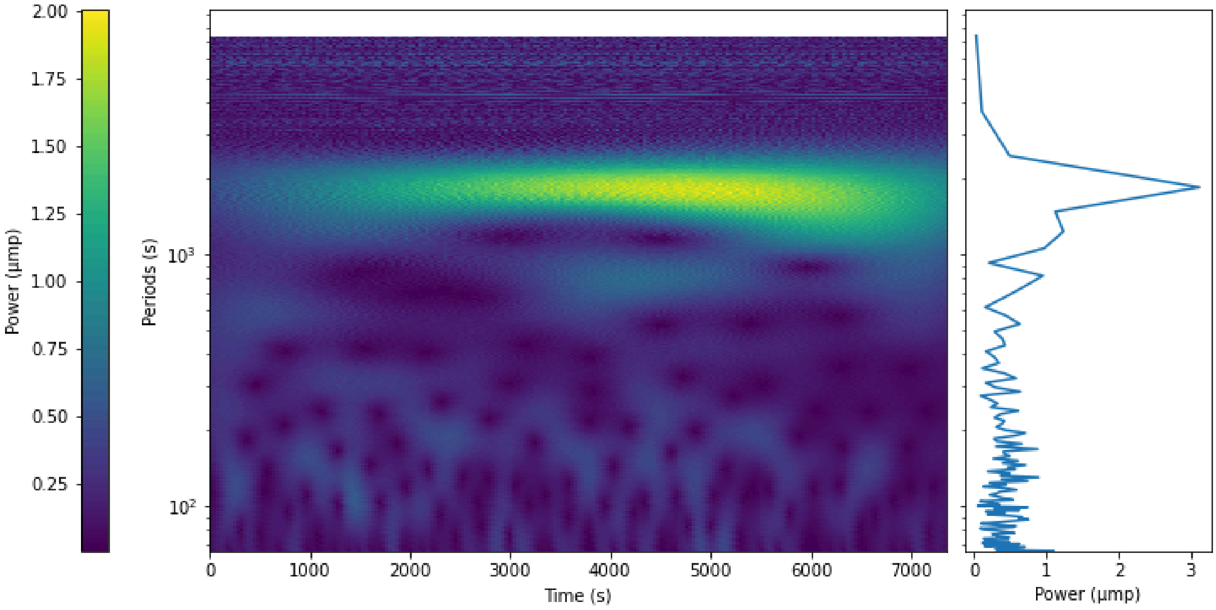

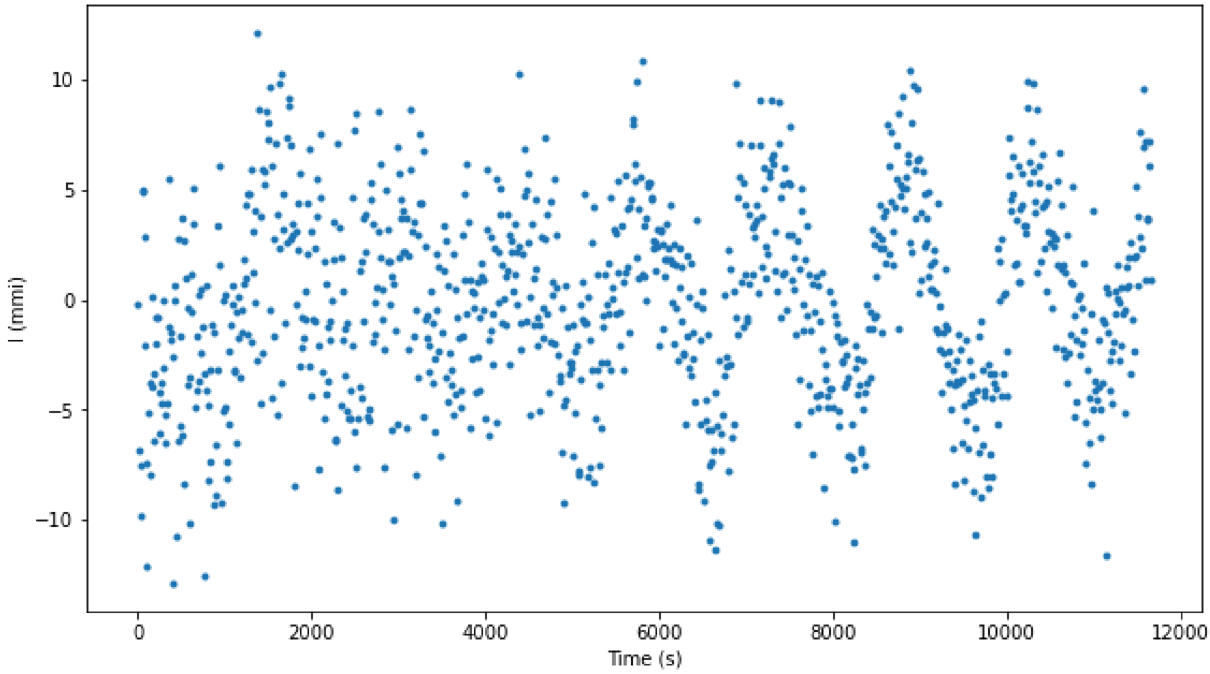

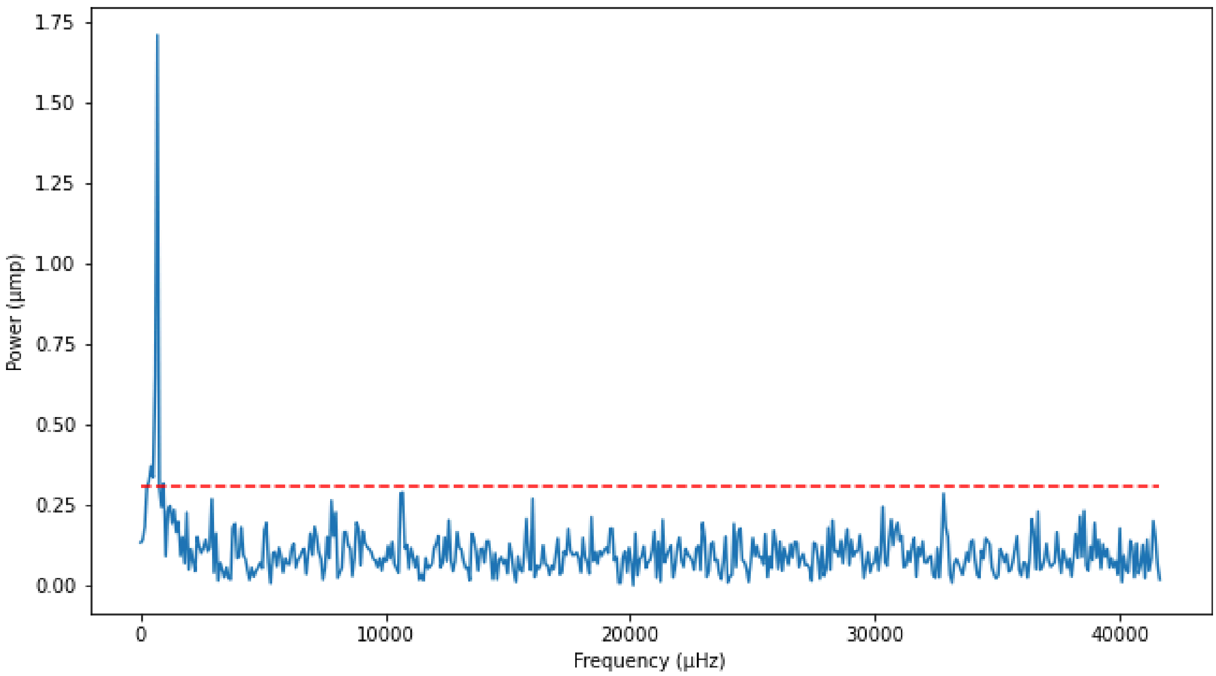


```
C:\Users\teach\AppData\Local\Temp/ipykernel_13912/2588248293.py:135: RuntimeWarning:
divide by zero encountered in true_divide
  periods_FT = 1/xf
```

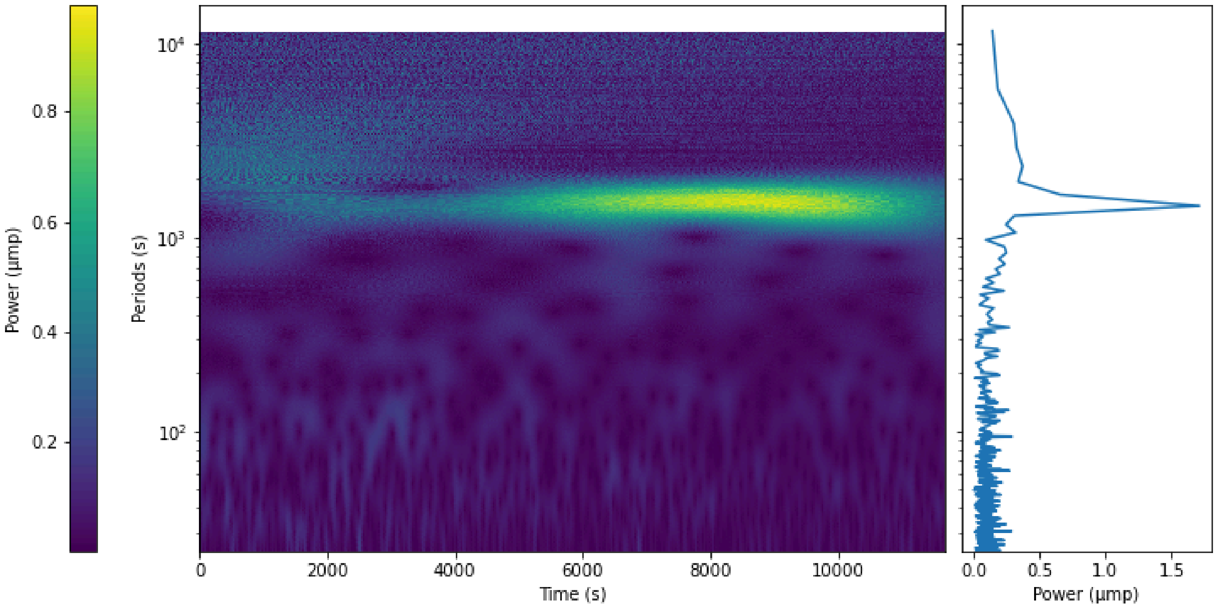
Power (µmp)
0.2
0.4
0.6
0.8
Periods (s)
10^2
10^3
10^4
0
2000
4000
6000
8000
10000
Time (s)
0.0
0.5
1.0
1.5
Power (µmp)

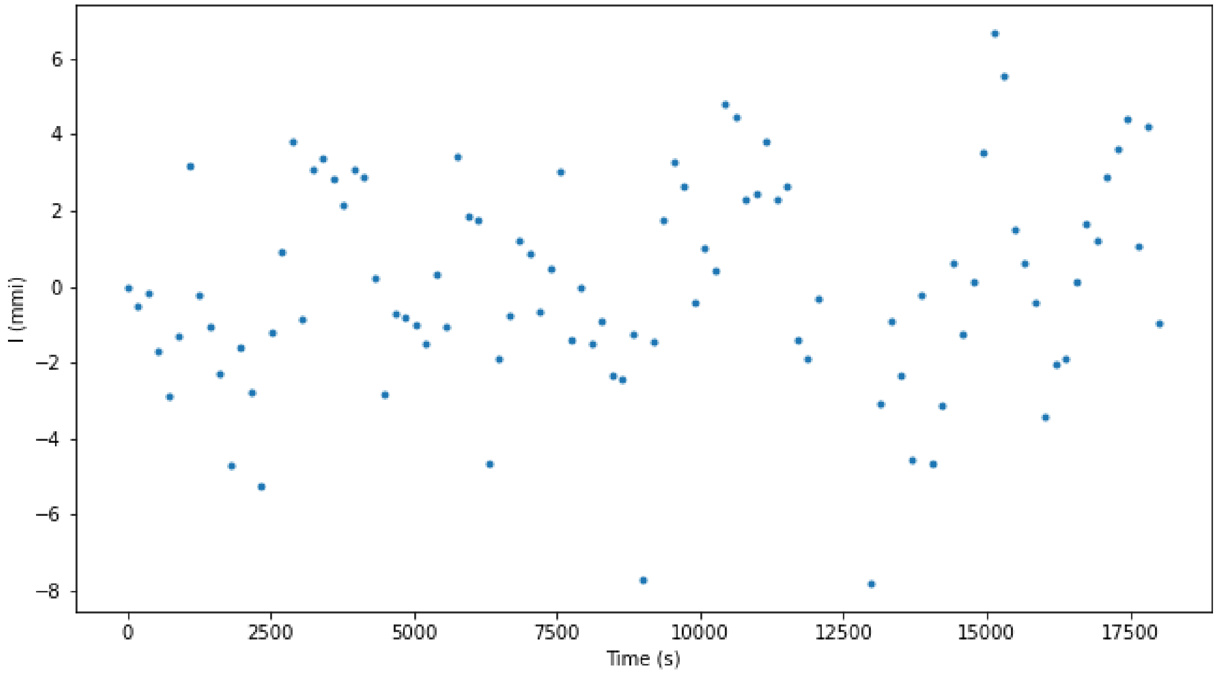
I (mmi)
6
4
2
0
−2
−4
−6
−8
0
2500
5000
7500
10000
12500
15000
17500
Time (s)

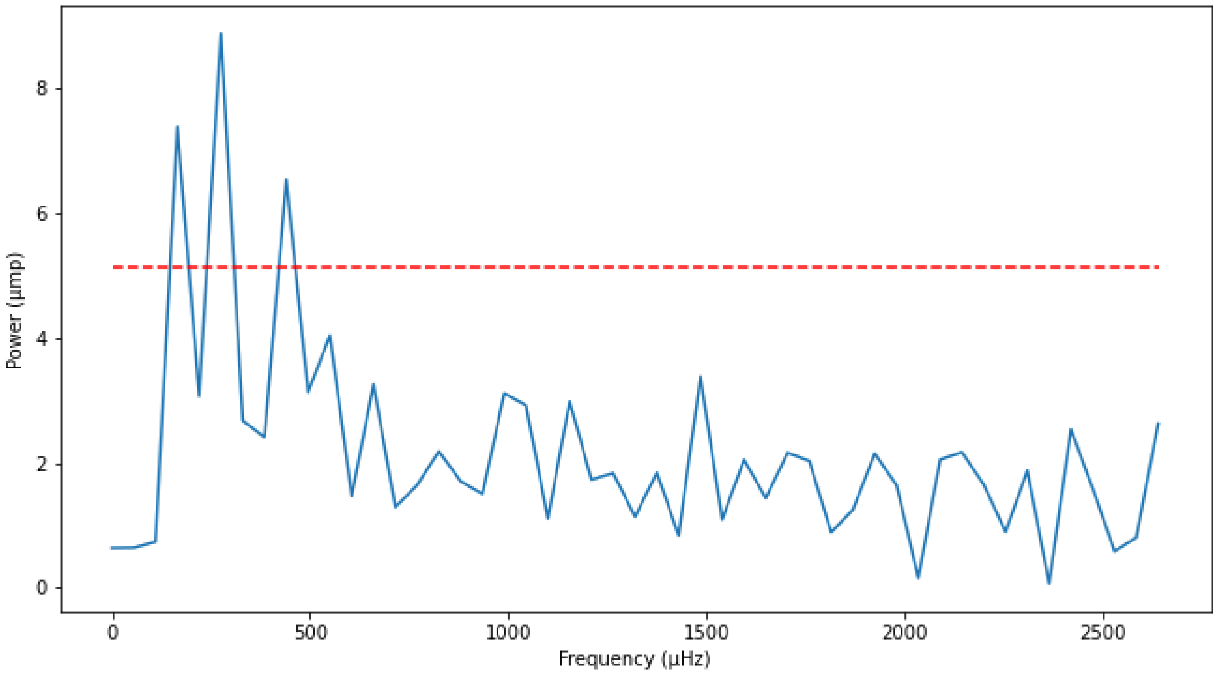
Power (µmp)
8
6
4
2
0
0
500
1000
1500
2000
2500
Frequency (µHz)

```
C:\Users\teach\AppData\Local\Temp/ipykernel_13912/2588248293.py:135: RuntimeWarning:
divide by zero encountered in true_divide
  periods_FT = 1/xf
```

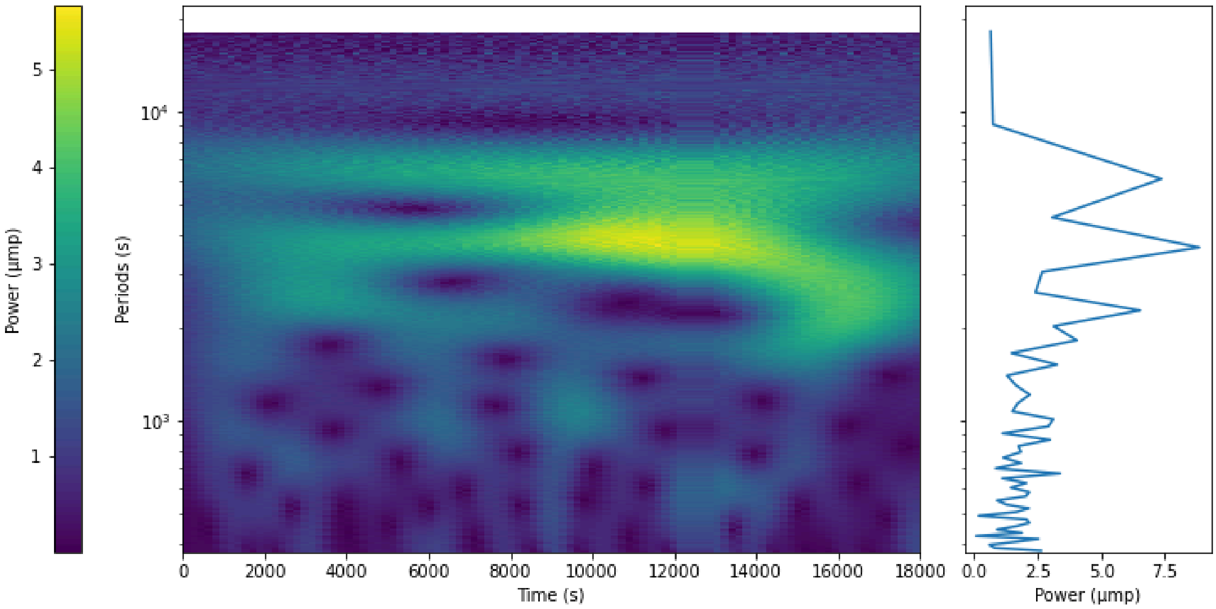

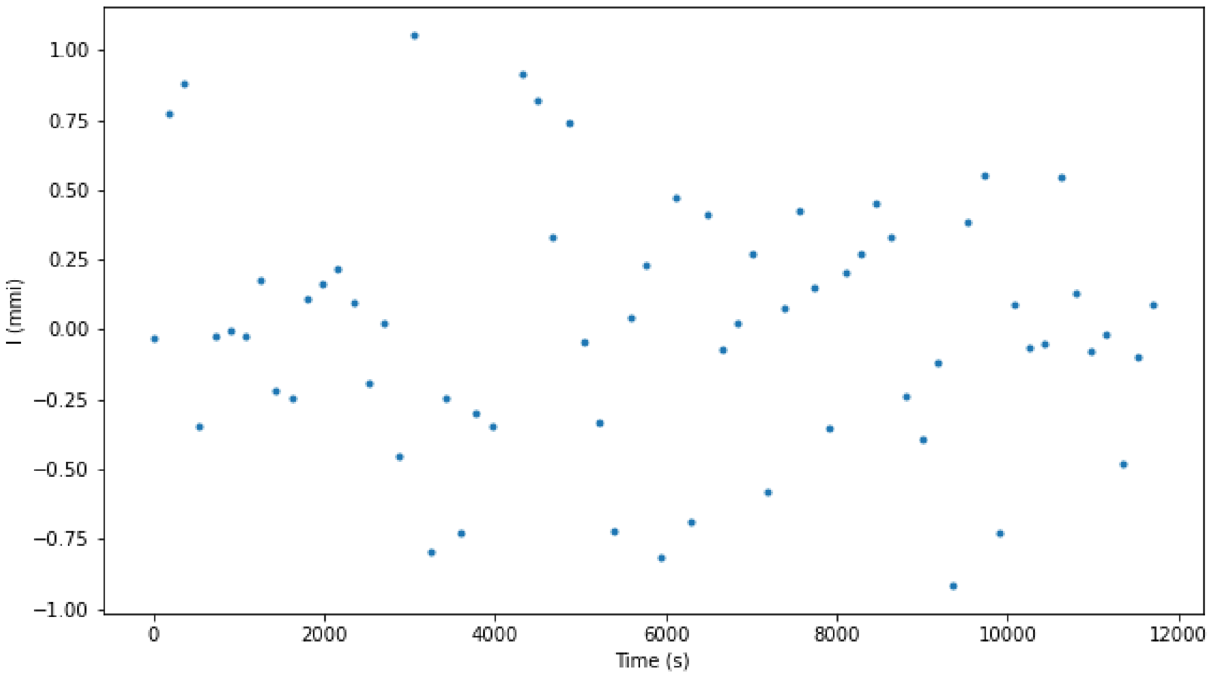

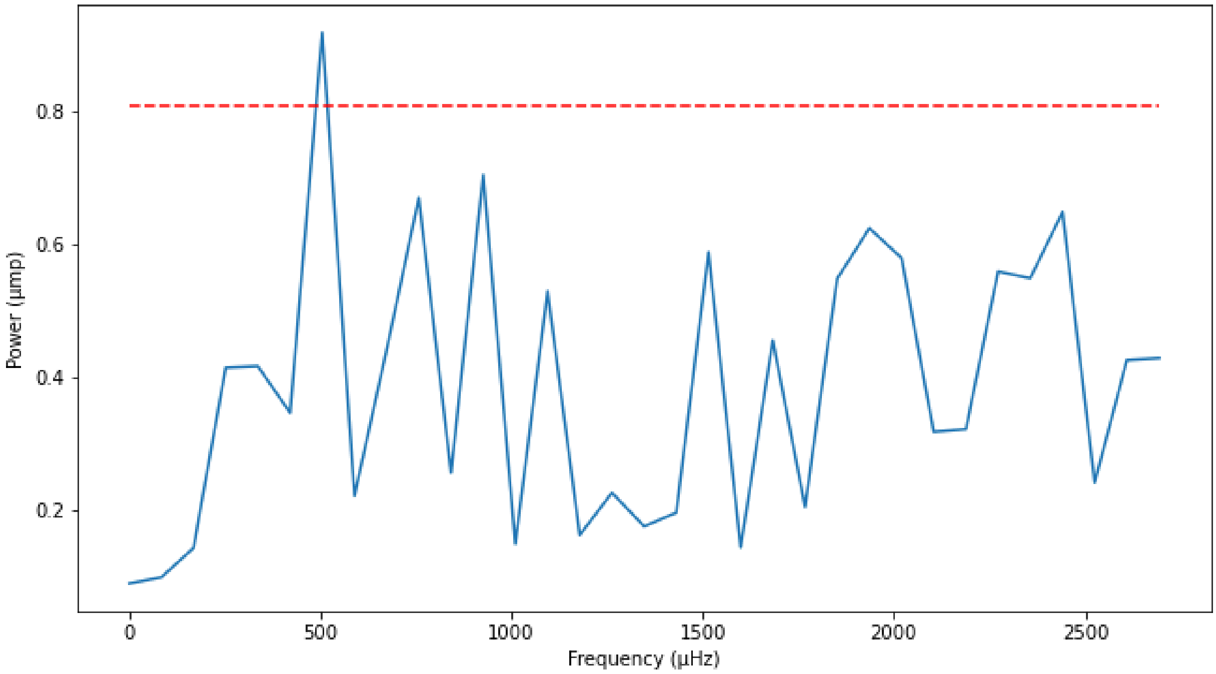


```
C:\Users\teach\AppData\Local\Temp/ipykernel_13912/2588248293.py:135: RuntimeWarning:
divide by zero encountered in true_divide
  periods_FT = 1/xf
```

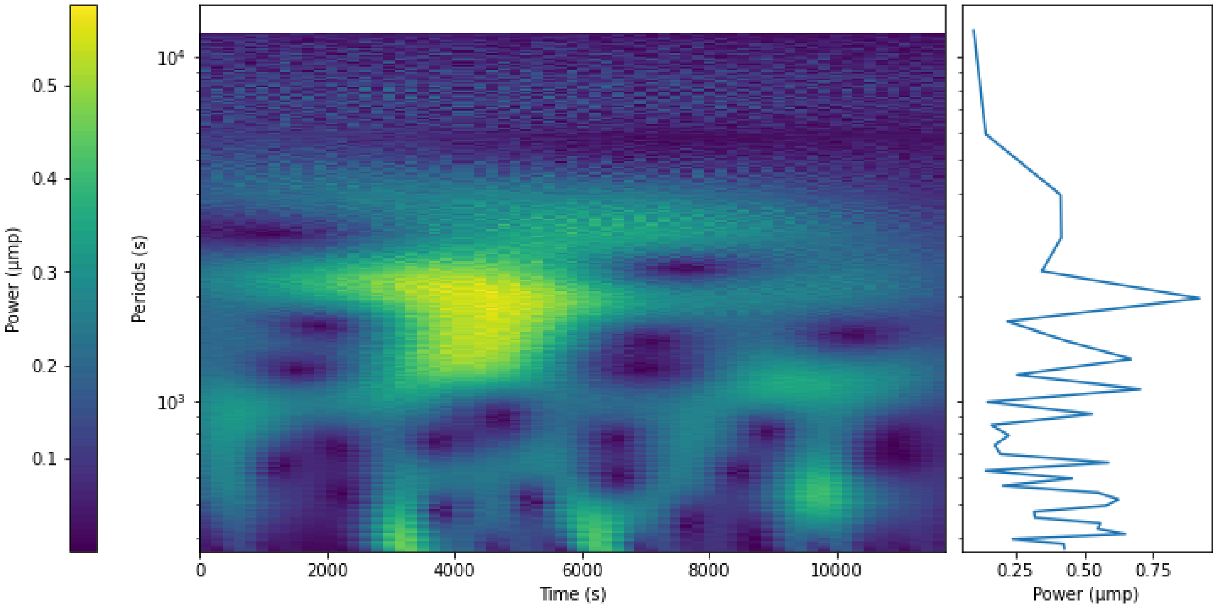

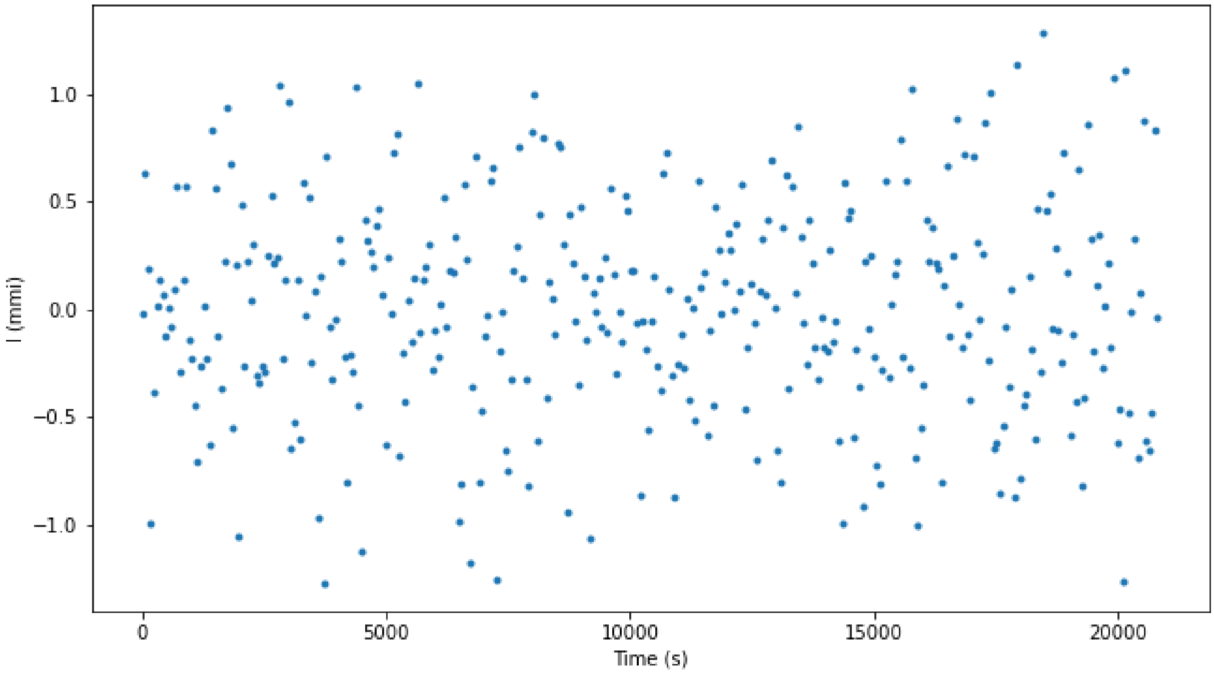

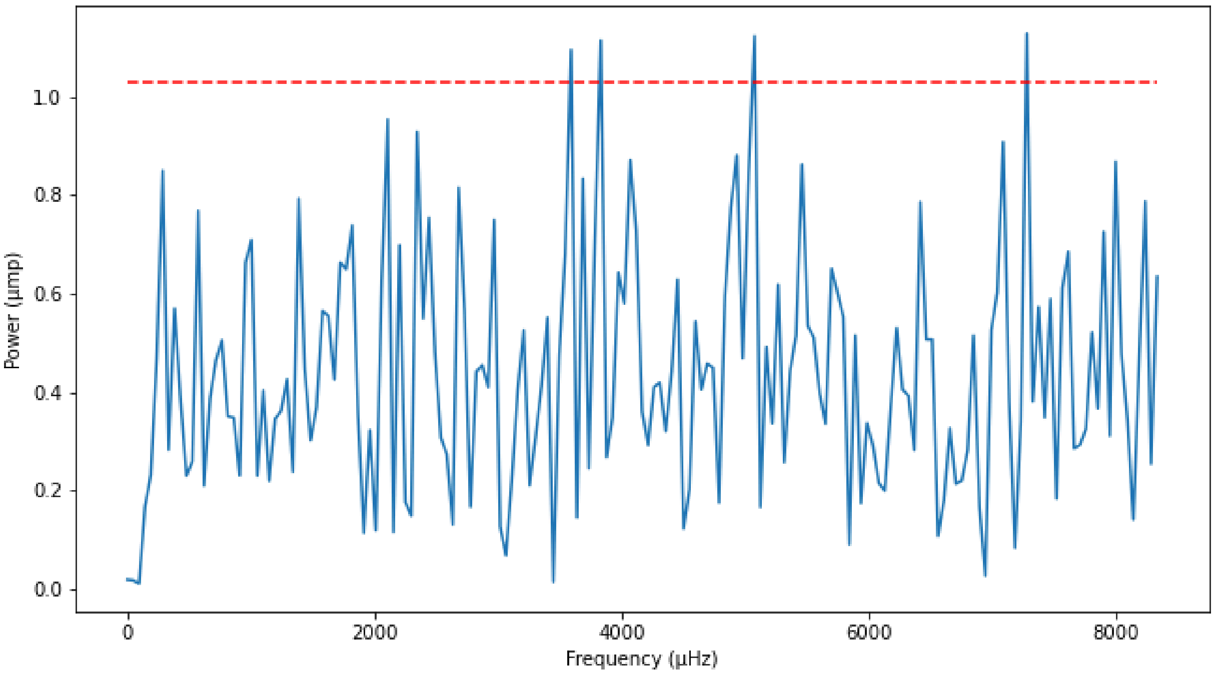


```
C:\Users\teach\AppData\Local\Temp/ipykernel_13912/2588248293.py:135: RuntimeWarning:
divide by zero encountered in true_divide
  periods_FT = 1/xf
```

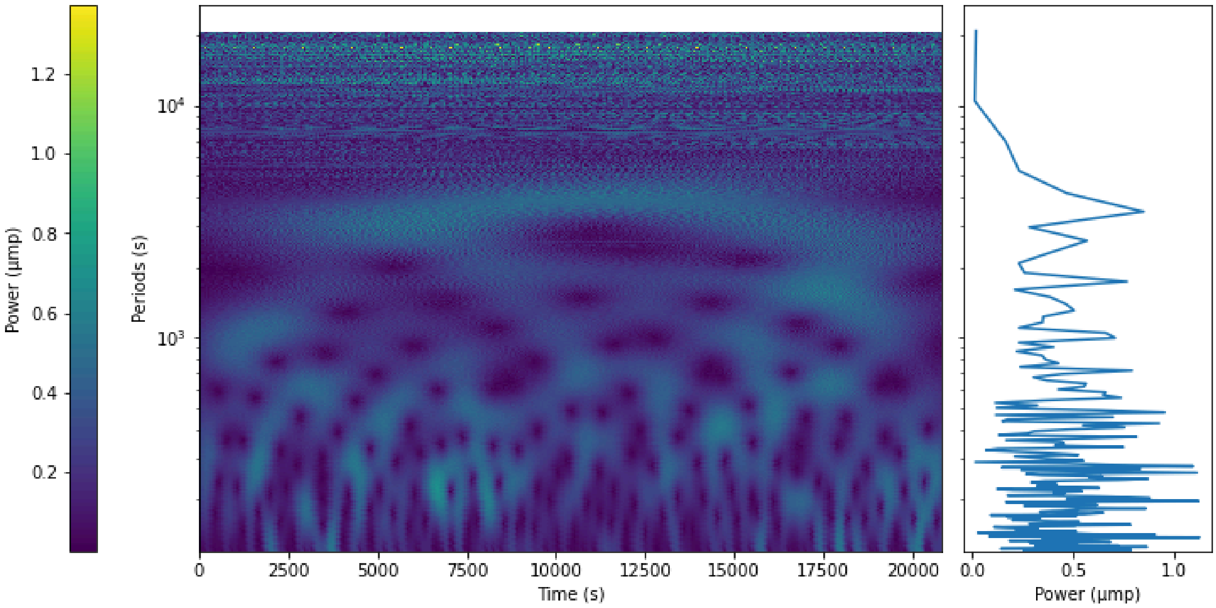
Power (µmp)
Periods (s)
Time (s)
Power (µmp)

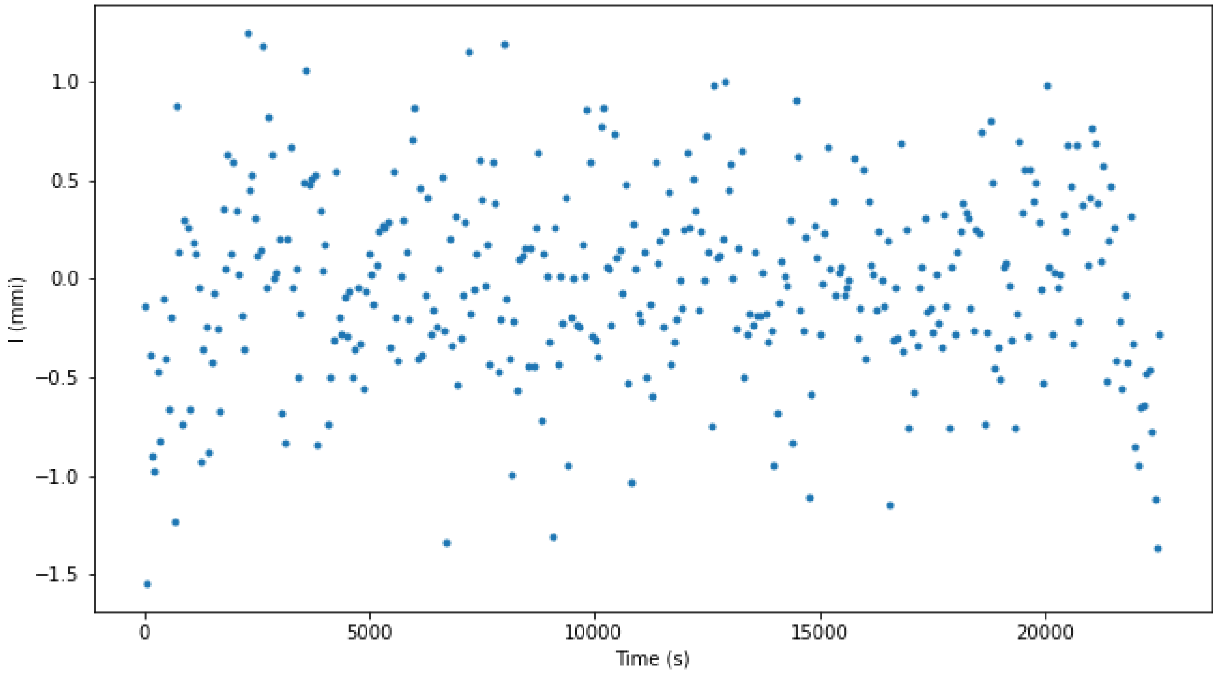
I (mmi)
Time (s)

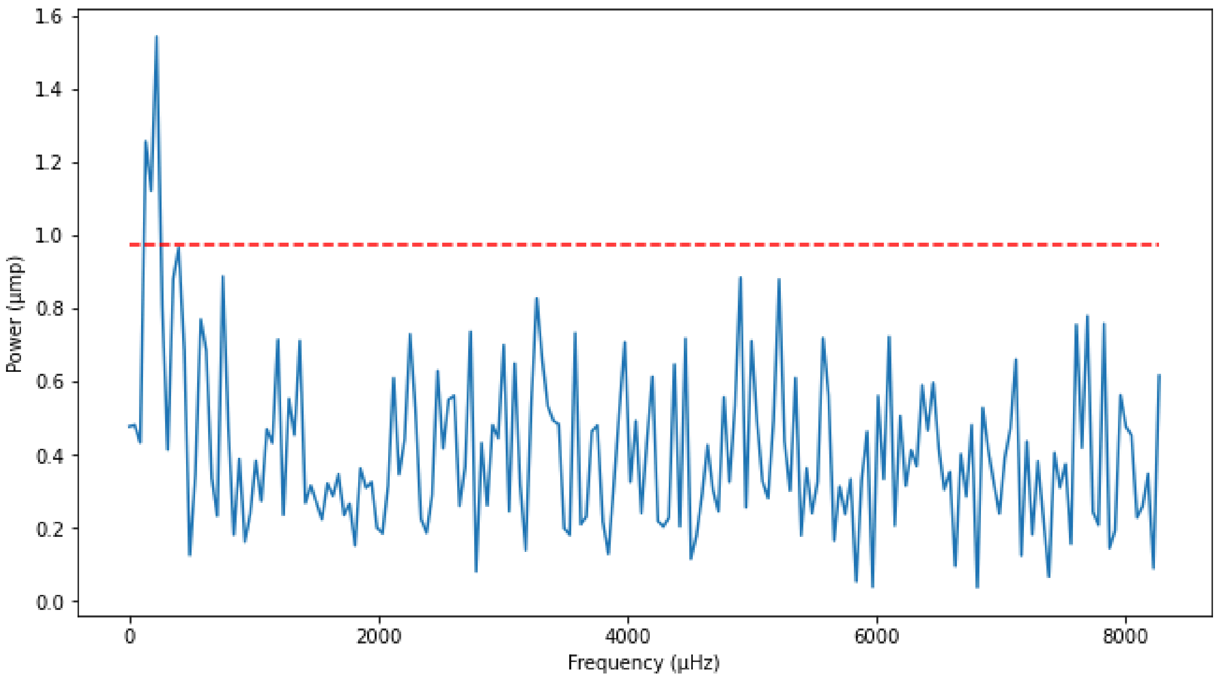
Power (µmp)
Frequency (µHz)

```
C:\Users\teach\AppData\Local\Temp/ipykernel_13912/2588248293.py:135: RuntimeWarning:
divide by zero encountered in true_divide
  periods_FT = 1/xf
```

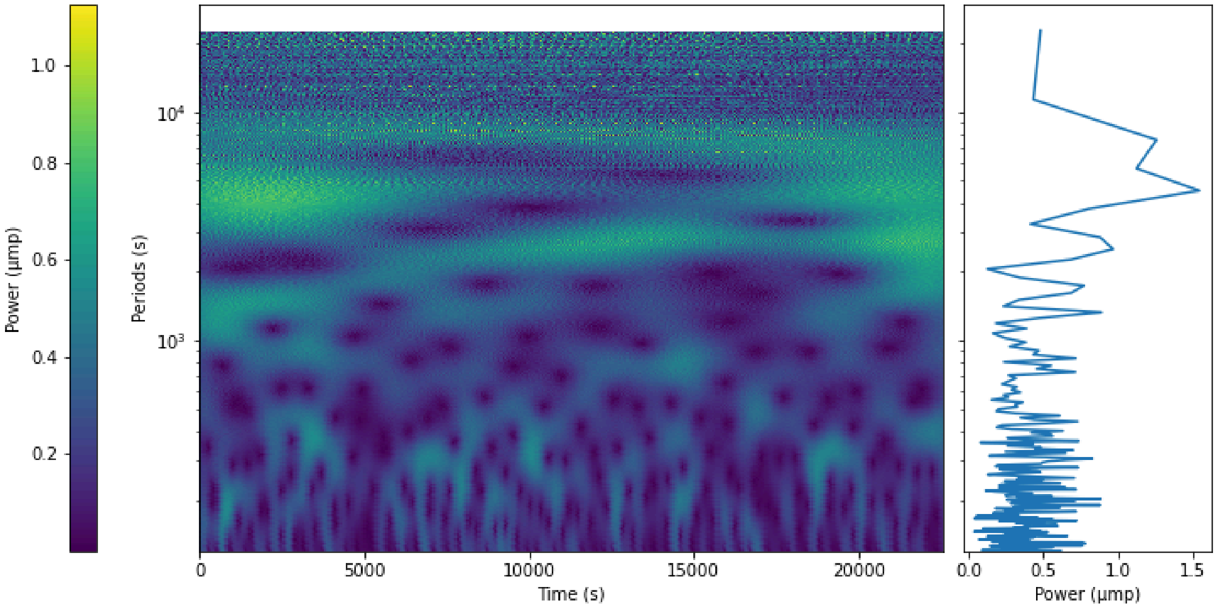

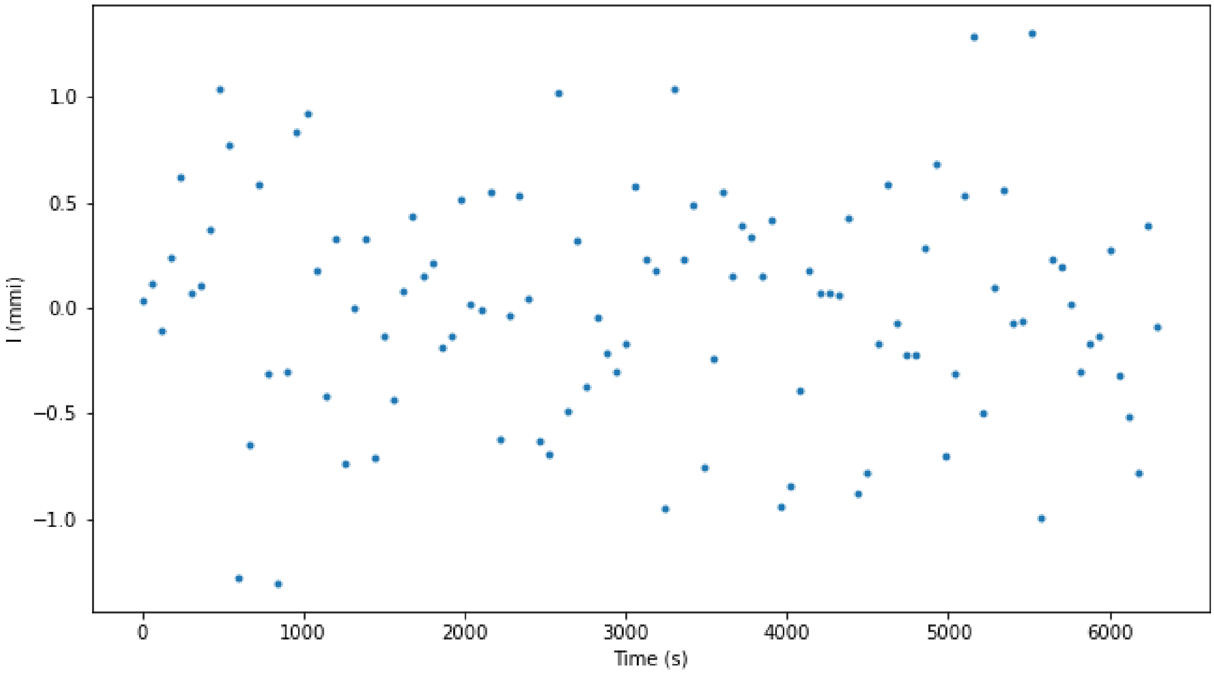

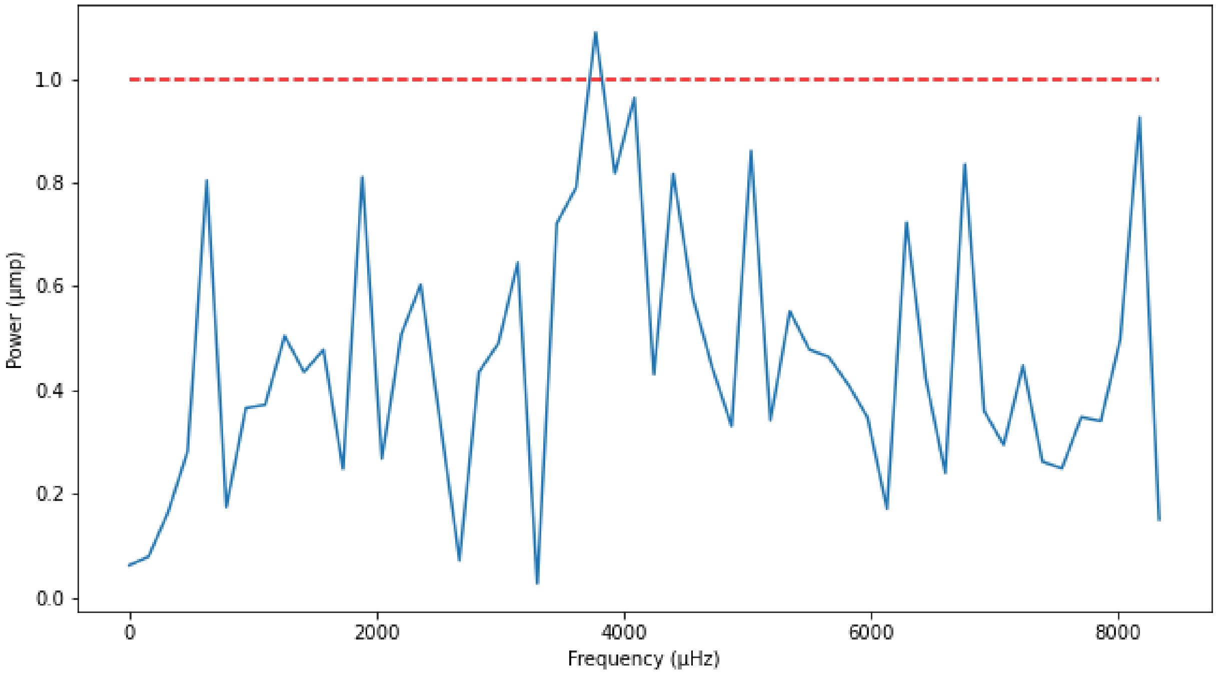


```
C:\Users\teach\AppData\Local\Temp/ipykernel_13912/2588248293.py:135: RuntimeWarning:
divide by zero encountered in true_divide
  periods_FT = 1/xf
```

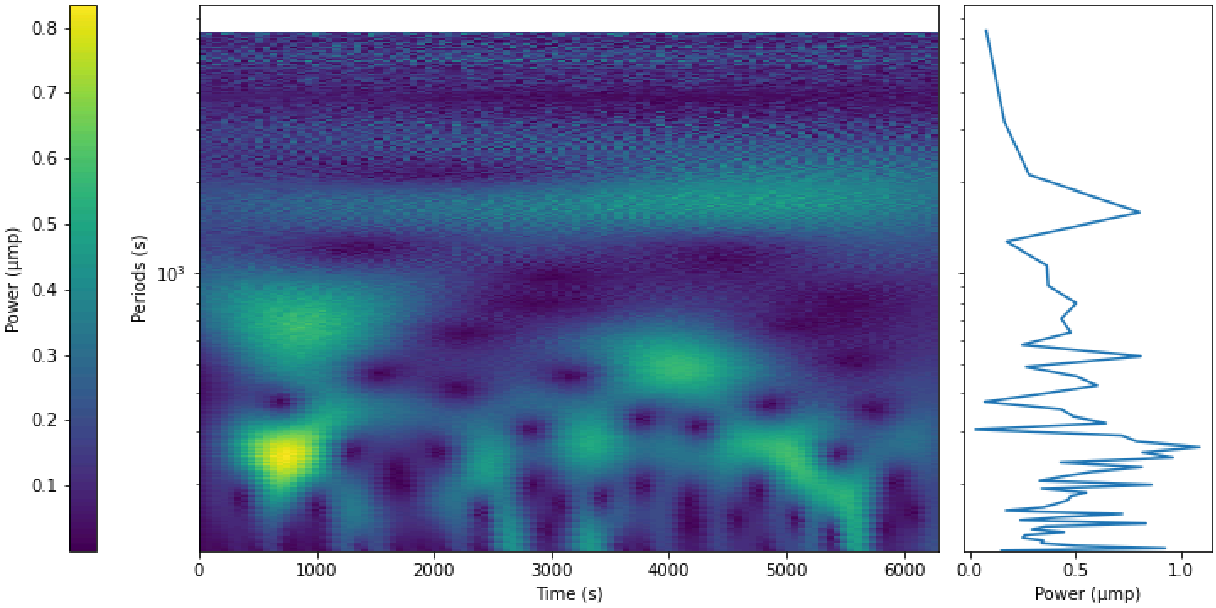

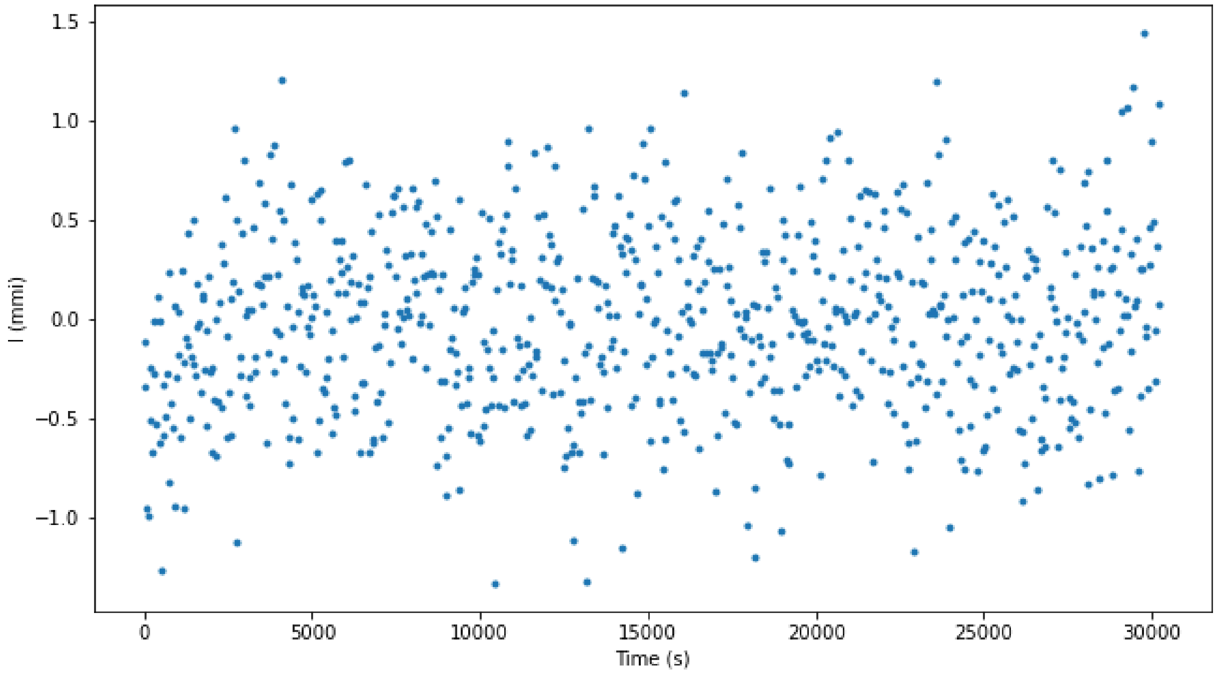

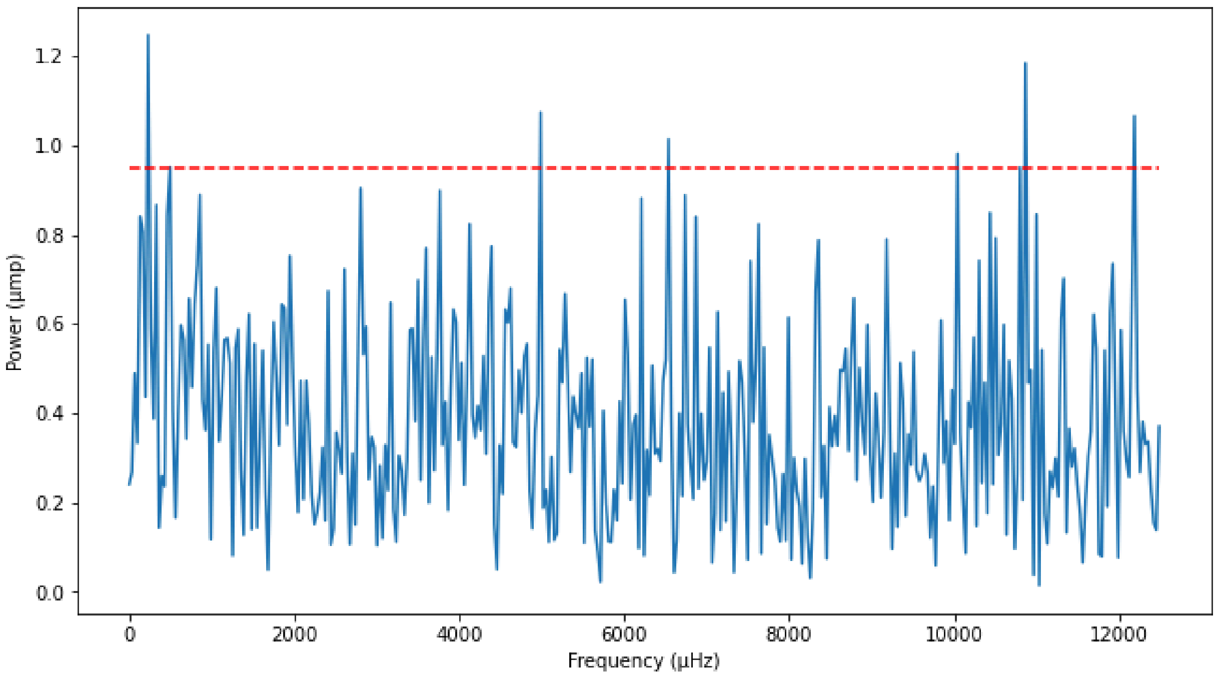


```
C:\Users\teach\AppData\Local\Temp/ipykernel_13912/2588248293.py:135: RuntimeWarning:
divide by zero encountered in true_divide
  periods_FT = 1/xf
```

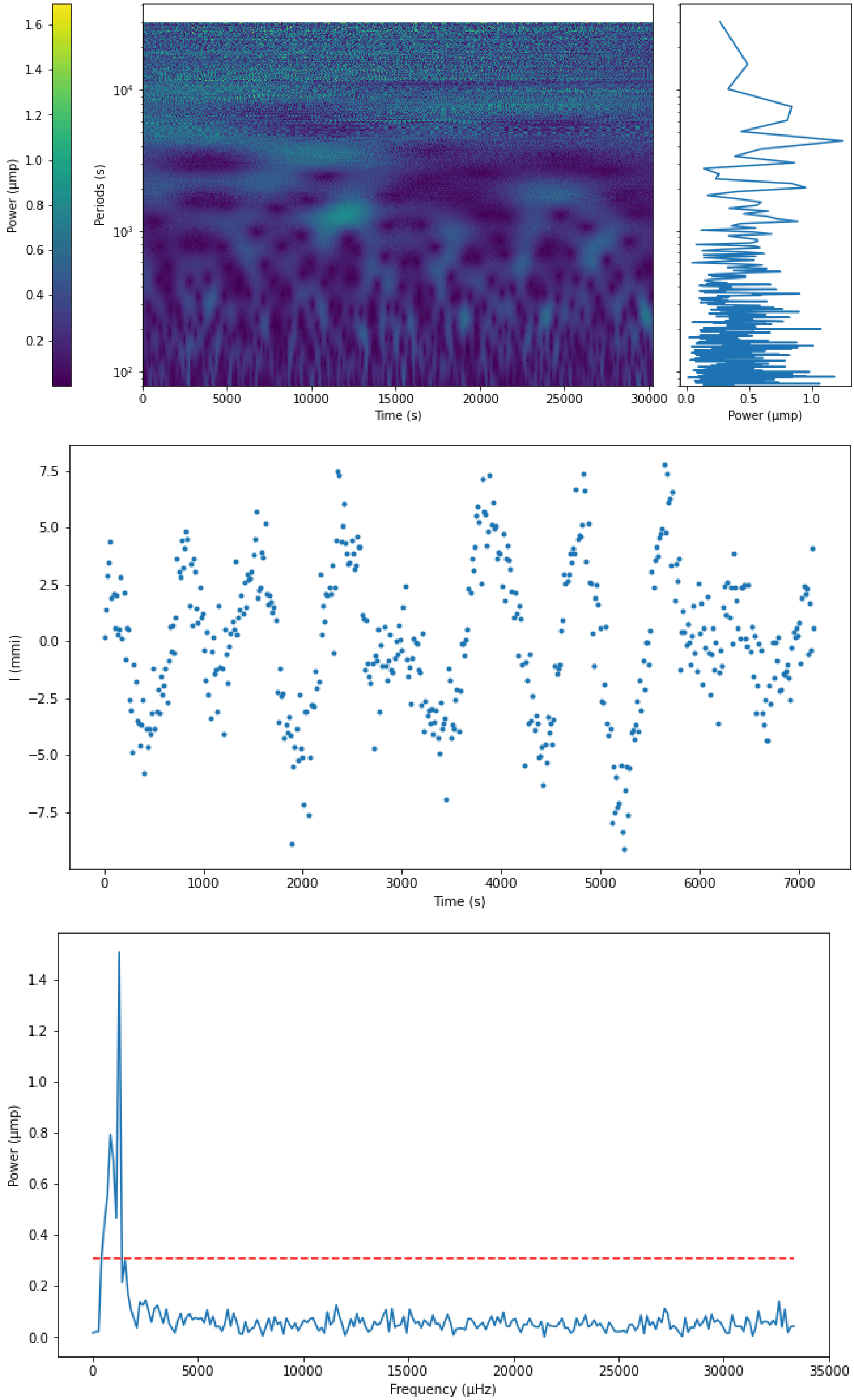
Power (µmp)
Periods (s)
Time (s)
Power (µmp)
I (mmi)
Time (s)
Power (µmp)
Frequency (µHz)

```
C:\Users\teach\AppData\Local\Temp/ipykernel_13912/2588248293.py:135: RuntimeWarning:
divide by zero encountered in true_divide
  periods_FT = 1/xf
```

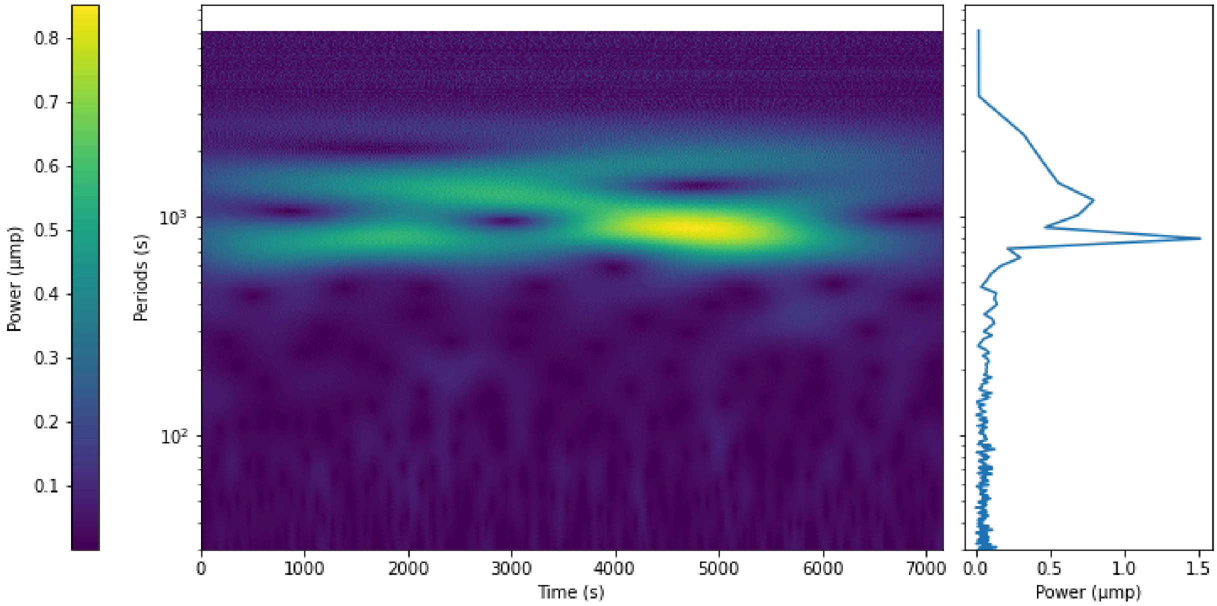

A.2 Synthetic light curve - Harmonics

Synthetic light curves - Harmonics

In [8]:

```
import matplotlib.pyplot as plt
import numpy as np
import math

import pywt
from scipy import signal
```

In [9]:

```
def sinus_signal(time,frequency,amplitude):
    sinewave = amplitude * np.sin(2 * np.pi * frequency * time)
    return sinewave
```

In [10]:

```
def butter_highpass(cutoff, f_nyquist, order=6):
    normal_cutoff = cutoff/f_nyquist
    b, a = signal.butter(order, normal_cutoff, btype='high')
    return b, a

def butter_highpass_filter(data, cutoff, f_nyquist, order=6):
    b, a = butter_highpass(cutoff, f_nyquist, order=order)
    y = signal.filtfilt(b, a, data)
    return y

def FT_and_CWT(time,signal):

    # perform fourier transform
    from numpy.fft import rfft, rfftfreq

    # Butterworth highpass filter
    sampling_period = np.diff(time).mean()
    sample_length = time[-1]
    f_min = 1/sample_length
    f_nyquist = (1/sampling_period)*(1/2)
    cutoff = 2*f_min
    signal = butter_highpass_filter(signal, cutoff, f_nyquist)


    yf = rfft(signal,norm="ortho")
    xf = rfftfreq(len(signal), sampling_period)

    yf = np.abs(yf)

    # perform CWT
    wavelet = "cmor1.5-1.0"

    # Calculating scales
    scale_min = 2
    scale_max = 2 * f_nyquist/f_min

    # logarithmic scale for scales, as suggested by Torrence & Compo:
    widths_1 = np.geomspace(scale_min, scale_max, num=500)
    cwtmatr, freqs = pywt.cwt(signal, widths_1, wavelet,
                              sampling_period=sampling_period)
    # absolute take absolute value of complex result
    cwtmatr = np.abs(cwtmatr[:-1, :-1])

    # converting frequency to period
    periods = 1/freqs
```

```
    return time, cwtmatr, freqs, periods, xf, yf


def plot_signal_FT_CWT(time,signal,title):

    #Plot signal

    #Generating data for CWT and FT
    time, cwtmatr, freqs, periods, xf, yf = FT_and_CWT(time,signal)

    #Plot scaleogram with Fourier transform

    #Plot result using matplotlib's pcolormesh (image with annoted axes)
    plt.rcParams['figure.constrained_layout.use'] = True

    fig, axs = plt.subplots(1, 2, figsize=(10,5), sharey=True,
                            gridspec_kw={'width_ratios': [3 ,1]})
    pcm = axs[0].pcolormesh(time, periods, cwtmatr)
    axs[0].set_yscale("log")
    axs[0].set_xlabel("Time (s)")
    axs[0].set_ylabel("Periods (s)")
    fig.colorbar(pcm, ax=axs[0], location='left',label="Power (μmp)")


    # converting frequency to period for FT
    periods_FT = 1/xf

    plt.plot(yf, periods_FT)
    axs[1].set_xlabel("Power (μmp)")
    axs[1].set_yscale("log")

    file_name_synthetic_scalogram_and_FT = title + 'synthetic_scalogram_and_FT.' + '
    plt.savefig('C:/Users/teach/OneDrive/Heldagsprøve/NTNU/Master LaTex/Pictures and
                file_name_synthetic_scalogram_and_FT, format = 'pdf', dpi = 300)
```

In [11]:

```
#generate time sequence
start_time = 0
end_time = 2200
sample_rate = 0.018 #with this sample rate one retrieves a value of about 56
                    #as the spacing values between adjacent values.
                    #56 is the step value for the data of Jn1 first
                    #run and hence is a good choice for comparison reasons.
time = np.arange(start_time, end_time, 1/sample_rate)
```

Harmonics with dominant fundamental frequency

In [12]:

```
#generate signal
harm_fund_freq_1 = sinus_signal(time, 1000*10**(-6), 10)
harm_fund_freq_2 = sinus_signal(time, 2000*10**(-6), 3)
harm_fund_freq_3 = sinus_signal(time, 3000*10**(-6), 2)
harm_fund_freq_4 = sinus_signal(time, 4000*10**(-6), 1)
harm_fund_freq_5 = sinus_signal(time, 5000*10**(-6), 1)

signal_fund_freq_1_to_3 = harm_fund_freq_1 + harm_fund_freq_2 + harm_fund_freq_3
signal_fund_freq_1_to_5 = harm_fund_freq_1 + harm_fund_freq_2 + harm_fund_freq_3
                        + harm_fund_freq_4 + harm_fund_freq_5
```

```
#Plot signal
plt.figure(figsize=(10,6))
plt.plot(time, harm_fund_freq_1, 'r', label='Fundamental frequency')
plt.plot(time, harm_fund_freq_2, 'g', label='First harmonic')
plt.plot(time, harm_fund_freq_3, 'b', label='Second harmonic')
plt.xlabel("Time(s)")
plt.ylabel("I (mmi)")
plt.savefig('C:/Users/teach/OneDrive/Heldagsprøve/NTNU/Master LaTex/Pictures and fig
            'harmonics with dominant fund.freq_1 to 3_separate signals_synthetic_lig
            + 'pdf', format = 'pdf', dpi = 300)
plt.legend()

plt.figure(figsize=(10,6))
plt.plot(time, signal_fund_freq_1_to_3)
plt.xlabel("Time(s)")
plt.ylabel("I (mmi)")
plt.savefig('C:/Users/teach/OneDrive/Heldagsprøve/NTNU/Master LaTex/Pictures and fig
            'harmonics with dominant fund.freq_1 to 3_synthetic_lightcurve.'
            + 'pdf', format = 'pdf', dpi = 300)
plt.show()

#Plot signal
plt.figure(figsize=(10,6))
plt.plot(time, harm_fund_freq_1, 'r', label='Fundamental frequency')
plt.plot(time, harm_fund_freq_2, 'g', label='First harmonic')
plt.plot(time, harm_fund_freq_3, 'b', label='Second harmonic')
plt.plot(time, harm_fund_freq_4, 'y', label='Third harmonic')
plt.plot(time, harm_fund_freq_5, 'm', label='Fourth harmonic')
plt.xlabel("Time(s)")
plt.ylabel("I (mmi)")
plt.savefig('C:/Users/teach/OneDrive/Heldagsprøve/NTNU/Master LaTex/Pictures and fig
            + 'harmonics with dominant fund.freq_1 to 5_separate signals_synthetic_l
            + 'pdf', format = 'pdf', dpi = 300)
plt.legend()

plt.figure(figsize=(10,6))
plt.plot(time, signal_fund_freq_1_to_5)
plt.xlabel("Time(s)")
plt.ylabel("I (mmi)")
plt.savefig('C:/Users/teach/OneDrive/Heldagsprøve/NTNU/Master LaTex/Pictures and fig
            'harmonics with dominant fund.freq_1 to 5_synthetic_lightcurve.'
            + 'pdf', format = 'pdf', dpi = 300)
plt.show()
```

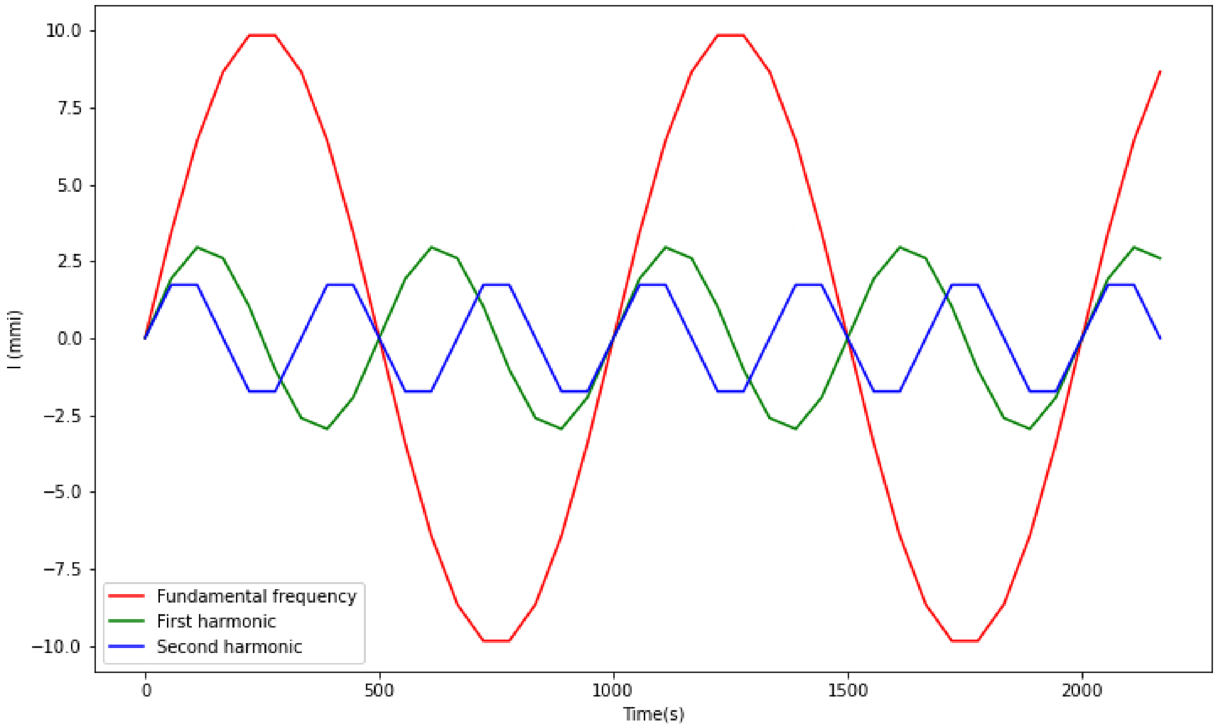
10.0
7.5
5.0
2.5
0.0
−2.5
−5.0
−7.5
−10.0
I (mmi)
0
500
1000
1500
2000
Time(s)
Fundamental frequency
First harmonic
Second harmonic

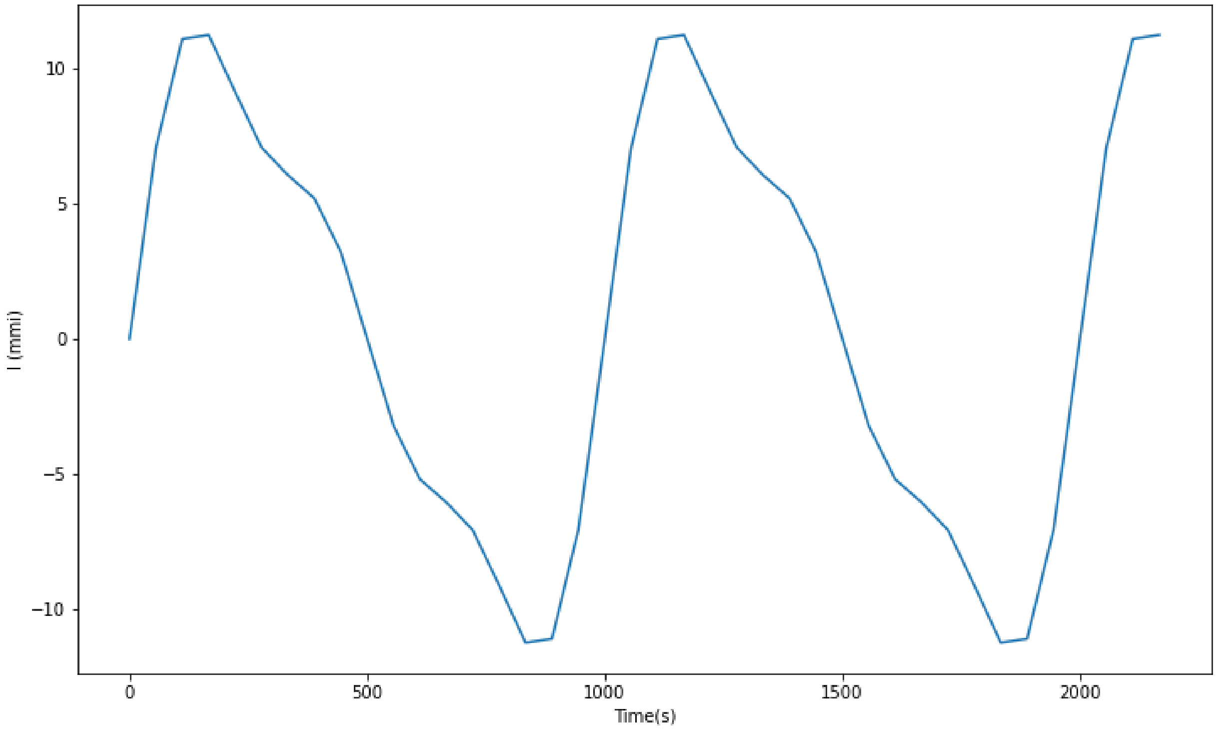
10
5
0
−5
−10
I (mmi)
0
500
1000
1500
2000
Time(s)

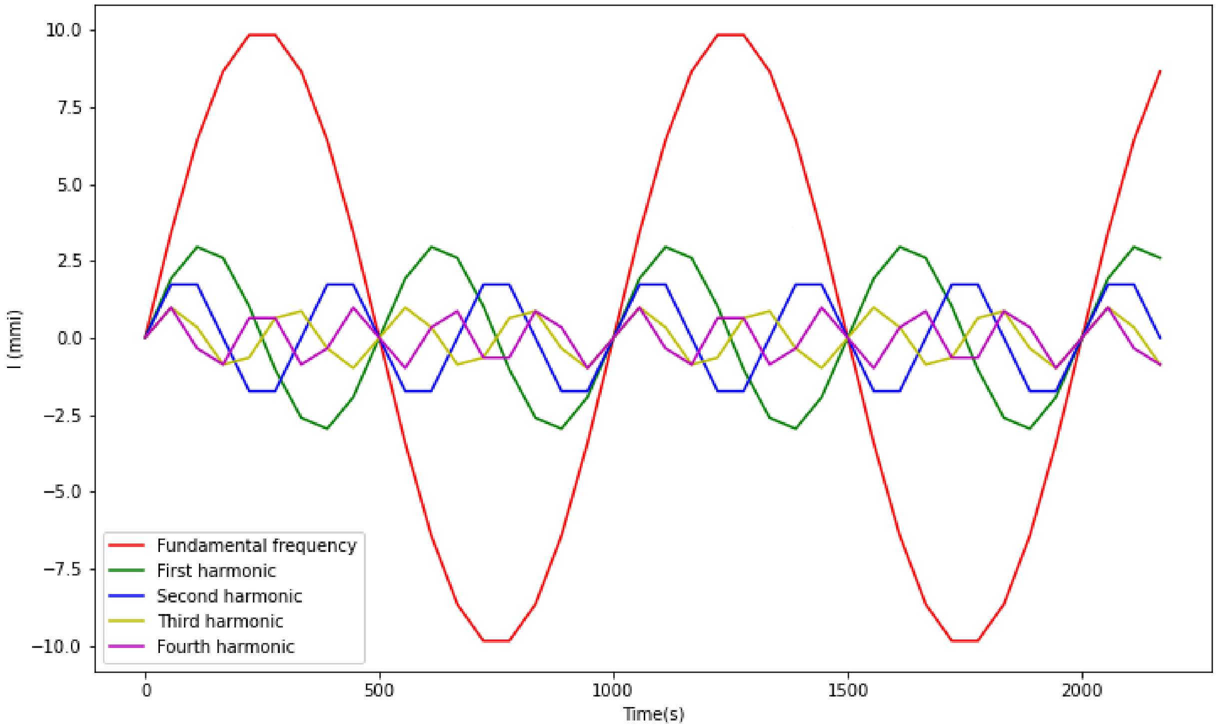

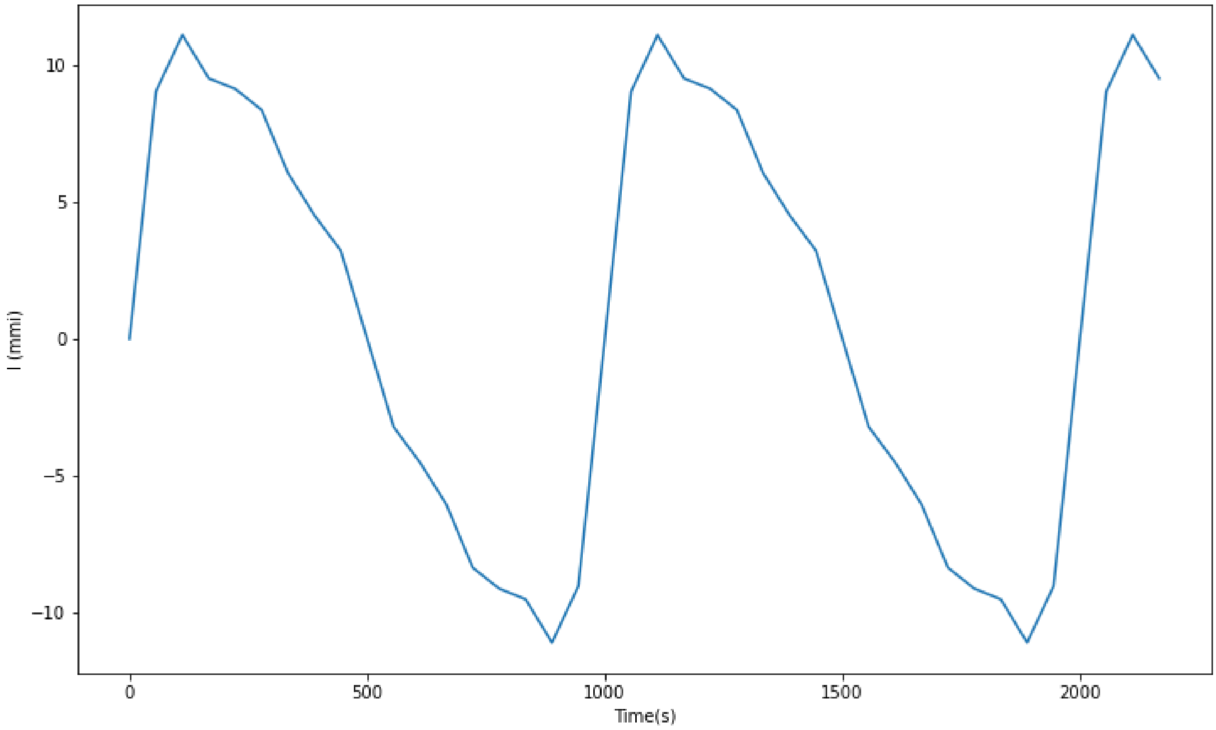

In [13]:

```
plot_signal_FT_CWT(time,signal_fund_freq_1_to_3,"harmonics with dominant fund.freque
plot_signal_FT_CWT(time,signal_fund_freq_1_to_5,"harmonics with dominant fund.freque
```

```
C:\Users\teach\AppData\Local\Temp/ipykernel_2496/812598757.py:70: RuntimeWarning: div
ide by zero encountered in true_divide
  periods_FT = 1/xf
C:\Users\teach\AppData\Local\Temp/ipykernel_2496/812598757.py:70: RuntimeWarning: div
ide by zero encountered in true_divide
  periods_FT = 1/xf
```

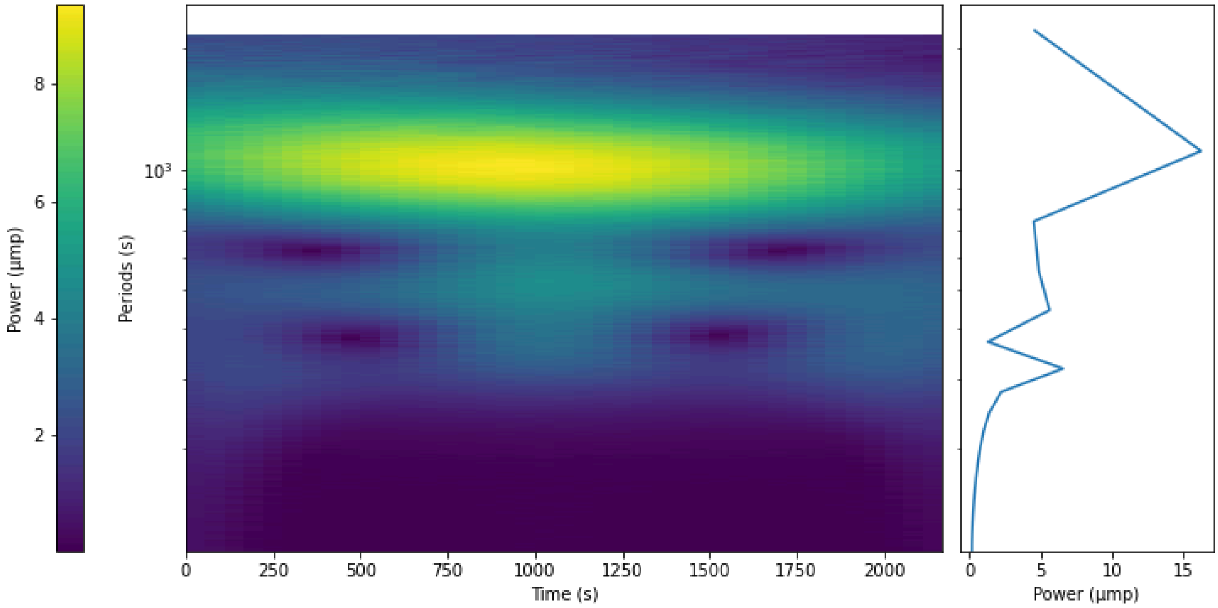

Power (μmp)
8
6
4
2
Periods (s)
10^3
0 250 500 750 1000 1250 1500 1750 2000
Time (s)
0 5 10 15
Power (μmp)

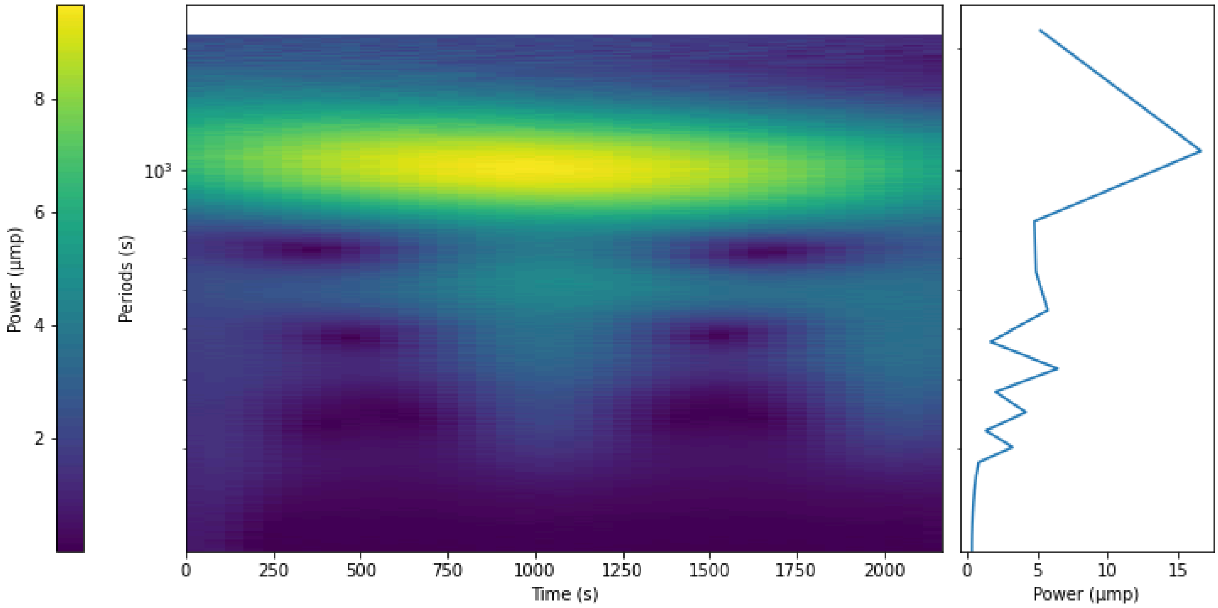

Power (μmp)
8
6
4
2
Periods (s)
10^3
0 250 500 750 1000 1250 1500 1750 2000
Time (s)
0 5 10 15
Power (μmp)

A.3 Synthetic light curve - Pulse shape

The function for doing the raised cosine pulse shaping was inspired by (31).

Synthetic light curves - Pulse shape

In [1]:

```
import matplotlib.pyplot as plt
import numpy as np
import math

import pywt
from scipy import signal
```

In [2]:

```
def butter_highpass(cutoff, f_nyquist, order=6):
    normal_cutoff = cutoff/f_nyquist
    b, a = signal.butter(order, normal_cutoff, btype='high')
    return b, a

def butter_highpass_filter(data, cutoff, f_nyquist, order=6):
    b, a = butter_highpass(cutoff, f_nyquist, order=order)
    y = signal.filtfilt(b, a, data)
    return y


# FALSE alarm probability function
def FAP(time,yf,FALSE_val):
    N = len(time)
    P_ave = 0
    for i in range(len(yf)):
        P_ave += (np.abs(yf[i]))**2
    P_ave = P_ave/N
    P_obs = math.log(N*(1/FALSE_val))*P_ave
    return P_obs
```

In [3]:

```
#Functions for sinus signal with varying amplitude
def sinus_signal_var_amp(time,frequency,amplitude_frequency,
                         amplitude_phase,amplitude_extent):

    amplitude = np.cos(amplitude_frequency*time + amplitude_phase)
    * amplitude_extent
    sinewave = amplitude * np.sin(2 * np.pi * frequency * time)

    return sinewave

def sinus_signal_const_amp(time,frequency,amplitude):

    sinewave = amplitude * np.sin(2 * np.pi * frequency * time)

    return sinewave

def sinus_signal_gen(frequency,amplitude,command):

    start_time = 0
    end_time = 10
    sample_rate = 1000
    time = np.arange(start_time, end_time, 1/sample_rate)

    #Define necessary parameters
    harm_num = 2
    amplitude_frequency = 0.1
    amplitude_phase = math.pi/2
    amplitude_extent = 10
```

```
    # Raised cosine pulse shape parameters
    fs = 5
    num_weights = 41
    alpha = 0.5
    x = 0.9999*np.arange(-int(num_weights/2),int(num_weights/2)+1,1)/fs
    raised_cos_weights = np.sinc(x)*(np.cos(alpha*np.pi*x)/(1-((2*alpha*x)**2)))

    #Function for RC pulse shape wave
    if command == "pulse_shape_RC":

        #Generate pulse vectors
        pulse1 = np.zeros(21,)
        pulse2 = np.zeros(21,)
        pulse3 = np.zeros(21,)
        pulse1[5] = 1
        pulse2[10] = 0.7
        pulse3[15] = 0.8

        #Pulse shape each symbol separately
        symbol1_rc = np.convolve(pulse1,raised_cos_weights).real
        symbol2_rc = np.convolve(pulse2,raised_cos_weights).real
        symbol3_rc = np.convolve(pulse3,raised_cos_weights).real

        #Pulse shape the combination of symbols
        symbols_rc = np.convolve(pulse1+pulse2+pulse3,raised_cos_weights).real

        for i in range(0,20):
            symbols_rc[i] = 0

        for j in range(41,61):
            symbols_rc[j] = 0

        #Shortening the length of the signal
        for i in range(0,16):
            symbols_rc = np.delete(symbols_rc,0)

        for i in range(45,61):
            symbols_rc = np.delete(symbols_rc,-1)

        #Repeat the pulse shape pattern
        signal = np.append(symbols_rc,symbols_rc)

        for i in range(8):
            signal = np.delete(signal,25)
        for i in range(4):
            signal = np.delete(signal,24)

        time = np.arange(0,46)
        harmonic_signals = []

        return time, signal, harmonic_signals
```

In [4]:

```
def FT_and_CWT(frequency,amplitude,command):

    # perform fourier transform
    from numpy.fft import rfft, rfftfreq

    time, signal, harmonic_signals = sinus_signal_gen(frequency,amplitude,command)

    # Butterworth highpass filter
    sampling_period = np.diff(time).mean()
    sample_length = time[-1]
```

```
    f_min = 1/sample_length
    f_nyquist = (1/sampling_period)*(1/2)
    cutoff = 2*f_min
    signal = butter_highpass_filter(signal, cutoff, f_nyquist)


    yf = rfft(signal)
    xf = rfftfreq(len(signal), sampling_period)

    yf = np.abs(yf)

    # perform CWT
    wavelet = "cmor1.5-1.0"

    # Calculating scales
    scale_min = 2
    scale_max = 2 * f_nyquist/f_min

    # logarithmic scale for scales, as suggested by Torrence & Compo:
    widths_1 = np.geomspace(scale_min, scale_max, num=500)
#     widths_2 = np.linspace(1,2048,num=500)
    cwtmatr, freqs = pywt.cwt(signal, widths_1, wavelet,
                              sampling_period=sampling_period)
    # absolute take absolute value of complex result
    cwtmatr = np.abs(cwtmatr[:-1, :-1])

    # converting frequency to period
    periods = 1/freqs

    return time, signal, harmonic_signals, xf, yf, periods, cwtmatr


def plot_signal_FT_CWT(frequency,amplitude,command):

    #Plot signal

    #Generating data for CWT and FT
    time, signal, harmonic_signals, xf, yf, periods, cwtmatr =
    FT_and_CWT(frequency,amplitude,command)
    title = command
    file_name_synthetic_lightcurve = title + '_synthetic_lightcurve.' + 'pdf'

    plt.figure(figsize=(10,6))
    plt.plot(time, signal)
    plt.xlabel("Time(s)")
    plt.ylabel("I (mmi)")
    plt.savefig('C:/Users/teach/OneDrive/Heldagsprøve/NTNU/Master LaTex/Pictures and
                file_name_synthetic_lightcurve, format = 'pdf', dpi = 300)
    plt.show()

    #--------------------------------------------------------------------------------

    #Plot scaleogram with Fourier transform

    #Plot result using matplotlib's pcolormesh (image with annoted axes)
    plt.rcParams['figure.constrained_layout.use'] = True

    fig, axs = plt.subplots(1, 2, figsize=(10,5), sharey=True,
                            gridspec_kw={'width_ratios': [3 ,1]})
    pcm = axs[0].pcolormesh(time, periods, cwtmatr)
    axs[0].set_yscale("log")
    axs[0].set_xlabel("Time (s)")
    axs[0].set_ylabel("Periods (s)")
    fig.colorbar(pcm, ax=axs[0], location='left',label="Power (µmp)")
```

```
    # converting frequency to period for FT
    periods_FT = 1/xf

    plt.plot(yf/10, periods_FT)
    axs[1].set_xlabel("Power (µmp)")
    axs[1].set_yscale("log")

    file_name_synthetic_scalogram_and_FT = title + 'synthetic_scalogram_and_FT.' + '
    plt.savefig('C:/Users/teach/OneDrive/Heldagsprøve/NTNU/Master LaTex/Pictures and
                file_name_synthetic_scalogram_and_FT, format = 'pdf', dpi = 300)
```

In [5]:

```
#Input values for plot_signal_FT_CWT function
frequency = 2.5
amplitude = 10
command = "pulse_shape_RC"

plot_signal_FT_CWT(frequency,amplitude,command)
```

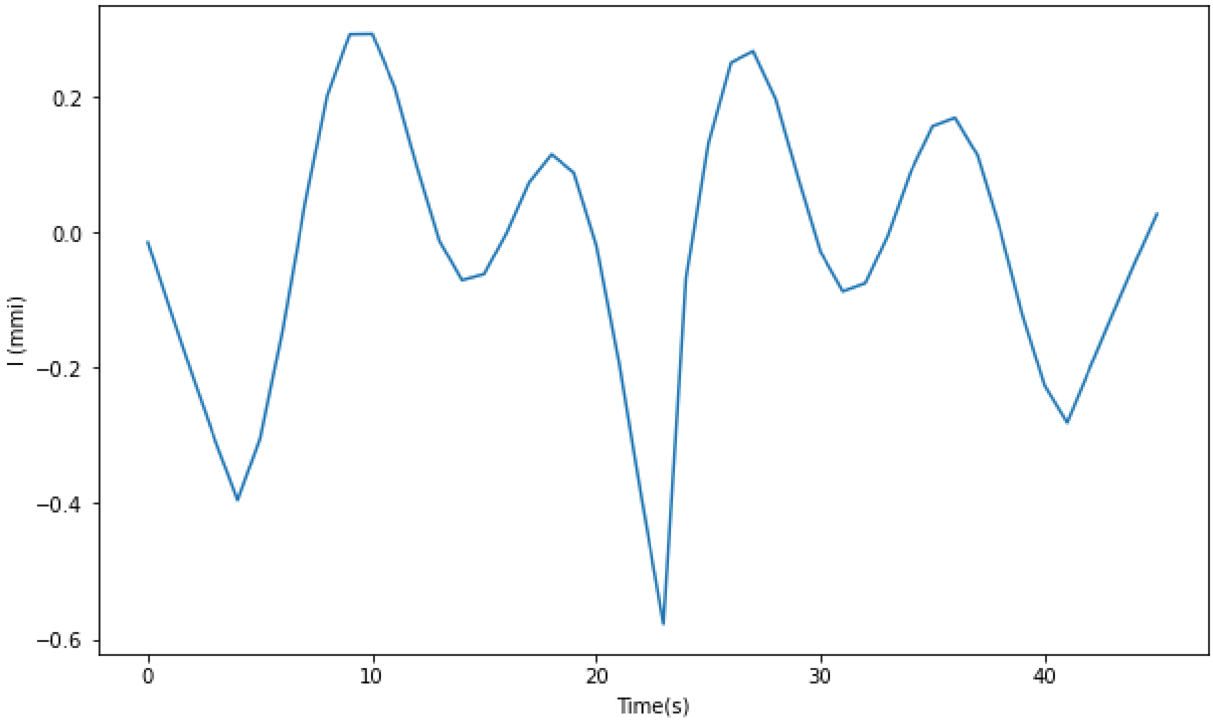


```
C:\Users\teach\AppData\Local\Temp/ipykernel_4044/2059480262.py:74: RuntimeWarning: di
vide by zero encountered in true_divide
  periods_FT = 1/xf
```

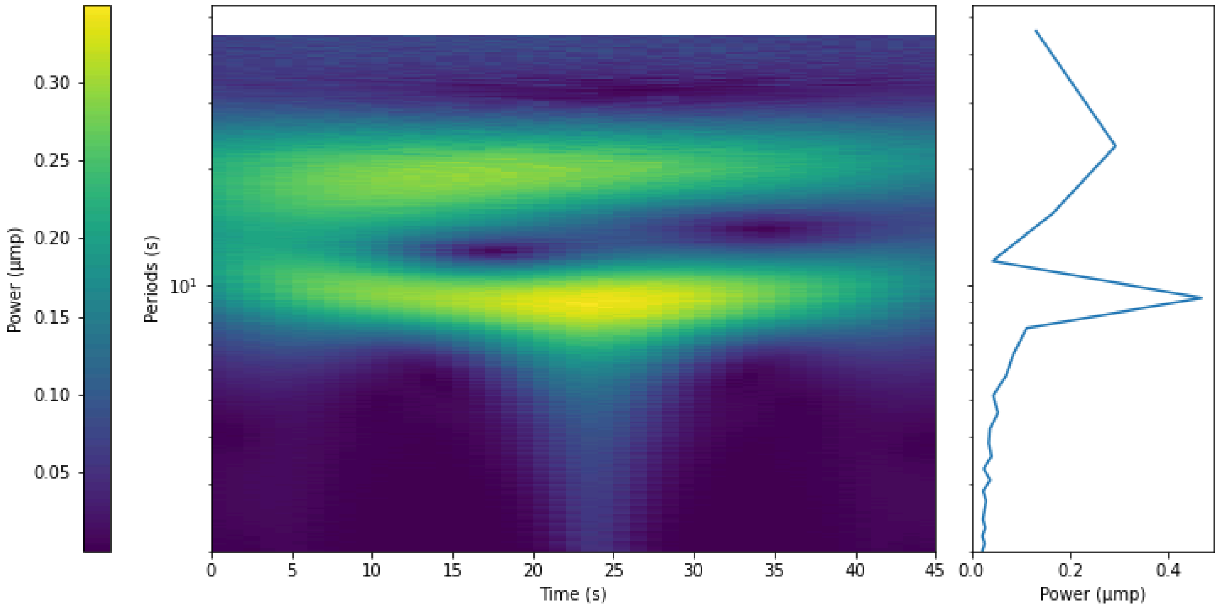
0.30
0.25
0.20
0.15
0.10
0.05
Power (µmp)
Periods (s)
10^1
0
5
10
15
20
25
30
35
40
45
Time (s)
0.0
0.2
0.4
Power (µmp)

NTNU

Norwegian University of
Science and Technology